THE
OBSERVATORY

A REVIEW OF ASTRONOMY

EDITED BY

D. J. STICKLAND

R. W. ARGYLE

S. J. FOSSEY

Vol. 127 No. 1196

2007 FEBRUARY

THE OBSERVATORY

Vol. 127 2007 FEBRUARY No. 1196

BRIGHTNESS OF CLOUDS AT NIGHT OVER A CITY

By R. H. Garstang
JILA, University of Colorado and NIST

The brightness of the sky on a cloudy night as seen at the zenith from the centre of a city has been calculated using a simple model of the city and a uniform cloud layer. The brightness of the centre of the city looking downwards from a satellite has also been calculated. Three methods of dealing with radiative transfer in the cloud have been tried. The brightness is primarily a function of the optical thickness of the cloud layer. Illustrative results are presented.

Introduction

Artificial outdoor lighting at night in cities has increased steadily for many years. Some of the light is necessary for human activities. Frequently the amount of light is excessive, and its undesirable effects are often called light pollution. Some of the light travels upwards into the atmosphere, and part of that light is scattered back towards the ground. This scattered light increases the brightness of the night sky on clear nights. A more obvious effect is the illumination of the clouds seen over a city at night. Some of the light penetrates through the clouds and is observed from satellites. It has been suggested that observations of cloud brightness from the ground inside a city and made frequently and over long periods might be a possible way of monitoring the growth of light pollution by residents in a cloudy climate. There do not seem to have been any previous measurements or calculations of cloud brightness over cities at night as seen from the ground, except in the case of a point source. There have been improvements to the light-pollution calculations valid for clear or hazy nights. For example, Kerola[1] successfully included polarization in his calculations. For our present purpose we felt that our original method of making approximate calculations of the upward light from a city and the resulting scattering of light downwards would be adequate if it were supplemented by adding approximate reflectivity and transmissivity calculations for the clouds. This paper combines these two aspects of the problem. The brightness as seen from a satellite has also been computed. Calculations have been performed to try to assess the importance of various factors leading to the observed brightness.

The city-light-emission model

The present author[2–4] devised a model of the light emitted by a city that has been very successful in calculations of the effect of a city on the brightness of the night sky at relatively distant observatories. The original model was not designed to work when the observer was inside the city, but it has been modified for this purpose. In this work the flat-Earth model is used; corrections due to the curvature of the Earth are neglected because they are only significant for distances of more than 50 km from a light source. In addition, a single exponential function is used in representing the molecular density of the air. The city is initially treated as a uniformly illuminated circle of radius R. The light emission is assumed to be proportional to the population (P) of the city. A fraction ($1–F$) of the light emitted shines down from the luminaires and then some fraction of that is reflected upwards to the clouds, mainly by road surfaces. An average ground reflectivity (rg) is assumed, based on road-surface reflectivities, with a Lambert distribution of the reflected light. An additional fraction (F) of the emitted light arises from light sources that are not well shielded, from which light escapes upwards and reaches the clouds. We used an empirical distribution of F that put most of the upward light directed at low angles to the horizon, and no light towards the zenith. To make things simpler we assume that the observer is at the centre of the city and observes light being scattered straight downwards from the zenith. This is a very convenient simplification because the symmetry allows the use of cloud models in which the azimuthal average intensities can be used. We also assume that the brightness above the clouds is observed from a satellite looking vertically downwards towards the city centre. For brevity we refer to these as 'city centre' and 'satellite'.

The input data for the model consists of P and R. The altitude, h, of the city above sea level can also be input if needed: it can usually be assumed to be zero for cities less than 300 m above sea level. We assume an emission of light proportional to the population, and in our older work we assumed 1000 lumens per head for visual observations. We have increased this because the levels of outdoor lighting are increasing, and Wim Schmidt (private communication) of Utrecht suggested to me that 1200 lumens per head would be better for the Netherlands and Germany. We adopted his value in our calculations. It is equivalent to a photon emission $phv = 4{\cdot}1 \times 10^{18}$ photons per second per capita in the V band. Our calculations are based on V-band photometry, and our brightness results are converted to cd/m^2. Other spectral regions could be studied by using appropriate photon intensities as input and modifying the extinction parameters in our programs. We used a fraction $F = 10\%$. The fraction F going upwards can be varied, and might be lowered to 5% or less in cities that have very tight light-pollution-control ordinances. In the usual absence of better information we assume that the reflectivity of the ground $rg = 0{\cdot}15$ for normal conditions. This can be increased to $0{\cdot}6$ for snow conditions if there has been some snow-plough activity that darkens the roads, and one might use $0{\cdot}8$ for fresh snow. Radiation reflected downwards from the clouds is reflected upwards again with the same ground reflectivity. The model takes into account Rayleigh scattering by molecules and scattering by aerosols. A parameter (K) is included in the model to allow for the clarity of the atmosphere: K is essentially the ratio of aerosol to molecular scattering, normalized so that $K = 1$ corresponds to standard sea-level visibility; $K = 0{\cdot}5$ is better for very clear air. The clouds are treated as a uniform plane-parallel horizontal layer having a cloud base at an altitude, H, that can be

prescribed, and an assumed total optical depth, $\tau^\star$. The intensity of light scattered downwards by the atmosphere is calculated by integrating first over the area of the city for an element of atmosphere at a given height above the observer, starting from the ground and continuing along the vertical from the observer upwards until the cloud base is reached. This gives the contribution to the observed brightness caused by city light scattered by the atmosphere between the ground and the cloud base. When the cloud base is reached the light intensity from a small area of the city reaching the cloud base immediately over the observer is calculated, the cloud reflectivity is used to calculate the downward intensity reaching the observer, and the result integrated over the city area. Similar calculations give the intensity emerging vertically upwards from the cloud. All calculations include the extinction of light along its upward and downward paths. When needed in calculations on light emerging from the top of the cloud, we used a calibration based on work by Slingo[5] that the geometric thickness of the cloud layer may be estimated as $0{\cdot}01\tau^\star$ km. For small cloud optical depths some city light can penetrate the cloud, be scattered by the atmosphere above the cloud, and pass downwards through the cloud to the city centre. We have made rough estimates of the intensity of this light and added them to our results when they are significant, which is only for optical depths $\tau^\star < 5$.

It is convenient to define a *standard city*. In the remainder of this paper this is defined as having $P = 1$ million, $R = 10$ km, $h = 0$, $rg = 15\%$, $F = 10\%$, and $phv = 4{\cdot}1 \times 10^{18}$ photons per second per capita in the photometric V band. $K = 1$ has been used throughout this paper. To examine the effects of city size we have used $P = 100\,000$ and $R = 3{\cdot}162$ km, and $P = 10\,000$ and $R = 1$ km, with the radii chosen to give the same population density of 3183 km^{-2} in each case. The other parameters used were as for the standard city unless otherwise stated. It should be noted that the population density of cities varies over an enormous range. For example, it is about 10 000 km^{-2} in New York and 320 km^{-2} in Oklahoma City. Population estimates are usually available, realistic estimates of radii are not. Anyone who desires to do calculations for a particular city should make a realistic estimate of the radius from maps and so avoid the situations when a city has incorporated large surrounding areas of low population that contribute little to light pollution, such areas being included in published values of city areas.

The scattering phase function for water droplets

When starting a calculation, the values of the altitude, H, of the cloud base must be prescribed with an assumed total optical depth, $\tau^\star$. Then one must calculate values for the reflectivity and transmissivity of a cloud layer from a suitable model. The principal problem in dealing with radiative transfer in a cloud is the very strong forward-scattering peak in the scattering phase function $P(\cos\Theta)$ for water droplets. Here Θ is the angle between an incoming light ray and an outgoing scattered ray. Although $P(\cos\Theta)$ is a very complex function the simple expression $P(\cos\Theta) = 1 + 3g\cos\Theta$ was shown by Shettle & Weinman[6] to be a valid approximation when used in the Eddington radiative-transfer method. The parameter g is the average value over the whole solid angle of $\cos\Theta$ weighted by $P(\cos\Theta)$, and is called the asymmetry factor. Fritz[7], Hansen[8], and others omitted the forward-scattering peak by just truncating it. Several more elaborate approaches have been made to this problem. Potter[9] treated the sharp peak as a Dirac delta function $\delta(1 - \cos\Theta)$, and this has become a very useful method. The scattering function P for larger angles (greater than about 15°) is extrapolated back to zero

angle of scattering. The photons in the sharp peak remain in the delta function until they are scattered by the extrapolated function. In later work the normalized phase function is written

$$P(\cos\Theta) = 2f\,\delta(1-\cos\Theta) + (1-f)(1+3g'\cos\Theta). \qquad (1)$$

Here f is the fraction of the photons that are included in the forward-scattering peak represented by the delta function. We truncated the phase function by omitting the high peak and extrapolating the function from $\Theta = 15°$ back to $\Theta = 0°$. The asymmetry factor g' is the asymmetry factor for the truncated phase function (omitting the delta function). We adopted the phase function given by Twomey *et al.*[10]. They used a Mie-scattering phase function for a mean drop radius of 4·3 microns at a wavelength 550 nm. They used conservative scattering applied to clouds with a liquid water concentration of 0·30 g m^{-3}, extinction coefficient 73 km^{-1}, and single-scattering coefficient $\omega = 1$. For similar clouds with absorption added they used an absorption coefficient 0·089 km^{-1}, and this is equivalent to a single-scattering coefficient $\omega = 0{\cdot}9988$. To simplify the calculations for our personal computer we represented the phase function (without the peak) by four exponential functions covering the Θ ranges 0–100, 100–135, 135–150, and 150–180 degrees. We calculated the values of $g = 0{\cdot}851$ and $g' = 0{\cdot}733$ for the original function and for the truncated function. We followed Joseph *et al.*[11] and imposed the condition that $P(\cos\Theta)$ from Eq. (1) has the same asymmetry factor as the original $P(\cos\Theta)$ function so that $g = f + (1-f)\,g'$ which then gives $f = (g-g')/(1-g')$. This corresponds to Mie scaling, and replaces Eqn. (2b) in Joseph *et al.*[11], which used Henyey–Greenstein scaling. It gives $f = 0{\cdot}443$. We checked this value by integrations of the original and of the truncated phase functions. We made no use of Henyey–Greenstein scaling in our work.

Cloud reflectivity by the Delta–Eddington approximation

Perhaps the simplest model to use for the cloud layer is the solution of the radiative-transfer equation by the Eddington approximation, as described by Shettle & Weinman[6]. A somewhat more elaborate model is the Delta–Eddington model, obtained by combining the Eddington approximation with the Dirac delta function approximation to the scattering function described above. The details may be found in Joseph *et al.*[11]. Those authors were interested in the case of the Sun shining on an infinite plane layer of uniform cloud. In that case the light source and the ground are on opposite sides of the cloud. We are interested in city light shining upwards. In this case the light source and the ground are on the same side of the cloud. The basic mathematical solutions still apply to our problem, but we must derive new boundary conditions. We chose to work in the first instance with a ground having zero reflectivity and later correct for ground reflectivity. In this situation the two boundary conditions for our problem are (*i*) there is no diffuse radiation entering the cloud from its top, and (*ii*) there is no diffuse radiation entering the cloud from its bottom. (The direct beams of light from the city do not contribute to the upward diffuse flux.) We take the optical depth of the cloud as increasing upwards from zero at the bottom of the cloud. Joseph *et al.*[11] showed that if we rescale the optical depth so that $\tau' = (1-\omega f)\,\tau$, rescale the single-scattering coefficient ω by $\omega' = (1-f)\,\omega/(1-\omega f)$, and use g' instead of g, the simple Eddington solutions can be used. We drop the primes but remember that we use scaled variables throughout. The scaled optical thickness of the cloud layer is $\tau_0 = (1-\omega f)\,\tau^{\star}$.

The solution for the intensity of radiation at angle μ can be written as $I(\tau, \mu) = I_0(\tau) + I_1(\tau)\mu$, where $\mu = \cos\theta$ and θ is the angle of the light beam relative to the upward normal, $\mu > 0$ for upward light and $\mu < 0$ for downward light. I_0 and I_1 are functions of the optical depth in the cloud. The equations refer to a total incident flux πF per unit cross-sectional area of the incident beam incident at an angle $\cos^{-1}\mu_0$ to the normal to the cloud layer. There are two cases. If the single-scattering coefficient of the water droplets in the cloud is ω, then $\omega = 1$ for conservative scattering with no absorption by the water droplets, and $\omega < 1$ when absorption by water droplets in the cloud is to be included. A simple solution exists for conservative scattering. A more complex solution is required in the non-conservative case when $\omega < 1$. In each case the two boundary conditions for our particular problem must be applied. The resulting boundary-condition equations replace Shettle & Weinman's[6] equations (17a) and (17b).

It was important to correct for the effects of the ground. This can be done in two ways. The boundary condition at the bottom of the cloud can be modified to include the diffuse radiation reflected upwards from the ground. Alternatively the method of Chandrasekhar[12] can be modified. We chose his method. His algebra was worked out for the planetary problem in which the Sun shines on the top of the atmosphere and the ground is below the atmosphere. We developed the algebra for the case when the light source (the city) and the ground are on the same side of the clouds. This gave a pair of equations which replace two of his[13] equations. In addition, Chandrasekhar assumed certain reciprocity relationships which do not hold for our approximate solutions of the radiative-transfer equations. Our scattering functions for radiation incident at μ_0 are defined as $S(\mu,\mu_0) = 4\pi I(0, \mu)/F$ with $\mu < 0$ for radiation emerging from the bottom of the cloud and $T(\mu, \mu_0) = 4\pi I(\tau, \mu)/F$ with $\mu > 0$ for radiation emerging from the top of the cloud. Then the effect of the ground depends on integrals of S and T that can be evaluated numerically in the computer program. Some direct light, which has been diffusely reflected from the ground, penetrates the cloud without being scattered. This must be added to the intensity seen above the cloud. It is not important for clouds with total optical depth greater than about 10.

For our purposes we need to put the appropriate values of the various parameters into the equations and calculate $I(0, \mu)$ and $I(\tau_0, \mu)$ as a function of μ. We use these as the angular reflectivity and transmissivity in our city model and calculate the total intensity reaching the observer from his zenith.

Cloud reflectivity by Twomey's matrix integration method

A method which starts from a very thin layer and repeatedly increases the layer thickness was described by Twomey *et al.*[14]. The intensities are calculated for a discrete set of emergent directions μ_i and a set of discrete incident directions μ_j, with i and j ranging from 1 to 10. The reflection matrix $\mathbf{S}(\mu_i, \mu_j)$ and the diffuse transmission matrix $\mathbf{T}(\mu_i, \mu_j)$ are calculated for a thin layer in which it may be assumed that only single scattering need be taken into account. Matrix equations were derived for the derivatives $\partial\mathbf{S}/\partial\tau$, $\partial\mathbf{T}/\partial\tau$, $\partial^2\mathbf{S}/\partial\tau^2$, and $\partial^2\mathbf{T}/\partial\tau^2$. These were integrated numerically at steps of constant $\Delta\tau$. This is essentially adding a large number of thin layers of equal thickness rather than a thickness-doubling procedure. The angular distribution of radiation was discretized in directions at angles θ to the normal to the layer given by $\mu = \cos\theta = 0{\cdot}05\ (0{\cdot}10)\ 0{\cdot}95$. Twomey *et al.* also stressed the importance of maintaining the normalization of the phase function to preserve flux conservation, and developed a sophisticated

method of achieving this in their initial thin layer. Twomey *et al*[10] carried out the method in detail. They presented results valid for optical depths greater than about 10. We used this method only for a few calculations and we will not discuss further details.

Cloud reflectivity by the doubling method

It seemed desirable to do some calculations by at least one other method. The doubling method was chosen. There is a large literature on the method, which was invented by H. C. van de Hulst, and developed by him and K. Grossman[15], J. E. Hansen[16], and J. F. Potter[9]. Grant & Hunt[17,18] gave an elaborate formulation of the basic theory. In their first paper they developed the interaction principle. This expressed the radiative intensities emerging from the top and bottom of a layer of cloud of infinite horizontal extent and uniform thickness as linear functions of the incident intensities on the top and bottom of the layer and of the radiative sources within the layer. They derived formulae for doubling the thickness of a layer. In their second paper[18] they discussed the required normalization of the phase function to ensure flux conservation. They also showed how the requirement of non-negativity of the reflection and transmission coefficients leads to an upper limit on the size of the thickness of an initial layer (their equation 3·8).

We used an implementation by Wiscombe[19,20]. This was designed primarily to study radiation fluxes, and used azimuth-averaged intensities. This method is particularly suitable for the present problem because we chose to calculate the cloud brightness at the zenith for an observer at the centre of the circular-city model, and this involves intensities which do not depend on azimuth. Wiscombe[20] considered reflection matrices $r_n(2^n\Delta\tau)$ and transmission matrices $t_n(2^n\Delta\tau)$, where $\Delta\tau$ is the optical depth of an initial thin layer, and the thickness has been doubled n times. The incident intensities are angularly discretized using m directions (we used $m = 10$) so that r_n and t_n are $m \times m$ matrices. They give the reflected and transmitted intensities from any incident direction into any emergent direction. Relationships based on the interaction principle of Grant & Hunt[17] were derived connecting r_{n+1} and t_{n+1} with r_n and t_n. Wiscombe developed a matrix form of the equation of radiative transfer. He discussed several ways of calculating the initial values $r_0(\Delta\tau)$ and $t_0(\Delta\tau)$ for the initial thin layer. He emphasized the importance of renormalizing the phase function of scattering to ensure conservation of flux, and gave a method due to Grant for doing the renormalization (ref. 20, Section 6); we used Wiscombe's equations (1), (3), (10), (11), and (12). The calculations require an azimuthally-averaged scattering phase function. We used the same function as we used in the Delta–Eddington method described above. In both the Delta–Eddington method and the doubling method the diffuse–direct flux separation is made in the equation of radiative transfer. In addition to any incident diffuse radiation, the city light enters the cloud as direct radiation. This travels in straight lines through the cloud layer. A fraction $\{1 - \exp(-\tau_0/\mu_0)\}$ of the light travelling in direction μ_0 is scattered in the cloud, and becomes part of the diffuse radiation. The remainder (which may be negligibly small) passes through the cloud and emerges unscattered. The direct–diffuse separation requires the introduction of source functions Σ^+ and Σ^- into the doubling formulae. Readers are referred to Wiscombe[19] (his eqns. (3) and (16); note that his eqn. (4) is not relevant in our problem) for the formulae and their derivation.

Units

The units used in this paper are in wide use in the lighting community but are not familiar to most astronomers. For clarification we note that the sky brightness V in mag/arcsec^2 for a brightness b in cd/m^2 is given by $V = 12{\cdot}60 - 2{\cdot}5 \log_{10} b$. Thus $b = 0{\cdot}1$ cd/m^2 is $V = 15{\cdot}1$ mag/arcsec^2. For a pristine mountain observatory, $V = 22$ mag/arcsec^2 corresponds to about $b = 0{\cdot}00017$ cd/m^2. For a daytime bright blue sky b is roughly 3000 cd/m^2. Thus for a large city the clouds can be roughly 1000 times as bright as the pristine night sky, and roughly 10 000 times fainter than the blue daylight sky. For observations from satellites a brightness of 1 cd/m^2 in the V band is equivalent to $0{\cdot}0137$ watts/m^2/sr/μm, where we have used the band width of the V band (90·6 nm). A city with a brightness of $0{\cdot}12$ cd/m^2 would give $1{\cdot}6 \times 10^{-3}$ watts/m^2/sr/μm. The *DMSP* satellites[21] when in their reduced-sensitivity range covered the intensity range $1{\cdot}57 \times 10^{-5}$ to $3{\cdot}17 \times 10^{-3}$ watts/m^2/sr/μm. This confirms that the system was not saturated by the light from cities. Detailed discussion of observations from satellites is outside the scope of this paper.

Results

Before starting a long series of calculations I wanted a check on my work to ensure that no major factor had been forgotten. There is a relatively compact area about 8 km from the centre of Boulder, Colorado, called Gunbarrel. It is partly inside and partly outside Boulder city limits. I estimated $P \approx 12\,000$ from census data and $R \approx 1{\cdot}4$ km from a local map. I ran the doubling method with cloud absorption for this area with cloud thicknesses $\tau^\star = 40$, 20, and 10. The results were, respectively, $0{\cdot}076$, $0{\cdot}058$, and $0{\cdot}034$ cd/m^2. Nancy Clanton, a lighting consultant who works in Gunbarrel, agreed to make a measurement. She obtained $0{\cdot}04$ cd/m^2, the accuracy being limited by her photometer. I felt that this was rough confirmation that I had no gross errors in my basic modelling.

It was necessary to fix the range of values of the total optical depth of the clouds for which calculations would be performed. Izakova *et al.*[22] made a study of the optical depths of stratocumulus cloud layers at the Meteorological Observatory of Moscow State University. In the visible spectral region they found that the optical depths on 279 occasions in the years 1980 to 1990 varied between the extremes of 2 and 170, with an overall mean of 46. Calculations have usually been performed for optical depths $0{\cdot}1$, $0{\cdot}2$, $0{\cdot}5$, 1, 2, 5, 10, 20, 40, 80, 160, and 320. The height of the cloud base above the ground has usually been assumed to be 1000 metres, but 2000 or 3000 metres have sometimes been used.

Table I shows results for calculations by the three methods described in this paper. Results are shown for no absorption ($\omega = 1$) and for $\omega = 0{\cdot}9988$, for an observer at the city centre and for observation from a satellite. (The value of ω was chosen so that our absorption coefficient would agree with that adopted by Twomey.) The results give an idea of the uncertainties in the calculations and an idea of the effects of allowing for absorption in the clouds. We have made many calculations by the Delta–Eddington method and by the doubling method. The doubling method is more accurate because it does not use the simple solutions of radiative-transfer theory, and we have used it in most of the results that we publish in this paper.

Fig. 1 shows the sky brightness for our standard city with $P = 1\,000\,000$ and $R = 10$ km as a function of the total optical depth of the cloud layer. Curve 1 is

TABLE I

*Brightness of clouds in cd/m² for standard city**

	ω	*Delta–Eddington*	*Twomey*	*Doubling*
City centre	1	0·244	0·181	0·209
City centre	0·9988	0·228	0·164	0·176
Satellite	1	0·0459	0·0423	0·0500
Satellite	0·9988	0·0376	0·0324	0·0300

*Standard city parameters used. The results by three methods are compared.
The differences between results with no absorption in the clouds ($\omega = 1$) and with absorption ($\omega = 0{\cdot}9988$) are shown for clouds with optical depth $\tau^\star = 40$ and cloud-base height 1 km.

for observations from the city centre and curve 2 is for observations from a satellite. In both cases the calculations assumed no absorption ($\omega = 1$). The brightness seen at the city centre increases steadily from a small value (light reflected by clear air) as the optical depth of the clouds increases and reaches a maximum for large cloud optical depths. The brightness of a large city seen by a satellite is a maximum for small $\tau^\star$, typically $\tau^\star \approx 2$. The thin clouds give some light scattering upwards beyond what would be seen from a city without any clouds. For large optical depths the brightness decreases because most of the city light is reflected downwards. To show the effects of absorption, curve 3 for the city centre and curve 4 for a satellite used the same parameters as curves 1 and 2 except for

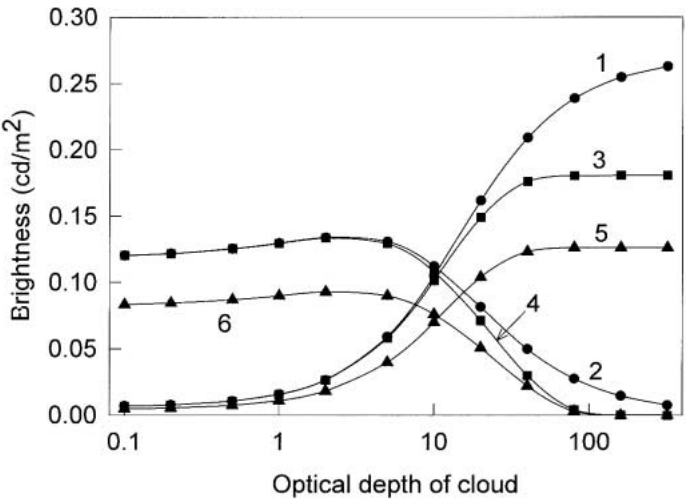

FIG. 1

The night sky brightness for a city with $P = 1\,000\,000$ on a cloudy night as a function of the optical depth of the cloud. Curves 1, 3, and 5 are for the zenith as seen from the city centre, curves 2, 4, and 6 are for a satellite looking vertically downwards towards the city centre. Curves 1 and 2 are for clouds with no absorption. Curves 3 and 4 are for clouds with absorption determined by the single-scattering coefficient $\omega = 0{\cdot}9988$. Curves 1, 2, 3, and 4 assume a city radius $R = 10$ km. Curves 5 and 6 assume a city radius $R = 12$ km and $\omega = 0{\cdot}9988$. All calculations used the doubling method.

$\omega = 0{\cdot}9988$. It is seen that absorption is important for $\tau^{\star} \geqslant 20$. The maximum brightness in curve 3 is less that that in curve 1 because of the absorption in the clouds. Curve 5 for the city centre and curve 6 for the satellite are calculated for the standard city except that the radius was changed to $R = 12$ km. The differences between curves 3 and 5 and between curves 4 and 6 are appreciable. The differences arise because in the larger city the population is farther from the city centre. This illustrates that for light-pollution calculations, with or without clouds, some effort must be made to get a good estimate of R.

Fig. 2 shows (curves 1 and 4) the city centre and satellite brightnesses for our standard city. Curves 2 and 5 are for the standard city except that $P = 100\,000$ and $R = 3{\cdot}162$ km. Curves 3 and 6 are for the standard city except that $P = 10\,000$ and $R = 1$ km. The radii give a constant population density 3183 km^{-2}. All calculations used the doubling method with $\omega = 0{\cdot}9988$. The differences from our standard city are not large considering that a factor 100 in population is involved. This is because for the larger cities a major part of the population is at larger distances from the centre of the city and in addition much of the light is incident on the cloud layer at larger angles to the vertical, at which the reflectivity is low. This illustrates that lights relatively close to the observer mainly determine the brightness of the clouds. This conclusion is more or less obvious and would also apply to observers well away from the city centre observing at their zeniths. Reduction in the population by a factor 10 only reduces the brightness for the smallest city (curve 3) by a factor 2 compared to the city with $P = 100\,000$ (curve 2).

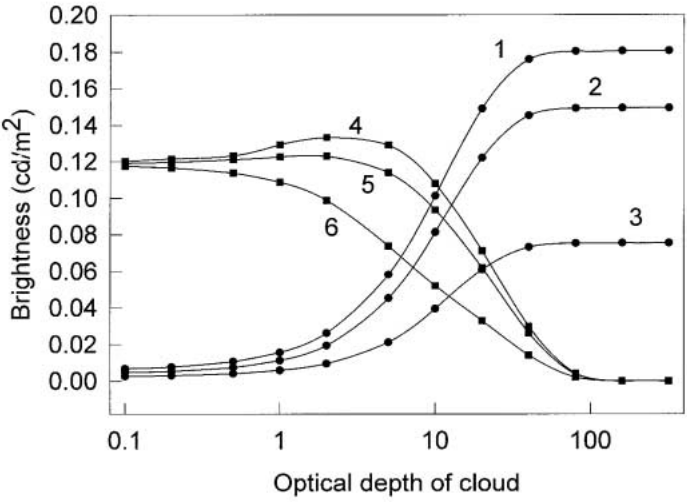

FIG. 2

Brightness of a cloud at night caused by a city. Curves 1, 2, and 3 are for observations towards the zenith for an observer at the centre of the city. Curves 4, 5, and 6 are for observations from a satellite looking vertically downwards towards the centre of the city. Curves 1 and 4 are for our standard city with $P = 1\,000\,000$ and $R = 10$ km, curves 2 and 5 are for our standard city except that $P = 100\,000$ and $R = 3{\cdot}162$ km, and curves 3 and 6 are for our standard city except that $P = 10\,000$ and $R = 1$ km. All the curves show the primary effects of different populations; the three cities have the same population density, 3183 km^{-2}. All calculations used the doubling method with $\omega = 0{\cdot}9988$.

All the calculations shown in Fig. 2 were for cities that have a population density ($P/\pi R^2$) = 3183 km^{-2}. Calculations were done for P = 1 000 000 and various values of the radius R from 7 to 18 km, which cover population densities 980 to 6500 km^{-2}. The brightness seen from the city centres was found to be very nearly proportional to the population density. This relationship holds only for very large cities.

The sensitivity of the results to the values of several parameters was examined. The light emission per capita has been assumed to be equivalent to 1200 lumens. This emission occurs linearly in the equations in our model, so our results can be easily adjusted for some other light emission rate. Table II shows the effect of different cloud-base heights. The brightness is reduced for larger cloud-base heights. Table II also shows the effect of shielding the city lights so that they give no direct radiation (F = 0) above the horizontal. (Upward light from road reflections is only slightly affected.) The conclusion is that while better shielding of city lights helps darken the night sky it cannot by itself give a major darkening of the sky as seen from the city. (This conclusion does not apply to mountain observatories, at which any value $F \neq 0$ from a distant city contributes to light pollution at the observatory.)

Table III shows the effects of ground reflectivity. Our usual assumption is rg = 15%, which is a compromise for roads and ground comprised of an unknown mixture of various materials. Fresh, dark asphalt has a reflectivity about $rg \approx 8\%$.

Table II

Effect of cloud-base height and well-shielded lights on brightness of clouds (in cd/m²) *

	F	*Cloud-base height (km)*		
		1	*2*	*3*
City centre	10%	0·176	0·149	0·131
Satellite	10%	0·0300	0·0291	0·0272
City centre	0	0·138	0·125	0·116
Satellite	0	0·0257	0·0257	0·0253

*Standard city parameters except for rows which had F=0.
Doubling method used. Clouds: τ^*=40, ω=0·9988.

Table III

Effect of ground reflectivity on brightness of clouds (in cd/m²) *

	Population	*Ground reflectivity (rg)*			
		8%	*15%*	*60%*	*80%*
City centre	1 000 000	0·110	0·176	0·934	1·81
Satellite	1 000 000	0·020	0·030	0·121	0·191
City centre	10 000	0·038	0·073	0·453	0·871
Satellite	10 000	0·0076	0·014	0·065	0·101

*Table shows the effects of ground reflectivity. rg=8% is for dark roads, 80% for fresh snow, 60% for snow after many roads ploughed.
Doubling method used. Clouds τ^*=40, ω=0·9988.
Standard city parameters except for rg values and where P=10 000, R=1 used.

In Table III we show the effects of $rg = 8\%$. As one might guess, it would nearly halve the cloud brightnesses. There is little chance that a large part of a city would change its road surfaces, so major reductions in *rg* are unlikely. Table III also shows the other extreme, for snow on the ground, where we guess the reflectivity $rg = 80\%$ for freshly fallen snow and $rg = 60\%$ after many of the roads have been snow-ploughed.

There are of course many uncertainties in the light-pollution model. The assumption of a uniformly illuminated circular city is the obvious first model to try. An actual city has a mixture of brighter (*e.g.*, shopping centres, main highways, and sports facilities) and darker areas (mostly residential areas). It would require very large calculations to model accurately even for a single city, might be impracticable to do it for many cities, and in any case it probably would not be worthwhile. The need in light-pollution studies for a whole city is for measurements on an area with relatively stable lighting. There are uncertainties in the atmospheric model (the use of a single exponential density function and the use of a single parameter to represent the aerosol content of the air). However, all the calculations in this paper required an integration over the area of the city, done over the radius *r*. It was possible to introduce a city illumination which was a function of *r*. Several functions were tried. For example, the brightness of the annulus $(R - 0{\cdot}5, R)$ was doubled and the remainder unchanged. This gave the contribution of this annulus to the total, and division by the area of the annulus gave the contribution per sq. km. This was used to get estimates of the contribution of sources near the edge of the city. Similar calculations for different annuli gave estimates of the contributions from different distances from the city centre. For larger cities the contributions from sources such as parking lots near the edge of the city have little effect on the brightness seen at the centre. The effect of a bright superhighway through a large city would be unimportant unless it passes less than a few kilometres from the observer. Observations from close to a city centre would seem to be the most useful for light-pollution modelling.

As a final item of interest we calculated the brightness at the city-centre zenith and downwards from a satellite at full moon. We used the Delta–Eddington method in the form appropriate to the solar case when the source and ground are on the opposite sides of the cloud. The values of μ_0, the cosine of the zenith distance of the full moon at its highest point in the sky, can vary between about 0·98 and 0·93 in Boulder, and between 0·91 and 0·82 at latitude 53°. We used $\mu_0 = 0{\cdot}9$. We assumed that full moon has apparent magnitude $V = -12{\cdot}74$, that one $V = 0$ star outside the atmosphere gives $2{\cdot}54 \times 10^{-10}$ lumens/cm^2, and that 1 lumen $= 4{\cdot}13 \times 10^{15}$ photons/second. This leads to a lunar photon emission of $1{\cdot}31 \times 10^{11}$ photons/second/cm^2 in the beam of light reaching the Earth. Our results are shown in Fig. 3. Curve 1 is the brightness seen from the city centre and curve 2 the brightness from a satellite at full moon. The maximum in curve 1 arises because the scattering of moonlight towards the observer increases as the clouds become thicker, but eventually the brightness decreases because for thick clouds most moonlight is reflected back into space. Curve 2 shows a slight minimum caused by absorption in thin clouds, followed by a high reflectivity for thick clouds. For comparison, curves 3 and 4 show the brightness of a city with $P = 100\,000$ and $R = 3{\cdot}162$ km for city-centre and satellite observations. The assumptions that the Moon is full and near the zenith constitute a worst-case scenario, so that the cloud brightnesses caused by the Moon will usually be much less than we have calculated.

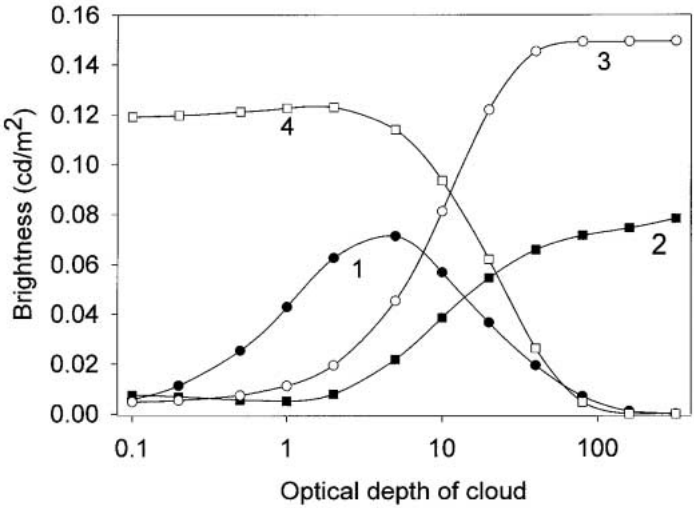

FIG. 3

Brightness of clouds due to full moon (Moon near zenith at $\mu_0 = 0{\cdot}9$): curve 1 as seen in the zenith direction from the ground, curve 2 as seen from a satellite looking vertically downwards. For comparison with the brightness of a city without moonlight, curve 3 shows the brightness of a city with population 100 000 and radius $3{\cdot}162$ km seen at the zenith from the centre of the city and curve 4 as seen from a satellite looking vertically downwards at the city centre. An observer at the centre of this city on a night of full moon would see a brightness given by adding curves 1 and 3; an observer looking downwards from a satellite would see a brightness given by adding curves 2 and 4.

The lack of detailed knowledge of the properties of the clouds on any night, and especially their optical thickness, means that one must resort to statistical studies. The suggestion has been made that monitoring of the light pollution of an individual city could be done by making measurements of the night-sky brightness over the city on numerous nights covering a period of many years. The above studies show that while this is possible in principle there are so many factors that are not known that extensive observations would be needed. If sufficiently sensitive photometric equipment were available at a price that amateur astronomers would be willing to afford, these extensive studies on individual cities would be possible. The prospects do not seem promising for this to become a widely-adopted approach to light-pollution monitoring.

Acknowledgements

I am indebted to Wim Schmidt and Robert Stencel for correspondence and discussions of the problems of cloud brightnesses. I thank Nancy Clanton and Randi Herman for a measurement of the night-sky brightness at Gunbarrel. I found Wiscombe's[20] (his Appendix A) advice on matrix computing very helpful in programming his method for my personal computer. I am grateful to the referee for a very careful reading of the manuscript and for many suggestions, most of which have been incorporated in the paper.

References

(1) D. X. Kerola, *MNRAS*, **365**, 1295, 2006.
(2) R. H. Garstang, *PASP*, **98**, 364, 1986.
(3) R. H. Garstang, *PASP*, **101**, 306, 1989.
(4) R. H. Garstang, *PASP*, **103**, 1109, 1991.
(5) A. Slingo, *J. Atmos. Sci.*, **46**, 1419, 1989.
(6) B. P. Shettle & J. A. Weinman, *J. Atmos. Sci.*, **27**, 1048, 1970.
(7) S. Fritz, *J. Meteor.*, **11**, 291, 1954.
(8) J. E. Hansen, *J. Atmos. Sci.*, **26**, 478, 1969.
(9) J. F. Potter, *J. Atmos. Sci.*, **27**, 943, 1970.
(10) S. Twomey, H. Jacobowitz & H. B. Howell, *J. Atmos. Sci.*, **24**, 70, 1967.
(11) J. H. Joseph, W. J. Wiscombe & J. A. Weinman, *J. Atmos. Sci.*, **33**, 2452, 1976.
(12) S. Chandrasekhar, *Radiative Transfer* (Oxford University Press), 1950, pp. 269–273.
(13) Ref. (12), p. 273, eqns. (201) and (202).
(14) S. Twomey, H. Jacobowitz & H. B. Howell, *J. Atmos. Sci.*, **23**, 289, 1966.
(15) H. C. van de Hulst & K. Grossman, in J. C. Brandt & M. B. McElroy (eds.), *The Atmospheres of Venus and Mars* (Gordon and Breach, London), 1968, pp. 35–55.
(16) J. E. Hansen, *ApJ*, **155**, 565, 1969.
(17) I. P. Grant & G. E. Hunt, *Proc. Roy. Soc.*, **A 313**, 183, 1969.
(18) I. P. Grant & G. E. Hunt, *Proc. Roy. Soc.*, **A 313**, 199, 1969.
(19) W. J. Wiscombe, *J. Quant. Spectrosc. Radiat. Transfer*, **16**, 477, 1976.
(20) W. J. Wiscombe, *J. Quant. Spectrosc. Radiat. Transfer*, **16**, 637, 1976.
(21) P. Cinzano *et al.*, *MNRAS*, **318**, 641, 2000.
(22) O. M. Izakova *et al.*, *Atmos. Ocean. Phys.*, **30**, 357 (Russian ed. p. 196), 1994.

SIR JAMES JEANS AND THE STABILITY OF GASEOUS STARS

By Alan B. Whiting
University of Birmingham

In 1925 Sir James Jeans calculated that a star made up of an ideal gas, generating energy as a moderately positive function of temperature and density, could not exist. Such stars would be unstable to radial oscillations of increasing size. It appears that the flaw in his calculation has never been clearly explained, especially the physical basis for it. I conclude it lies in an almost offhand assumption made about the form of the temperature perturbation. The episode provides a number of lessons about complicated calculations and their interpretation.

What is a star? The view in 1925

In the first decades of the 20th Century one of the areas of great astrophysical interest and activity was stellar structure. It was fairly clear that the Kelvin–Helmholtz theory of gravitational contraction (which lives on in our terminology of 'early-type' and 'late-type' stars) was inadequate, though its replace-

ment was not immediately available. The theory of relativity promised in principle a sufficiently long-lasting power source through the conversion of mass to energy, but details remained obscure. Using the 19th-Century science of thermodynamics and the 20th-Century theories of radiation, models of gaseous stars were constructed and elaborated, eventually forming the basis of the science of stellar structure as we know it today. But of course it was not clear at the time that such an approach would necessarily work. In fact Sir James Jeans, a major figure in astrophysics, put forward a theory involving liquid stars powered by a form of nuclear fission. A complete treatment of his theory and its fate is, however, beyond the scope of a short paper like this one. Here I intend to treat just one aspect of Jeans' work: his calculation that gaseous stars were unstable.

With the benefit of hindsight we can say that Jeans' calculation must have been in error. There are several possible explanations, from simple mistakes in algebra to new physics that was simply unknown in 1925. My initial aim in this study is to determine where Jeans' error lies, and especially whether it could have been detected using methods and knowledge available to him. Subsequently I will examine some of the implications of the episode for the practice of mathematical model building and for the process of science. It is possible to make many more connexions between Jeans' ideas and subsequent work, but for limitations of space I will maintain the focus on his calculation and things having a direct bearing on it.

Jeans' analysis

Jeans[1] presented his results in a *Monthly Notices* paper in 1925, but I will use as a reference the revised version[2] published in book form a few years later. The relevant parts are sections 105–111, found on pages 117–125. I will outline them here, referring the reader to the original for the details.

Jeans begins by writing the equation of motion for a shell at radius r within a star, supported by pressure and held together by gravity:

$$\frac{d^2r}{dt^2} = -\frac{1}{\rho}\frac{d}{dr}\left(p_G + \frac{1}{3}aT^4\right) - \frac{\gamma M_r}{r^2}, \tag{1}$$

where ρ is the mass density, p_G the gas pressure, a the radiation constant, T the temperature, γ Newton's constant, and M_r the mass within the radius r. Next Jeans accounts for energy raising the temperature of the material, doing pressure–volume work, being generated by some process as yet unspecified, and flowing out and in:

$$\rho C_v \frac{dT}{dt^2} - \left(p_G + \frac{1}{3}aT^4\right)\frac{1}{\rho}\frac{d\rho}{dt} = \rho G - \frac{1}{r^2}\frac{d}{dr}(r^2 H), \tag{2}$$

where C_v is the heat capacity of the material, G the rate of generation of energy per unit mass, and H the radiant energy flux.

Next the model is made more specific by assuming something like an ideal gas,

$$p_G \propto T\rho^{1+s}, \tag{3}$$

where s may be used to parametrize departures from ideal-gas behaviour; and an opacity similar to that of Kramers' expression,

$$k = \frac{c\mu\rho}{T^{3+n}}, \tag{4}$$

with k the coefficient of opacity, μ the molecular weight of the material, and c the speed of light. If $n = 1/2$ a Kramers opacity is recovered. Assuming an Eddington grey atmosphere, this expression allows us to write the equilibrium radiation flux H in a useful form.

Jeans assumed an energy-generation law in which

$$G \propto \rho^{\alpha} T^{\beta} \tag{5}$$

and, for convenience in notation, introduced λ as the ratio of gas pressure to radiation pressure.

To this point Jeans has built a star almost as one would do today. It is of course much simpler than the models one builds nowadays on a computer, but there should be nothing inherently unstable about these simplifications.

The next step is the stability analysis. The general problem of stability for a system as complex as this is difficult and complicated to treat analytically. Through various relations and assumptions Jeans reduced the problem to that of the perturbation in size, δr; and assumed a particular form of perturbation, a proportional change in radius (so that $\delta r/r_0$ is constant with radius). This still left too many terms in $\delta T/T_0$, so Jeans assumed also that it was constant with radius; that is, there was a proportional heating or cooling everywhere. I think this is a very important assumption, though it does not seem to have excited any comment before now.

With these assumptions and simplifications made, Jeans obtained the master equation of stability:

$$\begin{aligned} &\frac{d^3}{dt^3}\,\delta r \;+\; \frac{(7+n-\beta)G_0}{C_v T_0}\,\frac{d^2}{dt^2}\,\delta r \\ &\quad+\; \frac{\gamma M_r}{r_0^3}\left[\frac{\lambda+4}{\lambda+1}\left(\frac{3p_G+4aT_0^4}{\rho C_v T_0}-1\right)+\frac{3s\lambda}{\lambda+1}\right]\frac{d}{dt}\,\delta r \\ &\quad+\; \frac{\gamma M_r}{r_0^3}\,\frac{G_0}{C_v T_0}\left[\frac{\lambda+4}{\lambda+1}\,(3\alpha+\beta-n)+\frac{3s\lambda}{\lambda+1}\,(7+n-\beta)\right]\delta r = 0. \end{aligned} \tag{6}$$

If one cares to reproduce the algebra, one finds also that Jeans has assumed that λ does not vary with radius, nor C_v. In any realistic star it will, but not so much as to change the qualitative stability.

Equation (6) is a linear equation with constant coefficients (constant with respect to time; in general they may vary from shell to shell) so the solutions will be of the form $e^{\omega t}$. There are three possible values for ω, solutions of the equation

$$\omega^3 + B\omega^2 + C\omega + D = 0, \tag{7}$$

where B, C, and D are the coefficients in Equation (6). Following Jeans we note that any positive ω, or complex ω with a positive real part, denotes instability. Avoiding a real, positive ω gives the condition that D be positive. If we assume a

perfect gas, so $s=0$, this means

$$3\alpha+\beta-n>0. \tag{8}$$

So if the coefficients of energy generation are too small, the star will monotonically shrink or expand. Physically, this means that if compressing the star (say) does not generate enough additional heat to cause the pressure to rise and bounce back, the star keeps on shrinking. This is reasonable, and so far we have no argument with Jeans' calculations.

Avoiding a complex ω with a positive real part is a bit more involved, but if D is positive the condition reduces to

$$BC>D, \tag{9}$$

which means (for $s=0$)

$$(7+n-\beta)\left(\frac{3p_G+4aT_0^4}{\rho C_v T_0}-1\right)>3\alpha+\beta-n. \tag{10}$$

(The expression Jeans gives is a bit different, but in the last step of his derivation he appears to have made a substitution that is true only for critical stability, that is, only when the inequality is an equation. For purposes of finding the critically stable exponents no trouble should have resulted, however.)

Taking Equation (10) together with Equation (8), we find that the fraction in the brackets (something like the ratio of pressure energy to thermal energy) must be greater than unity. For a star in which only gas pressure is important it has the value 3/2, while if radiation pressure dominates it approaches 1. At unity, the two stability criteria together require

$$3\alpha+\beta-n=0, \tag{11}$$

an extremely restrictive condition; if a two-particle fusion reaction is postulated as an energy source so that $\alpha=1$, along with a Kramers opacity, it must go *slower* as temperature increases, and at an exact rate. The situation with a ratio of 3/2 is better, but still a two-particle reaction cannot depend even linearly on the temperature. Jeans' stability criteria exclude essentially all nuclear-fusion reactions as a possible source of stellar energy.

Oscillations and the thermal instability

What is the *physical* cause of Jeans' unstable stars? He interpreted the oscillations of increasing amplitude as being due to the increased heat-energy liberated by the reaction (whatever it is) during the dense phase of the oscillation requiring an expansion of a larger amplitude during the following phase. This is a plausible interpretation, but worth looking at in more detail.

The perturbed energy equation (from Equation 2) is

$$\rho C_v T\,\frac{d}{dt}\left(\frac{\delta T}{T}\right)\;-\;\rho G(\beta-7-n)\;\frac{\delta T}{T}=$$

$$-3\left(C_v T\,\rho^{1+s}+\frac{4}{3}aT^4\right)\frac{d}{dt}\left(\frac{\delta r}{r}\right)-\rho G(3\alpha+7)\,\frac{\delta r}{r}, \tag{12}$$

where the subscript noughts, meaning equilibrium values, have been suppressed for ease of notation. Now suppose we impose a sinusoidal oscillation in $\delta r/r$. The equation may now be thought of as a linear, first-order differential equation in the (proportional) temperature perturbation with a sinusoidal forcing function. The solution will be the sum of sinusoidal terms and the homogeneous solution, which is

$$\frac{\delta T}{T} \propto \exp\left(\frac{G}{C_v T}\,(\beta - 7 - n)t\right). \tag{13}$$

In order for the temperature to stay bounded, $\beta \leqslant 7 + n$. This is not as strict a requirement as Jeans found, but then this is a *different* calculation: we have found the temperature response to a forced radial motion of the star. It still puts an upper limit on the temperature sensitivity of the reaction, and in particular excludes the exponential dependence one expects for nuclear-fusion reactions. Jeans' interpretation is thus shown to be correct. In addition, having a physical source for Jeans' instability allows us to investigate more complicated situations.

Previous identifications of the flaw

For a calculation that appeared to show gaseous, fusion-powered stars impossible, Jeans' work has left very little lasting trace. Chandrasekhar's[3] 1939 work on stellar structure, very extensive in its listing of the literature, does not even mention it directly. He does refer to an unspecified 'belief' in instability resulting from a certain kind of energy-producing reaction (pp. 457, 468), but sees no convincing reason for it. Milne's[4] biography of Jeans describes the calculation in some detail, but as far as criticism notes only (p. 138) that in the calculation he parametrizes departures from the ideal gas laws in two incompatible ways. This does show that Jeans was not terribly interested in specifically how stars might depart from being ideal gases, but then Jeans says just that himself at the beginning of his calculation. At any rate, it has no effect on the stability analysis for ideal-gas stars. (It is possible that Milne thought Jeans' work might be essentially correct; in his description he shows scepticism about the gaseous model.) The much more recent work on pulsating stars by Cox[5] does mention Jeans' calculation (pp. 166 and 172). It is noted as being equivalent to a one-zone model of a star (an important point, and one discussed below), but no analysis of its flaw is given.

What appears to be the accepted answer for the flaw in Jeans' calculation appears in a pair of papers by Cowling[6,7] (the first of which is cited by Chandrasekhar). He pointed out that a proportional change in radius, with $\delta r/r$ constant in space, probably was not a normal mode for a star. Therefore (putting words in his mouth) giving it such a kick would excite a number of normal modes of different frequencies, and the perturbation would not remain a constant proportion. Jeans' perturbation calculation was then not strictly a *stability* determination, in which the star is left to itself after being kicked, but shows a response to a specific kind of forcing.

Cowling had found a flaw in Jeans' work that made its result questionable. But this is not the same thing as showing that the flaw in fact led to the erroneous conclusion. Indeed, it is not immediately clear how a combination of normal motions, each of them individually stable, should be unstable taken together. (More recently, Papaloizou[8,9] has shown that at least for some models of very-high-mass stars, the opposite can happen: mode mixing can stabilize otherwise unstable modes.)

Cowling did go on to impose a proportional radial oscillation on his analysis, and obtained essentially Jeans' result. But because he was dealing with oscillations assumed to be adiabatic or nearly so, the temperature perturbation was automatically of the same form as the radial perturbation; so Jeans' separate assumption about it was implicitly included. It is this assumption concerning the temperature perturbation that I think is the real problem with Jeans' analysis. The next step is to test this idea.

Non-proportional temperature perturbations

The straightforward way to check the effect of this assumption is to relax it. One perturbs Equations (1) and (2) again, this time allowing terms with various derivatives of $(\delta T/T)$ with radius, then collecting everything into a new and more accurate version of Equation (6). In principle it is possible. But instead of requiring one additional equation, the time derivative of Equation (1), and a bit of algebra, one needs nine additional equations and a truly horrible lot of algebra. It is not a practical pen-and-paper exercise and I do not believe Jeans would have seriously considered it.

Even writing down Equation (12) as it appears, with the relaxation of the constraint on the temperature perturbation, is not particularly enlightening. But by making the further assumption that the temperature perturbation is separable, so that

$$\frac{\delta T}{T} = R(r)X(t), \tag{14}$$

the expanded form of Equation (12) can be rearranged into

$$\rho C_v TRX' + \left[-\rho G\,(\beta-7-n)\,R-\left((7+n)\,H+\frac{1}{r^2}\frac{d}{dr}\left(\frac{r^2TH}{dT/dr}\right)\right)R'-\frac{HT}{dT/dr}\,R''\right]X = -3\left(C_vT\,\rho^{1+s}+\frac{4}{3}\right)\frac{d}{dt}\;aT^4\left(\frac{\delta r}{r}\right)-\rho G(3\alpha+7)\,\frac{\delta r}{r}, \tag{15}$$

where primes denote derivatives with respect to the independent variable. If we impose a sinusoidal variation in the radial perturbation as before and consider this an equation for X, we again have a first-order differential equation with a forcing term. This time the coefficients depend on the variation of the temperature perturbation with radius, which we do not know. But some qualitative reasoning about the relative sizes of the R, R', and R'' coefficients shows that the radial change in temperature perturbation need only be a small fraction of the perturbation itself to dominate the stability calculation.

Physically, Jeans' assumption of a strictly proportional temperature perturbation has the effect of pumping heat energy around the star in an unphysical way. It is not a large effect, taking many oscillations to grow significantly (so that the adiabatic assumption of Cowling and many others is a very good one for working out small pulsations), but enough to blow up the star eventually.

On a more abstract level, it appears that the problem with Jeans' analysis lies in ignoring the internal structure of the star, in requiring it to be in some sense a single unit. We may explore this idea with a toy star.

The toy star

Not as a serious mathematical model, but as a way of investigating some of the effects we expect to operate in a real star, I present here a very simple model. (This is similar in motivation and in general to that in Kippenhahn & Weigert[10], pp. 13–15, 235–238, and 407–408, though the details and the application are different.) Suppose we enclose a spherical quantity of ideal gas, of mass m and density ρ, with some mixture of radiation inside a hollow shell of radius r and mass M. The gas mass m is much smaller than M; the shell is supported by the pressure of gas and radiation, and is held in by gravity. Everything is at one temperature T and the surface radiates heat as a blackbody. Inside the shell there is an energy-generating reaction that goes as $\rho^\alpha T^\beta$. The equations of motion and energy balance are thus

$$\begin{aligned} M\,\frac{d^2r}{dt^2} &= -\,\frac{\gamma M_r^2}{r^2} + \left(\rho_G + \frac{1}{3}\,aT^4\right) 4\pi r^2 \\ mG &= mC_v\,\frac{dT}{dt} + \left(\rho_G + \frac{4}{3}\,aT^4\right) 4\pi r^2\,\frac{dr}{dt} + 4\pi r^2\,\sigma T^4. \end{aligned} \tag{16}$$

Perturbing these, the heat-balance equation becomes

$$U\,\frac{d}{dt}\left(\frac{\delta T}{T}\right) = (\beta-4)F_0\,\frac{\delta T}{T} - (\lambda+4)\,\frac{4r}{4c}\,F_0\,\frac{d}{dt}\left(\frac{\delta r}{r}\right) - (3\alpha+2)\,F_0\,\frac{\delta r}{r}, \tag{17}$$

where $U = \rho C_v T$ is the (unperturbed) thermal heat content and $F_0 = 4\pi r^2\,\sigma T^4$ is the (unperturbed) energy radiated away from the surface. The master stability equation is derived as before. The first condition for stability, avoiding a monotonic expansion or collapse, implies

$$3\alpha+\beta-2>0, \tag{18}$$

a lower limit on the energy-generating reaction. The second criterion reduces to

$$(4-\beta)\,(\lambda+4)\,\frac{4rF_0}{3cU} > 3\alpha+2. \tag{19}$$

The fraction can be interpreted as F_0/U, the reciprocal of the time required to radiate away internal heat energy without replacement, times 4/3 the time required for light to go from the centre of the sphere to the surface. For even a toy star the ratio of crossing time to radiative timescale should be very, very small, giving us almost independently of the value of β,

$$\alpha < -\frac{2}{3}, \tag{20}$$

that is, that the energy-generating reaction is required to go *more slowly* with increasing density.

If we look again at Equation (17) and impose a sinusoidal radial oscillation, we find that the temperature-perturbation response is given by a sinusoidal term plus

$$\frac{\delta T}{T} \propto e^{(\beta-4)\frac{F_0}{U}t}, \tag{21}$$

that is, if the energy-generation reaction produces energy faster than it can be radiated away, temperature increases exponentially on a radiative timescale.

Taken together, these results show the toy star behaving in a similar way to Jeans' gaseous stars, and for similar reasons. The energy-generation rate must be sensitive to temperature and pressure, but in an extremely restrictive and unphysical way. Too little sensitivity and the star implodes or explodes monotonically; too much and growing oscillations, due to excess heat energy, tear the star apart.

The stability of gaseous, fusion-powered stars

It is important to keep in mind just what all these calculations have, and have not, proven. Cowling called attention to the fact that (in my words) Jeans' analysis was not strictly a stability calculation, since the required form of perturbation was not a free one. Since he recovered Jeans' result by imposing Jeans' restrictive form of the radial perturbation, he concluded that this was the problem. It is true enough for most purposes, since pulsations are very nearly adiabatic and for those the perturbations are proportional. By focussing on the temperature perturbation I have shown that Jeans' physical explanation for his instability is correct, that is, that each oscillation (of the restricted type) produces more heat energy than steady motion dissipates. I have then shown that even a small departure from a strictly proportional temperature perturbation could plausibly stabilize a forced oscillation, so the physical mechanism that destabilizes a Jeans star does not operate. Thus a full stability analysis using his methods (possible in principle, though not likely in practice) would show that gaseous, fusion-powered stars are stable. Since Jeans' assumptions of the form of temperature and radius perturbations in some sense ignore the structure of the star, I constructed a structureless toy star and found it to be subject to the same kind of instability that Jeans found, thereby lending support to that interpretation.

In all this I have *not* proven the stability of gaseous, fusion-powered stars. Indeed it seems almost certain that such proof is beyond the specific techniques used by Jeans. Cowling[6,7] took a more in-depth approach, depending more on the details of gaseous stars (some of which had not been determined when Jeans wrote). In that sense he was less general; but in allowing any shape to the perturbations he was more general in the more important way. In the end, his work was accepted as the true answer.

It appears that the problem was inherently more complicated than Jeans anticipated, not allowing reduction to a single ordinary differential equation. It was, however, possible for him to see that relaxing the assumption concerning the temperature perturbation could have changed the conclusion, and thus that the calculation was actually inconclusive.

Lessons for mathematical modelling and the progress of science

Out of all this algebra has come one potentially useful insight into the structure of stars: a star *must* change its structure to be stable. Simple proportional expansion and cooling, or contraction and heating, is not quite enough. Our concern, however, is much more with the implications of the episode for the practice of science.

Jeans' mistaken calculation had very little direct effect on the progress of stellar modelling. Its main importance for us here lies, first, in its implications for the continuing practice of constructing mathematical models of astrophysical systems. The actual flaw was subtle in its introduction and effect and went undetected for a very long time. The lesson that mistakes happen and that they may not be found very soon is not a new one, but well worth underlining. Also worth emphasizing is the fact that every mathematical assumption has some physical implication and that the true influence of a simplifying assumption is not known until it is relaxed. Models have grown no simpler since Jeans' day, but simplifying assumptions with all their effects must still be made.

This episode is important, secondly, for its implications about the progress of science, *exactly* because it had little effect. A calculation that appeared to disprove a popular picture (it hardly yet amounted to a theory) made little impact, in spite of the fact that its flaw was not discovered for a decade. Indeed, one may say the flaw was never actually found, but rather a different (more complicated and more correct) calculation was performed that replaced Jeans' effort. Note that Cowling was investigating in great detail the stability of *gaseous* stars, not the liquid versions postulated by Jeans. This episode, then, illustrates the process of accepting a new theory as noted in Kuhn's[11] original work (notably chapter XII): the new theory need not answer all questions at once, and indeed might not even do as well as another theory in specific places. A theory is almost necessarily a vague and imperfect thing at the beginning. It is only after a long period of refinement that its true power is shown.

The author is grateful to an anonymous referee for many helpful suggestions, and especially for bringing to his attention several relevant papers and passages in the literature.

References

(1) J. H. Jeans, *MNRAS*, **85**, 914, 1925.
(2) J. H. Jeans, *Astronomy and Cosmogony, 2nd Edition* (Dover, New York), 1961; unaltered reprint of the 1929 version.
(3) S. Chandrasekhar, *An Introduction to the Study of Stellar Structure* (Dover, New York), 1958; unaltered reprint of the 1939 version.
(4) E. A. Milne, *Sir James Jeans* (Cambridge University Press), 1952.
(5) J. P. Cox, *Theory of Stellar Pulsation* (Princeton University Press), 1980.
(6) T. G. Cowling, *MNRAS*, **94**, 768, 1934.
(7) T. G. Cowling, *MNRAS*, **96**, 42, 1935.
(8) J. C. B. Papaloizou, *MNRAS*, **162**, 143, 1973.
(9) J. C. B. Papaloizou, *MNRAS*, **162**, 169, 1973.
(10) R. Kippenhahn & A. Weigert, *Stellar Structure and Evolution* (Springer-Verlag, New York), 1991.
(11) T. S. Kuhn, *The Structure of Scientific Revolutions, 2nd Edition* (University of Chicago Press, Chicago), 1970.

THE VARIABLE POLARIZATION OF AR LACERTAE

By Robert H. Koch
University of Pennsylvania

A number of linear and circular *V*-band polarization measures of the close binary AR Lac are published here for the first time and have been amalgamated with data from two other sources. The K0 component is a years-long polarization variable but without a firm cycle length or period as far as can be told presently. On the time scale of the Keplerian period, the polarization is sporadically variable and not enduringly phase-locked. From the polarization spectrum and ground- and spacecraft-based observations of the atmospheric structure of the K-component, the seat of the polarization is understood provisionally to be located in the assorted active clouds that populate the outer envelope of that star.

Introduction

The many aliases of AR Lac (*e.g.*, IRAS 22066+4529, HR 8448, HD 210334, 2EUVE J2208+45·7, 1RXS J220840·9+454432) show how accessible it has been to different detectors. Even this enumeration conveys only a fraction of its information, for the star is a cm-wavelength source as well. Photometrically and spectroscopically, the variable is known as a detached pair of G2 and K0 subgiants revolving and eclipsing in a period disagreeably close to 2·0 days. This period has had two lengthy episodes of bounded variability each at least 50 years long and, at present, the current period decrease seems to be waning. There is no agreement concerning the cause of this variability. The eclipses are complete, lasting ±0·063 *P*, but the light curve is far from stable, being inflected by the sporadically spotted photospheres of the two stars. By one artifice or another, these spotted areas have been modelled with simple geometries and temperature differentials against the photosphere for quite some time. Year after year, the literature for the object has become increasingly voluminous as the different levels of the stellar atmospheres have been probed by assorted spacecraft, and ever-newer (n_e, Z, T, $\Delta T/\Delta r$) models of the chromospheres and coronae have been computed. As HIP 109303, the star has a parallax of 23·79±0·59 mas and it serves as a favourably bright analogue to RS CVn, the prototype of spotted, cool, close binaries.

This paper is concerned with the information about AR Lac that can be gleaned from infrequent polarimetric monitoring of the binary.

Polarimetric history

The first attempt to observe AR Lac with a polarimeter was made by Hiltner[1], but he obtained no signal above noise during the 1949–1950 season. For any star on his programme, the smallest measured signal was 0·4%, a value larger than anything AR Lac has ever shown. The first detections seem to have been reported by Pfeiffer & Koch[2], who summarized their results in the 1976 dissertation of the

first author. Only means of six polar-coordinate parameters were given at that time and there was no claim of variability. The whereabouts of two of these observations are not known at present. In 1984 Liu & Tan[3] used the McDonald 0·9-m reflector to observe the star again and, in a brief summary, announced it to be a polarization variable. They[4,5] have published their observations twice since the original abstract, and the author is grateful to John Bangert and Gregory Shelton, the USNO Librarian, who provided a copy of these difficult-to-find publications. Finally, Vasil'ev *et al.*[6] sampled the visible-band linear polarization spectrum on seven nights, for which only integral values of the JD Numbers were published. The spectrum clearly is not interstellar but rather drops from the *U*-bandpass through *V*, then rises to a maximum at *R* and finally drops again at *I*. The signals are so small that a wavelength-dependent trend in θ cannot be discerned if it is present.

New polarimetric measures and their errors

At the Flower and Cook Observatory (FCO) in 1989 the author re-started a monitoring programme of this star using the instrument package described by Corcoran[7] and Holenstein[8], who contributed three of the observations. The programme was sustained in the 1990 and 1992 observing seasons. Scores of observations of null- and non-null-polarization standard stars assured that the zero point and scale of the present measures were consistently controlled. The unfortunate Keplerian period meant that good coverage of the cycle was impossible in one season and it was hoped that variability would be decisive enough so that any modulation could be easily recognized and understood. That turned out to be a delusion. The normalized Stokes parameters are collected into Table I. The data of the final three seasons are adequately phased by an ephemeris provided privately by C.-H. Kim:

$$\text{Primary Minimum} = 2\,446\,041\cdot9815 + 1\cdot9831635E.$$

The same period, but with the epoch corrected for period variability, was used to compute the phases for the 1970s measures.

TABLE I

Normalized Stokes parameters for AR Lacertae

JDN – 2 440 000	*Phase*	*q*(%)	*u*(%)	*v*(%)
2317·562	0·0073	−0·093	+0·100	
2338·691	0·1511	+0·081	−0·013	
2995·705	0·9377	−0·018	+0·107	
7803·674	0·3244	+0·045	+0·006	+0·004
7804·547	0·7646	+0·028	−0·006	−0·014
7811·615	0·3286	−0·052	−0·029	−0·113
7822·615	0·8753	+0·042	−0·025	−0·048
7824·563	0·8576	+0·035	−0·016	−0·062
7834·528	0·8824	−0·016	+0·006	−0·103
7840·520	0·9038	+0·010	+0·010	−0·063
7843·587	0·4503	−0·030	+0·006	−0·005
7855·515	0·4649	+0·027	+0·037	−0·005
7857·588	0·5102	+0·020	−0·059	−0·045

TABLE I (*concluded*)

JDN – *2 440 000*	*Phase*	*q*(%)	*u*(%)	*v*(%)
8004·753	0·7174	+0·000	−0·037	−0·075
8111·612	0·6005	−0·066	−0·038	−0·081
8118·703	0·1761	−0·033	−0·013	−0·054
8118·722	0·1857	−0·028	−0·012	−0·004
8118·743	0·1963	−0·027	+0·010	−0·004
8158·570	0·2789	+0·012	−0·045	−0·058
8158·590	0·2890	+0·063	+0·005	−0·052
8167·573	0·8186	+0·009	−0·006	−0·033
8167·593	0·8287	−0·009	+0·030	−0·039
8189·558	0·9044	+0·032	+0·010	+0·006
8189·578	0·9145	−0·000	−0·004	−0·080
8211·520	0·9786	−0·001	−0·001	
8211·538	0·9877	+0·023	+0·010	
8211·556	0·9968	−0·019	−0·035	−0·132
8211·581	0·0094	−0·054	+0·026	−0·082
8211·600	0·0190	−0·006	+0·037	
8211·619	0·0286	+0·049	+0·052	−0·127
8211·647	0·0427	−0·038	+0·020	−0·075
8216·607	0·5437	−0·003	+0·014	−0·021
8832·706	0·2085	−0·168	+0·077	−0·015
8836·801	0·2734	−0·089	+0·048	−0·049
8839·698	0·7342	−0·024	+0·098	+0·019
8864·690	0·3363	+0·148	+0·060	−0·001
8877·686	0·8894	+0·093	−0·039	−0·062
8882·620	0·3774	−0·244	−0·106	−0·028
8895·652	0·9487	+0·007	+0·035	−0·062
8897·617	0·9395	+0·114	−0·007	+0·026
8899·644	0·9615	+0·086	−0·018	−0·030
8899·673	0·9762	−0·050	+0·145	−0·046
8899·701	0·9904	−0·001	+0·295	−0·015
8901·646	0·9711	−0·015	−0·064	−0·007
8902·607	0·4557	+0·016	+0·181	−0·021
8918·513	0·4762	−0·020	−0·022	+0·017
8918·531	0·4853	−0·016	+0·052	+0·031
8919·560	0·0042	−0·204	+0·168	+0·013
8919·579	0·0137	−0·187	+0·056	+0·057
8921·539	0·0021	+0·074	+0·025	−0·034
8923·547	0·0146	−0·016	+0·070	−0·099
8923·575	0·0287	−0·159	+0·124	+0·009
8923·596	0·0393	−0·112	+0·076	+0·013
8930·616	0·5791	−0·247	+0 235	−0·002
2317·615	0·0144	+0·252	+0·015	

The final datum in Table I is a red one and all the rest were taken with the *V* filter.
The errors of the observations were monitored consistently and their mean 1σ-values are shown for each parameter of each season in Table II.

TABLE II

Errors of the individual normalized Stokes parameters

Season	δq(%)	δu(%)	δv(%)
1974, 1976	±0·04	±0·04	
1989	±0·026	±0·020	±0·021
1990	±0·024	±0·019	±0·024
1992	±0·018	±0·018	±0·025

Thus, there are really only two significant figures in the Table I parameter listings. In order to avoid a quantized appearance of Figs. 1, 3, 4, and 5, with numerous data falling unresolved atop each other, and to permit the reader to check the figures against the tabular entries, three decimal places are given in the table.

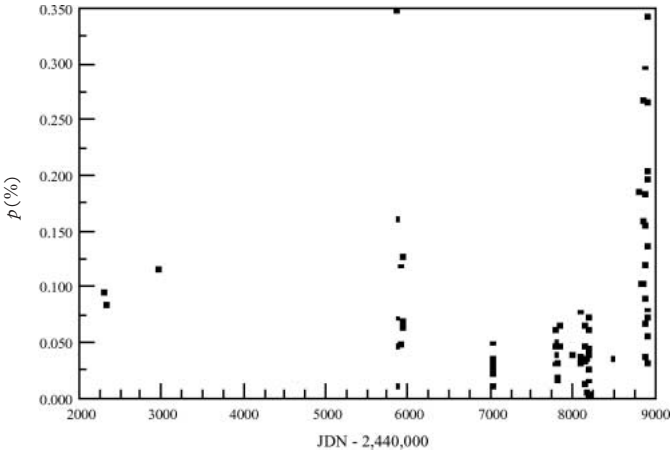

FIG. 1

All measures of the p parameter as a function of Julian Day Number. The data of Liu and Tan appear just before 6000 on the abscissa and the Crimean results just after 7000. All the rest come from the FCO.

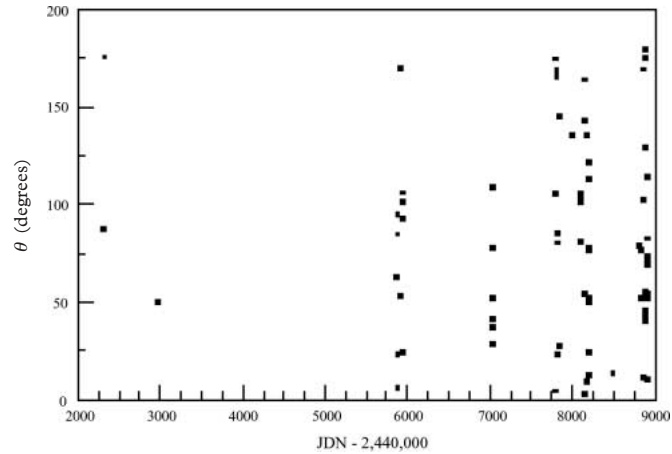

FIG. 2

All measures of the θ parameter as a function of Julian Day Number.

Long-term behaviour

Together with the results of Liu & Tan and of Vasil'ev *et al.*, the linear FCO observations in polar-coordinate form have been assembled into Figs. 1 and 2. Different seasonal behaviour can easily be seen, with the polarization being quiet and small from 1987 through 1991 but large and very variable in 1984 and 1992 and possibly in the 1970s. This conclusion is robust with respect to systematic error, since the 1984 and 1992 data came from different telescopes, polarimeters, and observers. For the same reasons, the same conclusion may be drawn about the quiet 1987, 1989, 1990, and 1991 measures.

The θ parameter, appearing in Fig. 2, is always noisy but not for a unique reason. From 1987 through 1991, the small values of p inevitably led to large uncertainties for θ, but the full range of θ is at least partly intrinsic during 1984 and 1992 when p was sometimes large.

It is first necessary to determine if there are zero-polarization measures. The maximum-likelihood precept of Stewart[9], applied to the measures of Table I, indicates that, for weighted averages of the errors of Table II, any individual value of $p < 0{\cdot}033\%$ should be considered unpolarized at the 1σ level. The data journal and Fig. 3 show that there are many such measures but a comprehensive understanding of this circumstance is not obvious. It could be, for example, that a seat of polarization is simply turned from the observer at some times.

The zero-polarization statistical level having been recognized, it is possible to learn more information than Figs. 1 and 2 convey: the distribution of the electric-vector values is essentially the same over the interval 0·00%–0·08%, *i.e.*, up to a level of about 2·5σ as Fig. 3 shows. Above this limit the figure shows that the orientation of the electric vector depends at times and in part on the value of p: for $p > 0{\cdot}08\%$ and the electric vector in the first quadrant, 20 measures give a

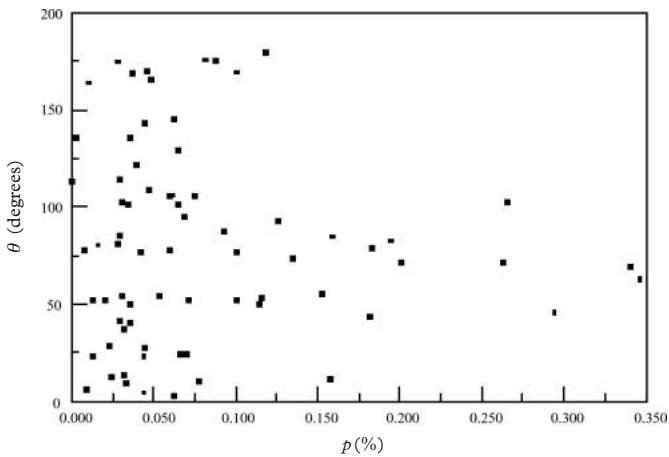

FIG. 3

The orientations of the electric vector against observed polarization values. The measure near 0·16% and 10° is not included in the mean value of θ noted in the text.

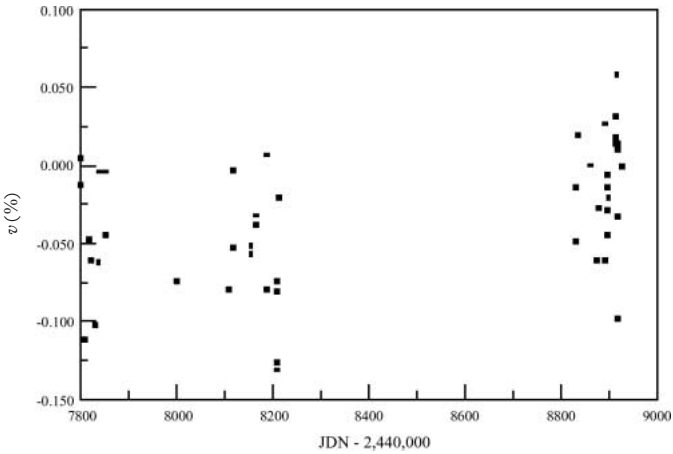

FIG. 4

All measures of the v parameter as a function of Julian Day Number. The range of the abscissa is more restricted than in Figs. 1 and 2.

mean $\theta = 71° \pm 4°$. Obviously, these come from only the 'high' seasons and they are only a fraction of those seasonal values. Had more measures been made, this pattern and mean may or may not have been confirmed. There is possibly another weakly preferred orientation of the electric vector near $\theta = 175°$.

Fig. 4 shows the accumulation of the v parameter against time. For this polarization component the data are comparably quiet (or noisy) in all three seasons but a positive gradient with time is apparent so that, approximately, the mean $v = -0{\cdot}01\%$ in 1992. A much larger positive gradient from 1990 to 1992 also appears for the mean linear polarization.

Light-curve information

The obvious first reference for the polarization information is the long-term photometric history collected by Lanza *et al.*[10] which interprets *V*-band light-curve changes from 1967 through 1992 as changes in photospheric spottedness. At the trivial level of just the light-curve changes, there can be seen neither a correlation nor an anti-correlation with the polarization history. The same conclusion results when the stars' seasonal covering factors are examined. On the other hand, there is a correlation between the non-dimensional quantity A_U, which scales the fractional minimum uniform spotted area averaged over all stellar longitudes of the K0 star, and the average polarization from 1984 through 1992. When the polarization is small, as from 1987 through 1991 with an average value of about $0{\cdot}036\%$, the value of A_U is close to $0{\cdot}03$. When as in 1984 and 1992 the polarization has a larger mean of about $0{\cdot}12\%$, the average value of A_U is also larger at about $0{\cdot}15$. This association may plausibly be extended to the other linear polarization coordinate: there is no reason to expect a favoured orientation of the electric vector if this parameter is averaged over a spotted global band engirdling

the K0 star. This is exactly what is shown by the noisy θ coordinate. It is, therefore, a possible deduction that the cool star's flux over the uniformly spotted area has been variably linearly polarized over the monitoring interval as the level of spottedness has varied. This does not necessarily mean that the polarizing mechanism is seated in the photospheric spots themselves. Because the number of polarization observations on any night is never larger than seven, it is impossible to attempt to correlate short-time-scale photometric changes with polarimetric ones. (A more general conclusion was kindly communicated by a referee, who confirmed the author's result that a periodogram analysis of the data yielded no periodicity whatever.)

The variability of the v coordinate in only two years should also be implicated in the same uniformly spotted-area index, but the sense of the change in v is to diminish as the p coordinate increases and the complete explanation must be more complex than just indicated.

Keplerian- and longitudinally-phased observations

The argument based on independent photometric information has allowed a weak inference about the spatial location for the seat of polarization. It is now useful to examine whether a more detailed conclusion may be gained by studying the measures when they are phased with the Keplerian ephemeris.

No enduring first or second harmonic of the normalized Stokes parameters exists when the data are so phased. In terms of the model of Brown, McLean & Emslie[11], this indicates no stable distribution of scatterers either in and near the orbital plane or at great distances above and below it. The variations on the original BME model by Manset & Bastien[12] do not change this conclusion at all. However, variations of the polarization parameters do exist within individual seasons and these were examined. The entire data set was compiled into two groups: the 'high' group of the 1970s, 1984, and 1992 and the 'low' one derived from the other seasons. To use the Crimean data, fictitious zone times (3 hours later than the Greenwich times for comparable dates amongst the FCO observations) were assigned to those observations. The independent variables for attempting an understanding of the data were both orbital phase and photospheric longitude with the conventions established by Lanza *et al*. An example of one 'pattern' is shown in Fig. 5.

The figure may be interpreted as indicating $u = +0{\cdot}1\%$ over the K-star longitude interval (360°–350°) during the rising branch of primary eclipse, followed by a diminished value of u over the interval (340°–290°), after which the parameter just shows high-frequency activity over the rest of the longitude and phase intervals. The 'pattern' might also partly be interpreted as simple removal of light dilution during the last half of the primary eclipse, but this interpretation cannot apply to the first half of the eclipse. These sorts of patchwork descriptions can hardly refer to a smooth distribution of scatterers on or above all longitude sectors and they are symptomatic of every failed attempt at economical understanding of all the linear parametric patterns.

For a stable envelope with a very high orbital inclination, the (q,u) pattern ultimately degenerates into a linear figure. Since for AR Lac $i = 87{\cdot}0°$, the subset of the 20 observations singled out in Fig. 3 seemed promising since they show a preference for the first quadrant. When these are examined, however, there is no appropriate Keplerian phase pattern to them.

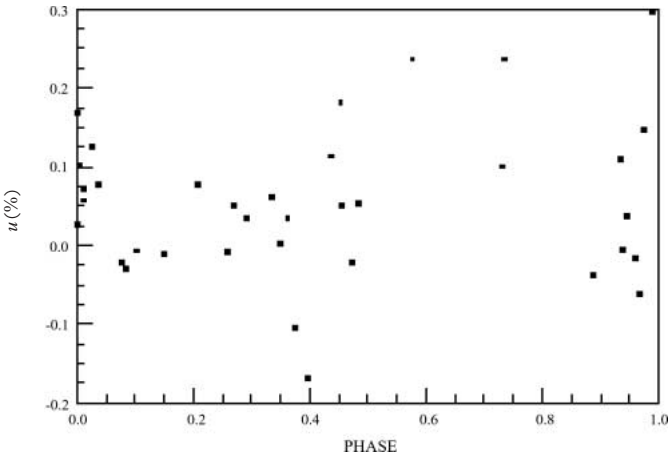

FIG. 5

The normalized u parameter from the 1970s, 1984, and 1992, all representative of the polarization's 'high' state.

It might be considered surprising that no phase-locked polarization pattern can be documented, but this is actually consistent with the pattern for A_D shown in Fig. 14c of Lanza *et al.* This photometric parameter measures non-dimensionally the longitude-dependent spottedness of each star and is seen to be almost flat at an average value of about 5% for the K0 star over the years of polarization monitoring. The modelling precision claimed for A_D itself is 5%–10%.

From Fig. 3 there has already been indicated a preferential value of θ if p is sufficiently large. For $p > 0{\cdot}13\%$, there are 13 measures and six of these occur within primary eclipse. Unfortunately that promising premise cannot be generalized for there also exist 13 other such eclipse measures for smaller values of p which show no preferential orientation.

During 1989 and 1990 the v parameter showed a noisy modulation with five observations attaining a minimum value of about $-0{\cdot}10\%$ when the 0° meridian of the K star (*i.e.*, its outside hemisphere) was turned to the observer. The other extremum near $v = -0{\cdot}03\%$ persisted over the rest of the cycle. In 1992 no such variability existed and the mean level was close to $-0{\cdot}01\%$.

There is no longitude or phase pattern when the total polarization (*i.e.*, the Pythagorean sum of all three normalized Stokes parameters) is examined. It must be concluded that the mean levels characteristic of the two polarization states are always associated with high-frequency, quasi-random signals so there are sources of variable polarization superposed on the source(s) correlated with the uniform spot distribution on the K star.

It was imagined that the polarization might be phase-locked to some period different from the Keplerian one, *e.g.*, a spin period somewhat shorter than $1{\cdot}98$ days. A small number of searches using different seasonal data sets and the q, u, and p parameters separately uncovered nothing. A definitive test of this possibility really needs data taken more densely in time than exists here.

A polarization resumé

A few basic decisions have to be made before any understanding can begin. (*a*) A matter correlated with null-value data has to do with the possible contamination of the measures by interstellar polarization. A faint interstellar line has been found near $-1{\cdot}0$ km s^{-1} in the Mg *k* blend; also $b = -8°$ is not a high Galactic latitude. There must, therefore, be some small interstellar polarization but the large parallax militates against any large value for it. Evidence pertaining to this matter exists in the measures of HD 202444, 203280, 210027, and 218045 reported by Koch and Clarke[13]. Interpolation among the Galactic coordinates and distances for these stars to the values appropriate for AR Lac strongly indicates that the interstellar value of *p* is no larger than $0{\cdot}01\%$ but also not much smaller than this value. With such a value for the interstellar component, Fig. 3 indicates AR Lac to have been unpolarized within measurement errors quite frequently despite the fact that every photometric and spectroscopic mapping of the photospheres and higher atmospheric layers has always required spots or clouds or extended high-temperature coronae. The interstellar component of the *v* parameter must be very small but cannot be known at present. (*b*) Have very large values of polarization been missed observationally? This is impossible to answer with complete certainty but the density of seasonal sampling from 1987 through 1992 suggests that the possibility is unlikely over that 5-year interval. (*c*) Has the polarization variability been at least cyclical or possibly periodic? Period lengths of about 17 years have been suggested in the past on the basis of light-curve changes. The relatively large polarization means attained in 1974–1976, 1984, and 1992 could be made compatible with a cycle length of the order of 8–9 years or, depending on the polarizing mechanism, possibly double that interval. Even if that were the case, the modulation could not be a smooth one. Any such waveform would have to keep the polarization at a 'high' value for some years, as in 1974–1976. It would also have to sustain low values, as over 1987–1991, and demand steep gradients between the 'high' and 'low' states. Any cycle would be in the nature of a succession of step functions.

Two possible polarizing mechanisms may be discounted quickly. The first is that of a third object (star or planet or coherent gas/dust cloud) orbiting the close binary with a period of several years. The waveform of the long-term polarization pattern must be similar to a sequence of step functions so that even a very eccentric orbit would not satisfy it. Secondly, it might be imagined that the 'high' states in three of the seasons are feeble analogues of the stream accretion operating in polars, the streaming material coming from the clouds mapped by spacecraft spectra or fluxes. This has the fundamental problem that the polarization 'high' states typically have to arise when the flow is transverse to the line of sight and it seems impossible to construct a long-term geometry whereby that condition is fulfilled as the orbital revolution runs its course. In addition, when the chronological sequence of the measures in the 'high' states is studied, there is no pattern to them whatever.

There is other polarization evidence of value. (*a*) Within its error, the last entry of Table I is consistent with the other data in the table and with the polarization spectra of Vasil'ev *et al.* Those spectra have a local maximum in the *R* bandpass, most probably associated with Hα emission, so the spectrum is not simply a Rayleigh-scattering one. Scaled down by about a factor of $9{\cdot}5$, the spectrum is very similar to Pfeiffer's[14] spectrum for RS CVn. Even if the polarizing mechanism is only a scattering one and not due in any way to a magnetic environment,

these spectra are more complicated and less steep than Rayleigh and, together with the cool stellar temperatures, implicate dust condensates somewhere in the stellar envelopes. If, however, an interstellar polarization spectrum with $p(V) = 0{\cdot}01\%$ is removed from Vasil'ev's values, the nett spectrum steepens toward a Rayleigh-type one. (*b*) Pfeiffer also noted a 5-year diminution of the visible-band polarization of RS CVn — possibly a fraction of a longer-term cycle. (*c*) The polarization signals are visible throughout the Keplerian cycle so that, if some seats of polarization are eclipsed, other comparable ones compensate by becoming visible at the appropriate times. (*d*) Lastly, the circular component is variable in the long-term and varies, as far as present evidence indicates, algebraically oppositely to the average linear signal.

More envelope information

There is much more information about layers above the photospheres than is conveyed by Lanza *et al.* The X-ray and radio coronae are variable, as Rodonò *et al.*[15] and Triglio *et al.*[16] have pointed out, and are best understood as two-component structures. Coronal modelling was somewhat ambiguous but one radio component has dimensions comparable to the orbital size and the second one could be a point source within the angular resolution. In the radio-emitting core layers, log (T_e) is of the order of 7 and is somewhat higher in the halo. For log (n_e), values of about $10{\cdot}3$ and 9 are appropriate averages for the same layers, respectively. At heights where the Mg XI ion is formed, Testa *et al.*[17] found log (T_e) and log (n_e) to be about $6{\cdot}8$ and $12{\cdot}5$, respectively. There was also confirmation that the coronal Z is less than solar. Pagano *et al.*[18] studied the chromospheric structure from the Mg II *k* lines observed in 1994. Whereas the G-star's chromosphere was compact and uniform, the K-star's layers were extended and non-homogeneous, so the authors mapped five discrete emitting regions up to $1{\cdot}2\,R_K$ above the K star's photosphere. Some of these emitting sectors are actually outside the star's Roche lobe. A bright region near the L_1 point was also discovered and the transition-region lines of C IV showed five flares over only five days. Griffiths[19] associated many hot and cool coronal loops with small footpoints on the stellar photospheres. The footpoints of the cool loops were anchored in cool spots of strong magnetic field which confined at least part of the coronal plasma. Values of log (n_e) between $11{\cdot}0$ and $9{\cdot}3$ were calculated for the loops whose tops lay only about $0{\cdot}15\,R_K$ above the photospheres. Amongst all these sources there is not a unique usage of the words 'corona' and 'chromosphere', which does not help to form a unified picture of the atmospheres. Only the electron densities in the high envelope levels bear directly on the present polarimetry but inferentially, below current angular resolution, there is also a multiplicity of relatively small structures which are themselves variable and these could be the scattering regions leading to the variable polarization.

Conclusion

No further information exists at this time and a decisive interpretation cannot be given now, but it is possible to outline model characteristics that must be satisfied by the measures of Table I and the other independent polarization results.

The beginning of an understanding recognizes that there must exist a shell within the extended K-star envelope where the density is low enough for the optically-thin scattering required by the small polarization values. This shell would

not be homogeneously filled but rather populated by the discrete clouds that are approximately co-rotating with the K-star and are also variable in dimension and number density. When at primary eclipse substantial light dilution is removed, the observed polarization sometimes increases, but large p values also occur at some other phase intervals. However appealing the possibility, these large values do not permit the general conclusion that there is an aspherical envelope with a preferential orientation aligned close to 70° with respect to the north direction on the sky; the necessary phase-locked progression is not demonstrated by the measures. At other times, data taken within primary eclipse do not reveal large polarization values so then the envelope could be populated by only a small number of scatterers or they could have assumed a nearly spherical geometry. The plasma furthermore must be low in metals compared to the Sun and not have a simple polarization spectrum. Since Z is about $0{\cdot}6 Z_{\odot}$, there is the possibility that the metal depletion is only apparent and not real because of grain condensation in the cool envelope and that grains alone are the seats of the polarization. Only detailed modelling can determine the form of the polarization spectrum from any condensate. It will also be necessary to account for the variability of the circular polarization component, possibly by appealing to the same dust component in the atmosphere.

It would have been much more useful if measures had been consistently taken with additional filters but the most important limitation of this work was self-imposed in another way. Had the data been assembled and studied promptly in 1992, four more seasons of monitoring would have become available before the polarization programme was terminated.

All of the observing effort for this star and for the standards that were treated in two previous papers was supported by a series of grants from the NSF. They are most gratefully acknowledged. I also note with appreciation several suggestions by the referee.

References

(1) W. A. Hiltner, *ApJ*, **114**, 241, 1951.
(2) R. J. Pfeiffer & R. H. Koch, *PASP*, **89**, 147, 1977.
(3) X.-F. Liu & H.-S. Tan, *BAAS*, **17**, 588, 1984.
(4) X.-F. Liu & H.-S. Tan, *Chinese A&A*, **11**, 244, 1987.
(5) X.-F. Liu & H.-S. Tan, *AcASn*, **28**, 139, 1987.
(6) V. P. Vasil'ev *et al.*, *AZh*, **70**, 1322, 1993.
(7) M. F. Corcoran, *ApJ*, **366**, 308, 1991.
(8) B. D. Holenstein, *PhD Dissertation, University of Pennsylvania*, 1991, p. 26.
(9) B. G. Stewart, *A&A*, **246**, 280, 1991.
(10) A. F. Lanza *et al.*, *A&A*, **332**, 541, 1998.
(11) J. C. Brown, I. S. McLean & A. G. Emslie, *A&A*, **68**, 415, 1978.
(12) N. Manset & P. Bastien, *AJ*, **120**, 413, 2000.
(13) R. H. Koch & D. Clarke, *The Observatory,* **125**, 355, 2005.
(14) R. J. Pfeiffer, *ApJ*, **232**, 191, 1979.
(15) M. Rodonò *et al.*, *A&A*, **346**, 811, 1999.
(16) C. Triglio *et al.*, *A&A*, **373**, 181, 2001.
(17) P. Testa *et al.*, *ApJ,* **617**, 508, 2004.
(18) I. Pagano *et al.*, *A&A*, **365**, 128, 2001.
(19) N. W. Griffiths, *ApJ*, **518**, 873, 1999.

ASTROPHYSICAL PARAMETERS FOR THE ECLIPSING BINARY IZ PERSEI

By R. W. Hilditch
School of Physics and Astronomy, University of St. Andrews, Scotland,
G. Hill
18A Stratford St., Auckland, New Zealand,
and T. A. Lister
School of Physics and Astronomy, University of St. Andrews, Scotland

New spectroscopic observations of the B-type eclipsing binary IZ Persei are analysed *via* cross-correlation and disentangling codes to determine orbital parameters and separated spectra of the two stars for the first time. These results are combined with analysis of photometric data from the *Hipparcos* satellite and new ground-based CCD photometry to yield the first determination of complete astrophysical parameters for both stars in this semi-detached system that is in the slow phase of Case-A mass transfer.

Introduction

The star HD 9234 (spectral type B8 in the *HD* catalogue) was discovered to be an eclipsing binary by Strohmeier[1]. He determined an orbital period of $3^{d}{\cdot}687661$ from photographic observations and the resultant light curve was of the EA or Algol type, suggesting either a detached system or a semi-detached system. It was assigned the variable-star name IZ Per and appears in the *Hipparcos* catalogue[2] as HIP 7145.

The first spectroscopic observations[3] were obtained at a reciprocal dispersion of 72 Å mm^{-1} and recorded on Kodak IIaO photographic emulsion, providing a dispersion of about $1{\cdot}4$ Å per pixel. Measurements of the radial velocity of the star were determined from the absorption lines Ca II λ3934, Hε, He I λ4026, Hδ, Hγ, and He I λ4471 on a total of 22 spectrograms. The resultant semi-amplitude of the dominant single spectrum was $K_1 = 52{\cdot}9$ km s^{-1}, and the orbit was found to be nearly circular. A spectroscopic investigation[4] of rotational velocities of stars in Algol-type systems suggested that the hotter component of IZ Per was of earlier spectral type, listed as B5?, and was rotating at $v \sin i = 185$ km s^{-1}, likely indicating non-synchronous rotation. This result was obtained from two spectra with a reciprocal dispersion of 16 Å mm^{-1}, recorded on baked IIaO emulsion (about $0{\cdot}3$ Å per pixel), and using only the He I λ4026 absorption line. Such a dispersion corresponds to a 3-pixel resolution of $0{\cdot}9$ Å or 67 km s^{-1}.

Three-colour photoelectric photometry was published by Srivastava & Padalia[5], containing complete coverage of the primary and secondary eclipses and most of the out-of-eclipse phases. Their analysis of these data *via* the Russell–Merrill method[6] suggested that primary eclipse was a total occultation and yielded a ratio of radii of the two stars of $k = 0{\cdot}84$, with the cooler secondary star being larger than the hotter primary star. These photoelectric data were re-analyzed[7] *via* the Wood method[8], which is based upon representing the stars as triaxial ellipsoids. Considerable discordance was obtained from the three light

curves between the values of stellar radii, orbital inclination, and mass ratio, but all showed that the hotter primary star eclipsed at primary eclipse is the slightly larger one of the two, contrary to the earlier investigation. It was concluded that the system was probably in a semi-detached state. Subsequent *UBV* photometry[9] suggested revised spectral types for the primary and secondary components of B2·5 III–V and B5 III–V respectively, with interstellar reddening of $E(B–V) = 0·4$, and indications of some intrinsic variability in the binary system, possibly of the β Cephei type.

A further light-curve analysis[10], made by means of the Wilson-Devinney code[11] and based upon unpublished *B* and *V* photoelectric photometry, demonstrated that the system was certainly semi-detached, with the cooler secondary star filling its Roche lobe and being somewhat smaller than the primary star. This analysis included a comment that some medium-dispersion spectroscopy had been secured which showed the primary star to be of spectral type B3–4. It also showed that the best representation of the complete light curve (specifically the out-of-eclipse ellipsoidal variations) was obtained by allowing non-synchronous rotation of the primary star at three times the synchronous value. A nearly simultaneous publication[12] reported a spectroscopic determination of the rotational velocity of the primary component of IZ Per to be only 98 ± 5 km s^{-1}, determined from one CCD spectrum with a dispersion of 0·2 Å per pixel (a three-pixel resolution of 0·6 Å or 40 km s^{-1}), and using the absorption lines of He I λ4471 and Mg II λ4481. As we show below, this latter measurement of $v \sin i$ is close to the synchronous value whereas the earlier spectroscopic measurement[4] is 1·8 times larger than synchronism.

This paper reports new spectroscopy and some CCD photometry which yield a complete specification of the astrophysical parameters of IZ Per for the first time. These new data do not resolve the issue of whether or not the primary star is rotating synchronously.

Orbital ephemeris

An analysis[13] of published times of minima of primary and secondary eclipses of IZ Per provided an orbital period of 3^{d}·687664, slightly revised from the original determination by Strohmeier, and some suggestions of a small-scale secular increase. A subsequent compilation and analysis by Símon[14] of all published times of minima determined photoelectrically or with CCD photometry showed that all the data were well represented by the linear ephemeris

$$T_{\text{pr.min.}} = 2\,444\,577·5874 + 3·687673E \qquad (1)$$

and that the orbital period had remained constant over the past 92 years. In all subsequent analyses in this paper we have adopted this orbital period. Our CCD photometry of one primary eclipse, defined by ≃ 800 observations, provides a time of minimum of HJD 2 453 693·5150 ± 0·0001, which has been used as the reference time. This time of minimum agrees with Símon's ephemeris to within 0^{d}·0001.

Spectroscopic observations

Spectroscopic observations of IZ Per were obtained by G. Hill during 1991 at the Herzberg Institute of Astrophysics, Victoria, Canada, using the 1·2-m tele-

scope and coudé spectrograph operating at a reciprocal dispersion of 20 Å mm^{-1}. A total of 21 spectra were secured with typical $S/N \simeq 50$, recorded with a Reticon diode array at a dispersion of 0·3 Å per pixel, giving comparison lines from an argon source with full width at half maximum (FWHM) of 0·9 Å (a three-pixel resolution of 63 km s^{-1} at 4250 Å). The spectra were wavelength calibrated, linearized, and continuum rectified using standard procedures. In Fig. 1, we present a montage of these rectified spectra, sorted according to increasing orbital phase, which shows that the H lines from the two stars are always seriously blended and explains why the first spectroscopic study at low resolution resulted in a spuriously low value for the semi-amplitude of the dominant primary component. It is also clear that both components contribute to the He I and Mg II lines, whilst C II λ4267 is due to the primary component alone.

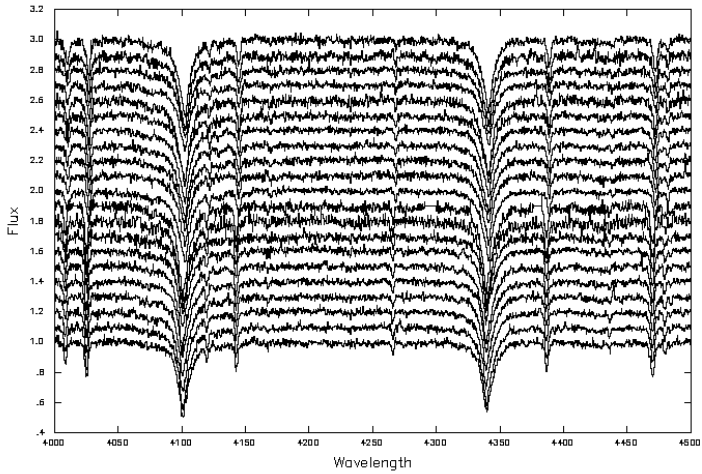

FIG. 1

Montage of 21 spectra of IZ Per displayed in order of increasing orbital phase from bottom (first quadrature, ten spectra, phase range 0·18—0·34) to top (second quadrature, 11 spectra, phase range 0·72—0·80).

Radial velocities and orbital solution

Radial velocities were determined for each component from the individual spectra by means of the cross-correlation code VCROSS[15]. The spectra of IZ Per were cross-correlated against a template spectrum of spectral type B2·5 V and using only the wavelength regions encompassing the He I lines, C II λ4267, and Mg II λ4481. In each of the resultant cross-correlation functions (ccfs), the principal peak was sensibly symmetrical, and fitted by a Lorentzian function to yield radial velocities of the primary component, which is of closely similar spectral type to that of the template. The procedure was then repeated with a template spectrum of spectral type A0V and using only the regions of the spectrum that would contain evidence of the very weak spectrum of the secondary component. These regions were λλ 4030–4070, λλ 4180–4260, λλ 4275–4320, and λλ 4477–4500, which minimized the influence of the primary-component spectrum. Again the principal peak in

TABLE I

Radial velocities of both components of IZ Per

HJD	*Orbital Phase*	*RV(pri)* km s^{-1}	*(O–C)(pri)* km s^{-1}	*RV(sec)* km s^{-1}	*(O–C)(sec)* km s^{-1}
2448297·6100	0·7724	57·5	−0·2	−258·2	−4·4
2448297·6326	0·7785	57·2	8·7	−231·8	20·6
2448297·6604	0·7860	64·5	8·0	−239·4	10·8
2448297·6885	0·7936	57·7	2·1	−264·4	−17·0
2448461·8157	0·3006	−88·7	1·6	210·1	11·3
2448461·8441	0·3083	−91·1	−2·0	212·8	17·8
2448461·8882	0·3203	−89·8	−3·0	167·4	−20·7
2448461·9216	0·3293	−91·6	−6·7	169·9	−12·2
2448516·6758	0·1772	−82·4	3·9	170·1	−16·5
2448516·7307	0·1921	−79·7	9·5	208·1	12·8
2448516·7772	0·2047	−92·5	−1·4	199·1	−2·1
2448516·8331	0·2199	−89·4	3·4	206·4	0·0
2448516·9321	0·2468	−94·9	−0·7	216·5	6·0
2448516·9859	0·2613	−98·8	−4·8	212·3	2·4
2448518·6540	0·7137	54·8	−1·7	−253·9	−3·8
2448518·7291	0·7341	60·7	2·7	−264·3	−9·3
2448518·7464	0·7387	61·9	3·7	−224·9	30·6
2448518·7954	0·7520	52·8	−5·6	−279·5	−23·4
2448518·8093	0·7558	54·4	−4·0	−266·1	−10·1
2448518·8266	0·7605	49·1	−9·2	−252·2	3·4
2448518·9634	0·7976	50·6	−4·4	−241·7	4·1

each of the ccfs was sensibly symmetrical and fitted by a Lorentzian function to yield radial velocities of the secondary component, which is of closely similar spectral type to that of the template. These values of radial velocity are listed in Table I, together with the Heliocentric Julian Dates of observation, the orbital phases according to the photometric ephemeris of Símon, and the observed-minus-calculated (*O–C*) values from the subsequent orbital solution.

Orbital solutions were determined *via* the code RVORBIT[16], adopting the above ephemeris and assuming a circular orbit. For the primary component alone, a semi-amplitude $K_1 = 76{\cdot}3 \pm 1{\cdot}1$ km s^{-1} and systemic velocity $\gamma_1 = -17{\cdot}9 \pm 1{\cdot}1$ km s^{-1} were determined, whilst for the secondary component, $K_2 = 234{\cdot}1 \pm 3{\cdot}3$ km s^{-1} and $\gamma_2 = -19{\cdot}6 \pm 3{\cdot}2$ km s^{-1} were found. The combined solution is listed in Table II. The necessary non-Keplerian corrections, required to account for the non-spherical shapes of the two stars and mutual heating effects, have to be calculated after the light-curve solution in an iterative process but are also provided in Table II for convenience.

The set of 21 spectra of IZ Per were also imported into the spectral-disentangling code TANGLE[17] to find an independent orbital solution for the system. This disentangling procedure makes no prior assumptions about the spectral types of the two stars, iteration zero starting with flat continua for both stars, but does require the orbital period to be defined, and we assumed circular orbits since there is no evidence to the contrary. The resultant orbital solution from TANGLE is also listed in Table II, and is in good agreement with the RVORBIT solution for the primary component, but less so for the secondary component. Setting aside the optimistic uncertainty on K_2 from the TANGLE solution, we have adopted the unweighted arithmetic-mean values and standard errors for the semi-amplitudes of the two components as being good determinations of these fundamental observables.

TABLE II

Orbit solutions

Parameter	*Primary*	*Secondary*
Semi-amplitudes $K_{1,2}$ km s^{-1} (RVORBIT)	76·3 ± 1·8	232·7 ± 2·1
Semi-amplitudes $K_{1,2}$ km s^{-1} (TANGLE)	79·4 ± 1·3	240·0 ± 0·5
Semi-amplitudes $K_{1,2}$ km s^{-1} (average)	77·9 ± 2·2	236·4 ± 5·2
Non-Keplerian corrections km s^{-1}	1·1	9·6
Final semi-amplitudes $K_{1,2}$ km s^{-1}	79·0 ± 2·2	246·0 ± 5·2
Final mass ratio q	3·11 ± 0·11	
Systemic velocity γ km s^{-1} (RVORBIT)	−18·6 ± 1·9	

With the orbital solution defined, the code MUTATE[17] was used to determine the average spectrum of each component of IZ Per, and these are plotted in Fig. 2. The disentangled spectrum of the primary component was compared with the Walborn & Fitzpatrick[18] atlas of O-type and early-B-type spectra, and a spectral type of B3 adopted. That of the secondary component is judged to be close to B9, since it shows He I lines, and Mg II λ4481 being somewhat stronger than He I λ4471. A cross-correlation of the well-defined disentangled spectrum of the primary component against the B2·5V template (η Lyr at RV[19] = −9·0 km s^{-1}) provided a measured systemic velocity of −18·8 ± 0·5 km s^{-1}, in excellent agreement with the result from RVORBIT. Curiously, the disentangled spectrum of the secondary component gave a systemic velocity of −61·8 ± 3·1 km s^{-1} when cross-correlated against the A0 V template (Vega at RV[19] = −15·0 km s^{-1}) using the same spectral regions as in the individual velocity measurements. We are not able to provide any explanation for this curious discrepancy, but we note that the solution for the orbital semi-amplitude is unaffected.

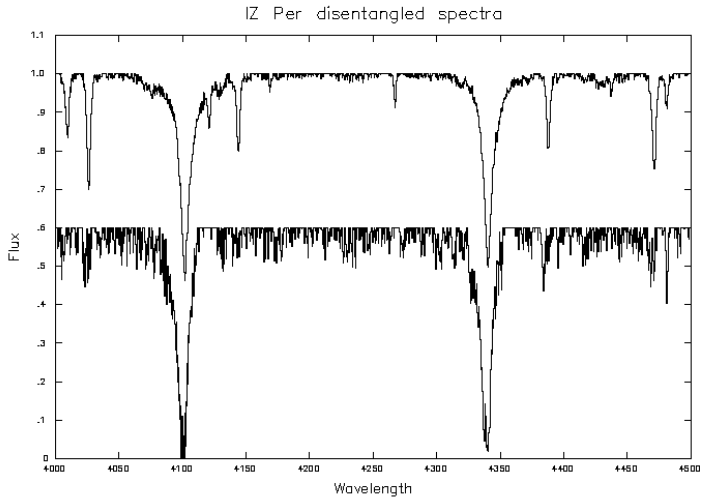

FIG. 2

Disentangled spectrum of the primary component of IZ Per (upper plot), and of the secondary component (lower plot) displaced by −0·4 in relative flux for clarity. The obvious absorption lines are He I λλ4009, 4026, 4144, 4383, 4471, Hδ, Hγ, Mg II λ4481 in both spectra, and C II λ4267 in the primary component spectrum.

Photometric observations

The photometric observations obtained by the *Hipparcos* satellite were contemporaneous with our spectroscopic data and provide a nearly complete light curve. The out-of-eclipse phases and the primary eclipse are fairly uniformly sampled, but unfortunately the phase range 0·45–0·55 covering mid-secondary eclipse is devoid of observations. To provide a more complete light curve for analysis, we observed IZ Per with the 0·9-m *James Gregory Telescope* at the University Observatory, St. Andrews, using a photometer that incorporates an Andor CCD camera. The CCD array has 1024 × 1024 13-μm pixels, giving a field of view of about 18 × 18 arcminutes with this *f*/3 Schmidt-Cassegrain telescope. The image scale is ≃ 1 arcsecond per pixel, but poor seeing and the telescope optics provide stellar images typically of 3–4 arcseconds in diameter, which are therefore well sampled.

Observations of the IZ Per field were obtained through a narrow-band filter with a central wavelength of 5300 Å and half-width 100 Å, and therefore close to the central wavelength of the H_p band. Integration times were usually 30s, and the readout time of the CCD is 1s. Observations were secured on three nights, covering a nearly complete primary eclipse (phases 0·93–0·07), most of secondary eclipse (phases 0·40–0·53), and near the light-curve maximum (phases 0·17–0·26). These CCD data were reduced using the automated pipeline reduction program[20] for photometric CCD observations written for the *SuperWASP* project. Differential magnitudes were formed between various possible comparison stars in the IZ Per field of view, and the comparison star (HD 232458) at the smallest angular distance and south-west from IZ Per was found to be sensibly constant in brightness over the three nights of observation to within ± $0^m·01$. A final set of differential magnitudes on the narrow-band instrumental system was then formed between IZ Per and HD 232458. These data were plotted against orbital phase together with the *Hipparcos* H_p data, and it was found that a simple zero-point shift of the λ5300 data up the magnitude axis was sufficient to make the two light curves overlap completely to within an eye-estimated uncertainty of ± $0^m·003$ and at all duplicated phases.

It was decided to form a binned light curve combining the 168 H_p and the 2387 λ5300 observations by taking the average values (magnitudes and phases) of all data points within each of 200 phase bins of width 0·005 in phase. Since some phase bins were empty of data, the resultant binned and combined light-curve data listed in Table III contains 138 data points, each with the average phase, average magnitude, average uncertainty (ε) from photon-counting statistics, and the number of observations per bin (n_{obs}). It may be seen that both eclipses are very well sampled, with typical uncertainties per bin of $0^m·003$, whilst most of the out-of-eclipse phase bins have only one or two *Hipparcos* observations with typical uncertainties of $0^m·015$.

Solution of the combined light curve

The detailed shapes and depths of the two eclipses in an eclipsing-binary light curve are defined by the sizes and shapes of the stars, their ratio of surface brightnesses, and the orbital inclination. The brightness changes out of eclipse also contribute to the solution, but not as strongly. In this light-curve analysis, we have adopted the standard procedure of weighting the observations according to $1/(\varepsilon\sqrt{f})$, where ε is the uncertainty in each data point, and f is the flux value relative to the adopted reference level at the quadrature phase 0·25. Thus the well-defined eclipse curves dominate the solution.

Table III

Combined H_p and λ5300 light curve of IZ Per

Bin number	*Orbital phase*	H_p (*mag.*)	ε (*mag.*)	n_{obs}	*Bin number*	*Orbital phase*	H_p (*mag.*)	ε (*mag.*)	n_{obs}
1	0·0024	9·171	0·002	24	2	0·0074	9·104	0·003	26
3	0·0125	8·995	0·003	26	4	0·0175	8·882	0·003	25
5	0·0224	8·781	0·003	26	6	0·0274	8·675	0·003	26
7	0·0324	8·582	0·004	27	8	0·0375	8·497	0·003	27
9	0·0425	8·415	0·002	24	10	0·0473	8·348	0·003	23
11	0·0525	8·281	0·004	23	12	0·0576	8·224	0·005	24
13	0·0625	8·172	0·004	22	14	0·0651	8·147	0·003	1
15	0·0719	8·077	0·014	2	16	0·0758	8·073	0·013	2
17	0·0825	8·033	0·014	2	18	0·0864	8·019	0·011	2
22	0·1076	7·972	0·014	3	23	0·1116	7·971	0·011	1
25	0·1217	7·931	0·013	1	26	0·1271	7·950	0·014	2
27	0·1324	7·936	0·011	1	29	0·1428	7·937	0·014	2
30	0·1478	7·924	0·016	2	31	0·1526	7·921	0·013	1
32	0·1563	7·917	0·015	2	34	0·1690	7·927	0·003	15
35	0·1711	7·926	0·003	22	36	0·1773	7·907	0·016	2
37	0·1817	7·917	0·014	3	38	0·1876	7·909	0·003	31
39	0·1936	7·904	0·009	10	40	0·1976	7·903	0·003	43
41	0·2023	7·899	0·003	47	42	0·2074	7·894	0·003	47
43	0·2125	7·889	0·003	50	44	0·2174	7·886	0·003	46
45	0·2206	7·890	0·004	11	46	0·2283	7·880	0·004	30
47	0·2315	7·879	0·003	23	48	0·2371	7·876	0·012	2
49	0·2426	7·872	0·003	25	50	0·2475	7·869	0·003	36
51	0·2517	7·868	0·003	22	52	0·2571	7·878	0·012	1
53	0·2609	7·874	0·009	1	58	0·2896	7·882	0·010	1
59	0·2934	7·889	0·016	1	60	0·2973	7·879	0·013	2
61	0·3012	7·875	0·015	2	65	0·3225	7·889	0·019	1
66	0·3264	7·875	0·016	1	68	0·3370	7·882	0·020	1
70	0·3466	7·873	0·016	1	71	0·3505	7·851	0·019	1
73	0·3630	7·886	0·015	2	74	0·3688	7·893	0·012	1
75	0·3726	7·905	0·008	1	76	0·3762	7·898	0 015	1
77	0·3819	7·913	0·012	2	78	0·3875	7·909	0·010	1
79	0·3929	7·893	0·011	1	80	0·3979	7·895	0·014	2
81	0·4031	7·927	0·004	23	82	0·4075	7·931	0·003	40
83	0·4122	7·938	0·007	26	84	0·4176	7·945	0·006	31
85	0·4227	7·945	0·003	40	86	0·4275	7·954	0·003	46
87	0·4322	7·964	0·003	43	88	0·4374	7·985	0·003	49
89	0·4423	7·996	0·003	37	90	0·4474	8·015	0·003	46
91	0·4522	8·031	0·003	41	92	0·4574	8·050	0·003	49
93	0·4624	8·069	0·003	49	94	0·4674	8·088	0·003	43
95	0·4724	8·106	0·003	40	96	0·4774	8·124	0·003	42
97	0·4824	8·143	0·003	40	98	0·4873	8·158	0·003	37
99	0·4925	8·170	0·003	40	100	0·4975	8·176	0·003	36
101	0·5022	8·177	0·003	35	102	0·5075	8·168	0·002	32
103	0·5122	8·153	0 002	29	104	0·5175	8·136	0·002	30
105	0·5225	8·117	0·002	26	106	0·5274	8·098	0·002	22
108	0·5395	8·063	0·018	1	109	0·5434	8·040	0·008	1
113	0·5636	7·982	0·013	1	114	0·5675	7·962	0·014	1
118	0·5877	7·937	0·016	1	133	0·6639	7·864	0·010	1
136	0·6756	7·878	0·010	1	140	0·6997	7·873	0·012	1
144	0·7200	7·879	0·013	1	145	0·7238	7·869	0·012	1
149	0·7441	7·875	0·016	1	150	0·7480	7·879	0·011	1
157	0·7838	7·882	0·013	1	158	0·7877	7·925	0·018	1
159	0·7923	7·894	0·013	2	160	0·7962	7·910	0·012	2
162	0·8079	7·898	0·012	1	163	0·8112	7·913	0·012	1
164	0·8164	7·911	0·011	2	165	0·8203	7·867	0·018	1
167	0·8314	7·912	0·016	1	168	0·8353	7·911	0·013	1

TABLE III (*concluded*)

Bin number	*Orbital phase*	H_p (*mag.*)	ε (*mag.*)	n_{obs}	*Bin number*	*Orbital phase*	H_p (*mag.*)	ε (*mag.*)	n_{obs}
169	0·8425	7·922	0·016	4	172	0·8574	7·930	0·015	2
173	0·8640	7·939	0·009	2	174	0·8679	7·917	0·015	2
175	0·8707	7·948	0·008	1	176	0·8796	7·930	0·018	1
177	0·8835	7·967	0·012	1	178	0·8888	7·963	0·013	1
179	0·8929	7·971	0·015	2	183	0·9124	8·034	0·014	3
184	0·9165	8·036	0·013	4	186	0·9290	8·124	0·003	12
187	0·9322	8·145	0·003	42	188	0·9373	8·186	0·003	41
189	0·9424	8·234	0·003	43	190	0·9475	8·290	0·002	42
191	0·9525	8·349	0·002	39	192	0·9574	8·415	0·003	41
193	0·9622	8·490	0·004	38	194	0·9674	8·580	0·004	45
195	0·9723	8·668	0·003	40	196	0·9775	8·776	0·002	33
197	0·9825	8·885	0·003	30	198	0·9874	8·996	0·004	31
199	0·9925	9·105	0·003	29	200	0·9973	9·170	0·002	25

We used the LIGHT2[21] light-curve-synthesis code to analyse these data, adopting the spectroscopically defined mass ratio $q(\text{pri/sec}) = 3\cdot11$, as described earlier, as a fixed quantity. We also adopted a mean surface temperature for the primary component of $T_{\text{pri}} = 19000$ K on the basis of the disentangled spectrum being classified as B3, together with the temperature scale of Böhm-Vitense[22]. The model for the system derived from the light-curve analysis in combination with the orbital solution provides a determination of the ratio of fluxes between the two stars at different chosen wavelengths. This ratio of fluxes is a required input parameter for the spectral-disentangling solution discussed earlier. The orbital solution for the two velocity semi-amplitudes is insensitive to this ratio of fluxes, and the spectral-disentangling result is also robust against significant changes in this ratio. All of these issues were checked by several iterations of the whole procedure. The nett result is that the disentangled spectra shown in Fig. 2 are those with the final flux ratio, which may be compared directly with model-atmosphere flux spectra at different temperatures, discussed below. Suffice it to state here that these confirm the temperature adopted above for the primary component. The published *uvby* photometry[23] of IZ Per also confirms this result, again discussed below.

The LIGHT2 code was used to solve the light curve at fixed mass ratio, fixed primary component temperature, and adopting a primary component rotating synchronously (102 km s^{-1}) and at $1\cdot8\times$ synchronism, close to the two published values of $v \sin i = 98$ km s^{-1} and 185 km s^{-1}. The results for the $1\cdot8\times$ synchronism solution are listed in Table IV and both solutions are plotted in Fig. 3. The mean radius of the primary component is reduced by 0·0028 in the synchronous solution, and the orbital inclination is reduced by 0°·2, both negligible amounts. The overall fit of the non-synchronous-solution light curve is better than that of the synchronous solution in the out-of-eclipse regions, but there are no differences in eclipses. This latter finding is in agreement with the earlier photometric study[10] with its unpublished light curve. The geometrical elements derived in that study are very similar to those listed here, although the mass ratio is somewhat different. The uncertainty on the mean T_{eff} for the secondary component given in Table IV is that from the formal solution of the light curve and does not take account of any uncertainty in the mean T_{eff} of the primary component.

The solution of the light curve confirms that the system is in a semi-detached state, with the less-massive, smaller and cooler secondary component filling its

Roche lobe and the more-massive, larger and hotter primary component being detached from its Roche lobe. The system IZ Per is confirmed to be a normal Algol-type binary, presumably, from its recently constant orbital period, in a quiescent phase of the longer-lived slow-mass-transfer stage of Case-A binary-star evolution.

TABLE IV

Solution of combined light curve

Parameter	*Primary*	*Secondary*
Mean relative radius	0·3170 ± 0·0009	0·2913 ± 0·0009
Fraction of Roche lobe filled	0·79	1·00
Mean $T_{\rm eff}$ (K)	19000 adopted	9500 ± 50
Gravity-darkening exponent	0·25	0·25
Limb-darkening coefficient	0·32	0·49
Heating fraction	0·75	0·90
Electron-scattering fraction	0·25	0·10
Mass ratio	3·11 fixed	
Orbital inclination	88°·22 ± 0°·22	

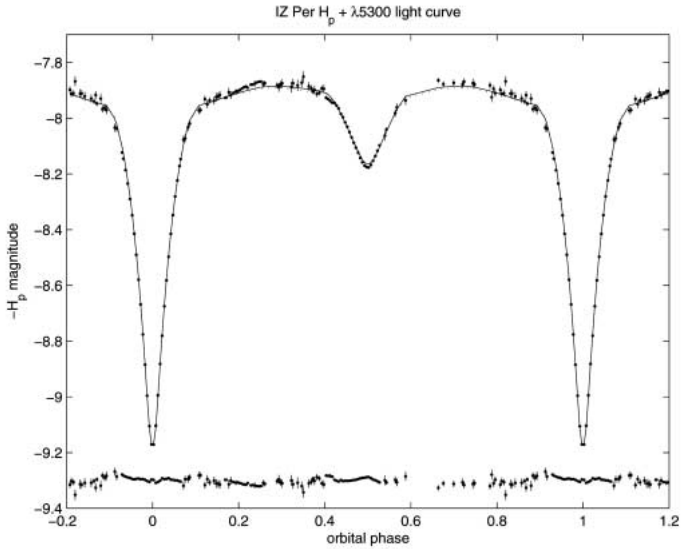

FIG. 3

The combined H_p and λ5300 light curve, plotting average values within 138 bins, with associated uncertainties. The solid line is the final model fit adopting $v \sin i = 185$ km s^{-1} for the primary component, and the (*O*–*C*) values are plotted at a vertical offset of $-9^{\rm m}\cdot30$ for clarity. The dotted line (just visible) is the final fit adopting synchronous rotation of the primary component.

TABLE V

Astrophysical parameters for IZ Per

Parameter	*Primary*	*Secondary*
Mass ($M_\odot$)	$9 \cdot 97 \pm 0 \cdot 55$	$3 \cdot 20 \pm 0 \cdot 17$
Radius($R_\odot$)	$7 \cdot 51 \pm 0 \cdot 13$	$6 \cdot 90 \pm 0 \cdot 12$
log g	$3 \cdot 684 \pm 0 \cdot 028$	$3 \cdot 264 \pm 0 \cdot 027$
$T_{\rm eff}$ (K)	19000 ± 1000	9500 ± 1000
log $T_{\rm eff}$	$4 \cdot 279 \pm 0 \cdot 023$	$3 \cdot 978 \pm 0 \cdot 046$
$\log(L/L_\odot)$	$3 \cdot 852 \pm 0 \cdot 093$	$2 \cdot 575 \pm 0 \cdot 184$
M_V	$-2 \cdot 98 \pm 0 \cdot 26$	$-1 \cdot 55 \pm 0 \cdot 48$

Astrophysical parameters

The final astrophysical parameters for both components of IZ Per are listed in Table V. An uncertainty of ± 1000 K was adopted for the primary component (and hence also the secondary component) from comparisons between the disentangled spectrum of the primary component and model-atmosphere spectra, discussed below.

Two observations[23] of IZ Per were obtained in the *uvby* photometric system at non-eclipse phases. These values were in good agreement and mean values were adopted of $(b–y) = 0^{\rm m} \cdot 119$, $m_1 = 0^{\rm m} \cdot 049$, and $c_1 = 0^{\rm m} \cdot 403$. Applying standard de-reddening procedures[24] for B stars to these values resulted in intrinsic colours for the IZ Per system of $(b–y)_0 = -0^{\rm m} \cdot 081$, $m_0 = 0^{\rm m} \cdot 113$, $c_0 = 0^{\rm m} \cdot 363$, and $E(b–y) = 0^{\rm m} \cdot 200$.

We compared these observed *uvby* colour indices of IZ Per with those expected from a binary composed of a B2 · 5 or B3 primary and the secondary defined by the flux ratios between the two components from the final light-curve solution at the effective wavelengths of the *uvby* filters. The average *uvby* colour indices for B2 · 5 and B3 stars[24] coupled with the flux ratios from the light-curve solution then yielded intrinsic colour indices for our model of IZ Per that agreed with the observed values to within ± $0^{\rm m} \cdot 01$–$0^{\rm m} \cdot 02$, in particular bracketing the temperature-sensitive c_0 index. These data confirm the spectral classification of B3 for the primary component.

The interstellar reddening value of $E(b–y) = 0^{\rm m} \cdot 200$ provides a total extinction in the standard V band of $A_V = 4 \cdot 3E(b–y) = 0^{\rm m} \cdot 86$. The observed V magnitude of IZ Per at orbital phase 0 · 845 is $V = 7^{\rm m} \cdot 80$[22], and the light curve shows that the system is $0^{\rm m} \cdot 04$ brighter at quadratures (phases 0 · 25 and 0 · 75). The flux ratio between the two stars is very well defined by the light curve solution at $f_{\rm pri}/f_{\rm sec} = 3 \cdot 938$, whilst the absolute visual magnitude of the primary component (Table V) is $M_V = -2^{\rm m} \cdot 98 \pm 0^{\rm m} \cdot 26$. The total absolute visual magnitude for the IZ Per system is then $M_{V,\rm total} = -3 \cdot 23 \pm 0 \cdot 26$ and the distance to IZ Per is $1062 \pm {}^{135}_{120}$ pc. This value may be compared with the *Hipparcos* parallax for IZ Per of $\pi = 1 \cdot 68 \pm 0 \cdot 91$ mas, corresponding to an uncertain distance of $595 \pm {}^{703}_{209}$ pc, which brackets the determination from our astrophysical parameters.

The properties of the IZ Per binary system are very similar to those of the semi-detached eclipsing binary *u* Her[25], and both seem to be well matched by the binary-evolution models published by Nelson & Eggleton[26], which find good agreement between the observational data on Algol-type binaries and their conservative Case-A evolution models.

Disentangled spectrum of the primary component

The disentangled spectrum of the primary component of IZ Per may be compared directly with a library of spectra[27] calculated from model atmospheres and displayed at a resolution of 1 Å, close to the resolution of our spectra at 0·9 Å. These model atmospheres were calculated for a standard solar composition, which may be applicable to the mass-gaining primary component of IZ Per. It was found from the library of spectra that the maximum depths of the He I lines occurred at an effective temperature $T_{\rm eff}$ = 19000 K. In Fig. 4 we plot the full spectrum of the primary component between λλ 4000–4500 Å together with the model spectra at $T_{\rm eff}$ = 19000 K, surface gravity log g = 3·50, and v sin i = 100 km s^{-1} and 200 km s^{-1}. The overall fit is remarkably good and confirms the adopted spectral classification of B3 and the adopted temperature calibration[21]. However, it is also clear that the depths of the He I lines in the disentangled spectrum are systematically greater than the models, particularly so for the singlet series lines rather than the triplet series. The H lines are well matched in depth but the model lines are somewhat narrower than in the disentangled spectrum. A selection of absorption lines is shown in more detail in Fig. 5. Perhaps these differences suggest that the helium abundance in the atmosphere of the primary component of IZ Per is rather greater than the solar value, whilst that of carbon (*cf.*, the C II λ4267 line) is lower than solar. A complete model-atmosphere analysis would be required to establish these factors, preferably by using new spectra at a resolution of 0·1 Å.

With regard to the axial rotation speed of the primary component, it should be noted that the synchronous rotation value of 100 km s^{-1} gives good line depths,

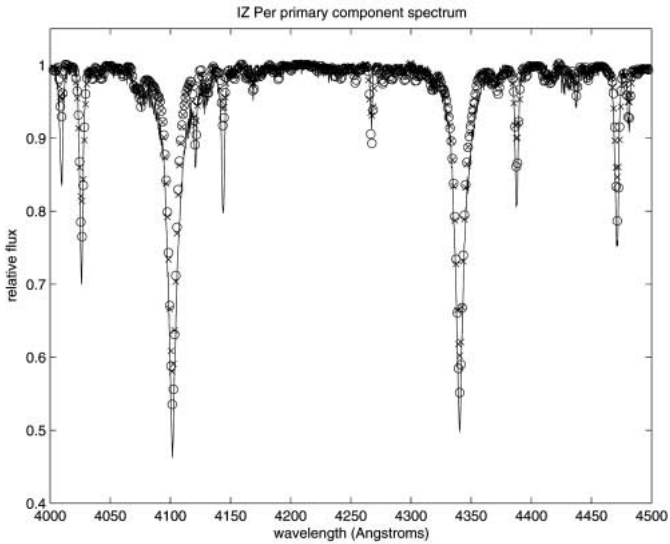

FIG. 4

The disentangled spectrum of the primary component of IZ Per plotted as a solid line from 4000 to 4500 Å. To show the model atmosphere spectra for comparison over the full wavelength range of the observed spectra, the model with v sin i = 100 km s^{-1} is plotted as open circles, whilst that with v sin i = 200 km s^{-1} is plotted as crosses.

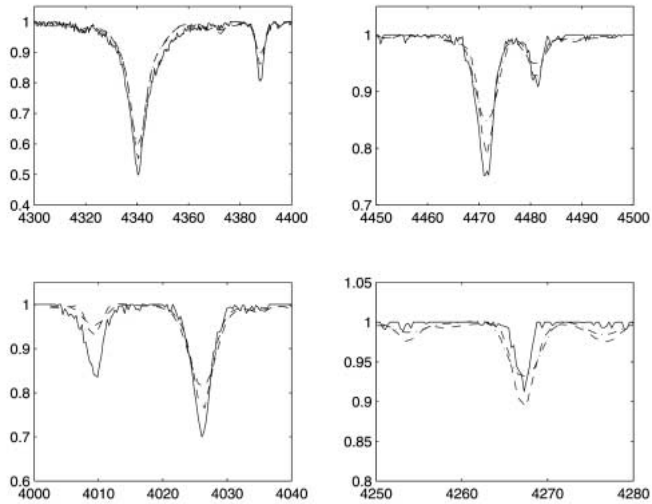

FIG. 5

Four selected regions of the disentangled spectrum of the primary component of IZ Per, plotted as a solid line for Hγ and He I λ4388, He I λ4471 and Mg II λ4481, He I λ4009, λ4026, and C II λ4267. The two model spectra are shown as dashed lines (v sin i = 100 km s^{-1}) and dashed-dotted lines (v sin i = 200 km s^{-1}).

but the line widths seem too narrow compared to the disentangled spectrum, and the 2 × synchronism value of 200 km s^{-1} gives shallower and broader lines as expected. But it is very clear that the resolution of these spectra is not sufficient to distinguish between the synchronous and non-synchronous rotation values for the primary component. The three-pixel spectral resolutions used in the two v sin i studies were, respectively, 0·9 Å and 0·6 Å, and perhaps the latter study has sufficient resolution to distinguish between these competing values of v sin i. Further spectroscopic studies at a resolution of 0·1 Å would resolve this matter and the issue of the chemical abundance of the primary component in such a mass-exchanging system[28].

Conclusions

The final astrophysical parameters for the components of IZ Per are as precise as the present data set and the procedures for analysis will allow. To make further progress, particularly determining the rotational velocity of the primary component and the chemical abundances of both stars, would require high-resolution spectra and complete light curves, preferably at several monochromatic wavelengths, and defined by observations with uncertainties of ± 0^{m}·002.

References

(1) W. Strohmeier, *Kl. Veröff. Rem. Sternw. Bamberg*, Nr. 24, 1958.
(2) M. A. C. Perryman *et al.*, *The Hipparcos and Tycho Catalogues* (SP-1200, ESA Publications, Noordwijk), 1997.
(3) I. Yavuz, *A&A*, **2**, 388, 1969.
(4) E. P. J. van den Heuvel, in A. Slettebak (ed.), *Stellar Rotation* (Reidel, Dordrecht), 1970, p. 178.
(5) R. K. Srivastava & T. D. Padalia, *BAC*, **21**, 359, 1970.
(6) H. N. Russell & J. E. Merrill, *Princeton Contr.*, No. 26, 1952.
(7) F. Mardirossian *et al.*, *A&AS*, **40**, 57, 1980.
(8) D. B. Wood, *A Computer Program for Modeling Non-Spherical Eclipsing Binary Systems* (Goddard Space Flight Center, Greenbelt, Maryland), 1972.
(9) R. K. Srivastava, *ApSpSci*, **132**, 125, 1987.
(10) G. W. Wolf & S. R. D. West, in K. C. Leung & I.-S. Nha (eds.), *New Frontiers in Binary Star Research* (ASP Conf. Series, **38**), 1993, p. 312.
(11) R. E. Wilson, *ApJ*, **356**, 613, 1990.
(12) P. B. Etzel & E. C. Olson, *AJ*, **106**, 1200, 1993.
(13) R. K. Srivastava, *ApSpSci*, **129**, 143, 1987.
(14) V. Símon, *A&AS*, **134**, 1, 1999.
(15) G. Hill, *PDAO*, **16**, 59, 1982.
(16) G. Hill, *RVORBIT*, unpublished DAO manual, 1986.
(17) T. J. Harries, R. W. Hilditch & I. D. Howarth, *MNRAS*, **339**, 157, 2003.
(18) N. R. Walborn & E. L. Fitzpatrick, *PASP*, **102**, 379, 1990.
(19) D. E. Holmgren, G. Hill & W. A. Fisher, *A&A*, **236**, 409, 1990.
(20) D. L. Pollacco *et al.*, *PASP*, **118**, 1407, 2006.
(21) G. Hill, *PDAO*, **15**, 297, 1979.
(22) E. Böhm-Vitense, *ARAA*, **19**, 295, 1981.
(23) R. W. Hilditch & G. Hill, *Mem.RAS*, **79**, 101, 1975.
(24) D. L. Crawford, *AJ*, **83**, 48, 1978.
(25) R. W. Hilditch, *The Observatory*, **125**, 72, 2005.
(26) C. A. Nelson & P. P. Eggleton, *ApJ*, **552**, 664, 2001.
(27) U. Munari *et al.*, *A&A*, **442**, 1127, 2005; and http://gaia.esa.int/spectralib/.
(28) M. J. Sarna & J.-P. de Greve, *QJRAS*, **37**, 11, 1996.

SPECTROSCOPIC BINARY ORBITS FROM PHOTOELECTRIC RADIAL VELOCITIES

PAPER 192: HD 172401

By R. F. Griffin
Cambridge Observatories

HD 172401 is a K-giant star that has often been used as a spectrophotometric and radial-velocity reference in studies of galaxies, but its own interest has until now been overlooked. It is shown to be a binary system with a period of 24 years and a very high eccentricity (0·85).

Introduction

The subject of this paper is a 7^m star in the extreme eastern peninsula of Ophiuchus; it is to be found less than half a degree following the variable star X Oph (which is marked in star atlases such as *Norton*), or, in a broader context, it is halfway between Altair (α Aql) and Rasalhague (α Oph).

There is just one paper that gives HD 172401's V and B magnitudes, and also its spectral type; that paper[1], by Fernie, is really about X Oph, for which HD 172401 formed a convenient nearby standard. The magnitudes $V = 6^m{\cdot}98$, $(B-V) = 1^m{\cdot}07$ were determined at Mount Wilson by Arp (who was at that time a colleague of Fernie's at the Goethe Link Observatory), and the classification K0 III was made on a plate obtained with the Newtonian spectrograph of the Goethe Link 36-inch reflector.

Even though HD 172401 was only of oblique interest in that paper, it did at least receive *some* attention itself. It was the start of a career in which the star was 'always the bridesmaid, never the bride'! — until now. Out of 14 papers listed for it by *Simbad*, in no fewer than ten the star is mentioned merely as a 'template' or standard for spectrophotometry and/or radial velocity, for comparison with galaxies — except in the one case[1] already mentioned — although it is difficult to see how it could act as a standard of radial velocity when its own velocity was unknown. In the remaining four papers, one gives the polarization of its light (which tells us nothing about the star itself), two give spectrophotometric indices in the context of a large programme (but deduce nothing from them about the star), and the fourth refers merely to its entry in a catalogue. In the 'galaxy' papers, the magnitude and/or type as given by Fernie[1] is sometimes listed, but in one case[2] (where its spectral type appears to be unknown) its radial velocity is given, as $-73{\cdot}0$ km s^{-1}, and in another[3] it is given as $+23{\cdot}6$ km s^{-1}. Those are the only radial velocities that have ever been proposed for HD 172401, to the writer's knowledge, and as will become apparent below they are both wildly in error.

Hipparcos measured the magnitude of HD 172401 as $7^m{\cdot}01$; the parallax corresponds to a distance modulus of about $6^m{\cdot}8 \pm 0^m{\cdot}5$, and so to an absolute magnitude of about $+0^m{\cdot}2$ with the same uncertainty. The star is clearly a normal giant, and its classification[1] as K0 III agrees well with its colour index.

New radial velocities and orbit

The radial velocity of HD 172401 was first measured rather casually by Dr. J. E. Gunn and the writer during an observing run in 1978 with our spectrometer[4] on the 200-inch Palomar telescope, in response to a request from a third party (identity now forgotten!) to know its radial velocity for use in connection with a project on galaxies. The velocity was found to be $-0{\cdot}7$ km s^{-1}. Four years later, after a similar request was received from Dr. R. L. Davies, the star was re-observed with the Cambridge spectrometer, and its velocity was found to have changed —it was then about $+7$ km s^{-1}. The object was thereupon transferred to the spectroscopic-binary programme and observed once a month when it was conveniently accessible in the sky. Its velocity declined only very slowly, so after a few years the frequency of observation was halved. The decline seemed to become ever slower, approaching only asymptotically the original Palomar level. The slower it became, the higher was the implied eccentricity of the orbit, and it was obvious that a point would ultimately be reached at which there would have to be a sudden rise which must on no account be missed. Accordingly, when the velocity finally was down to zero in 2000 and was, within possible observational error, the same as in the

original observation, the observer felt a need to watch very carefully for the impending rise which might be of any degree of abruptness. The frequency of observations was accordingly restored to one a month, and was maintained even when the object was not *conveniently* accessible — indeed there was a measurement in every calendar month in 2002. At last a rise began in 2003, slow at first, and then violently accelerating just at the season of the year when the star was almost out of reach and the nightly window of accessibility was very short and the weather uncooperative! The rise was, however, tolerably well documented, and the nodal passage and initial decline have been carefully monitored. The systematic measurements now cover the full cycle, and there seems little to be gained by deferring publication any longer, unless indeed it is put off until after the next periastron passage in late 2027, when the orbital period will be determinable within an uncertainty of less than a day. Such deferral would not be a wise course for the current observer, so the orbit is presented now.

For reasons sufficiently excused above, there is the unusually large number of 174 radial-velocity measurements available; they are set out in Table I. The main sources are the original radial-velocity spectrometer at Cambridge (42 velocities), the Haute-Provence *Coravel* (34), and the Cambridge *Coravel* (87). The usual adjustment of $+0{\cdot}8$ km s^{-1} to the Haute-Provence measures brings them into systematic accord with the 'original Cambridge' ones with which they are in part satisfactorily intermingled, while an adjustment of $-0{\cdot}2$ km s^{-1}, which is in line with accumulating experience of the matter (*cf.* Paper 190[5]), has been applied to the Cambridge *Coravel* values. The two *Coravel*s yield very similar residuals with respect to the velocity curve and have been equally weighted; the 'original Cambridge' data have warranted a weighting of $0{\cdot}15$. Then there are three minor sources of velocities — Palomar (2), the Dominion Astrophysical Observatory (7), and the ESO *Coravel* (2); they have all been somewhat arbitrarily weighted $^1/_3$, a value that does, however, do reasonable justice to their residuals. The orbit then readily follows; it is illustrated in Fig. 1 and its elements are:

$P = 8631 \pm 59$ days
$\gamma = +2{\cdot}44 \pm 0{\cdot}03$ km s^{-1}
$K = 7{\cdot}52 \pm 0{\cdot}05$ km s^{-1}
$e = 0{\cdot}8485 \pm 0{\cdot}0020$
$\omega = 307{\cdot}3 \pm 0{\cdot}6$ degrees
$(T)_2 =$ MJD $53096{\cdot}5 \pm 1{\cdot}5$
$a_1 \sin i = 472 \pm 5$ Gm
$f(m) = 0{\cdot}0565 \pm 0{\cdot}0015\ M_\odot$
R.m.s. residual (wt.1) $= 0{\cdot}27$ km s^{-1}

Discussion

The orbital period is long for a spectroscopic binary, but is not quite the longest to be documented in this series of papers — it has been exceeded[6] by the rather uncertain value of 9749 days for HD 22046 in Paper 165 and the 9610 days for 85 Peg in Paper 177. Of course the designation of a binary as being a spectroscopic one is artificial, and binaries observable visually usually have longer periods than that of HD 172401, periods ranging up to thousands of years; in the cases of common-proper-motion pairs which have not yet shown any detectable relative motion, even astrometrically, the periods may run into millions of years. The eccentricity of the orbit determined here is high, but again it is not the highest to be found in this series — there have been seven higher, including three above $0{\cdot}9$; a discussion of high eccentricities is to be found[7] in Paper 173.

The mass function requires the companion star to have a mass of not less than $0{\cdot}75\ M_\odot$ if the primary is supposed to be of $2\ M_\odot$; it could be a white dwarf but

Table I

Radial-velocity observations of HD 172401

Except as noted, the sources of the observations are as follows:
1978–1991 — original Cambridge spectrometer (weighted 0·15 in orbital solution);
1992–1998 — Haute-Provence Coravel (wt. 1); 1999–2006 — Cambridge Coravel (wt. 1)

Date (UT)	*MJD*	*Velocity km s^{-1}*	*Phase*	*(O−C) km s^{-1}*
1978 May 23·44★	43651·44	−0·7	0·906	+0·2
1982 July 9·98	45159·98	+7·4	1·081	+0·7
16·01	166·01	+8·0	·081	+1·4
19·93	169·93	+7·0	·082	+0·4
1983 May 10·10	45464·10	+4·7	1·116	−0·9
June 9·04	494·04	+5·4	·119	−0·1
July 2·98	517·98	+5·4	·122	0·0
Aug. 3·90	549·90	+3·4	·126	−2·0
Sept. 18·83	595·83	+5·3	·131	+0·1
Oct. 13·20★	620·20	+4·3	·134	−0·9
24·14†	631·14	+5·9	·135	+0·7
Nov. 21·71	659·71	+6·7	·138	+1·6
1984 Apr. 17·13	45807·13	+4·2	1·155	−0·6
May 13·06	833·06	+4·8	·158	+0·1
July 28·92	909·92	+4·7	·167	+0·1
Aug. 30·88	942·88	+5·5	·171	+1·0
Sept. 22·82	965·82	+3·2	·174	−1·3
Dec. 10·70	46044·70	+4·9:	·183	+0·6
1985 May 31·05	46216·05	+4·0	1·203	−0·1
July 6·97	252·97	+3·9	·207	−0·1
Oct. 5·81	343·81	+4·2	·218	+0·3
Nov. 2·76	371·76	+3·4	·221	−0·5
1986 Apr. 5·15‡	46525·15	+3·2	1·239	−0·5
May 14·05	564·05	+3·6	·243	0·0
June 15·01	596·01	+4·4	·247	+0·8
July 4·00	615·00	+3·8	·249	+0·2
Aug. 24·88‡	666·88	+3·2	·255	−0·3
Sept. 25·85	698·85	+3·1	·259	−0·4
Oct. 11·78	714·78	+3·1	·261	−0·3
Nov. 8·75	742·75	+4·2	·264	+0·8
1987 Mar. 4·21‡	46858·21	+3·1	1·277	−0·2
May 5·08	920·08	+3·2	·284	0·0
June 23·00	969·00	+2·4	·290	−0·8
July 4·96	980·96	+3·9	·291	+0·7
18·16§	994·16	+2·6	·293	−0·6
Oct. 12·82‡	47080·82	+3·9	·303	+0·8
Nov. 6·99§	105·99	+2·7	·306	−0·3
Dec. 7·71	136·71	+3·7	·310	+0·7
1988 Feb. 1·62†	47192·62	+3·3	1·316	+0·3
Mar. 14·19‡	234·19	+3·3	·321	+0·4
June 1·05	313·05	+2·9	·330	0·0
July 11·98	353·98	+1·9	·335	−0·9
Sept. 12·88	416·88	+2·0	·342	−0·8
Nov. 2·76‡	467·76	+2·6	·348	−0·1

TABLE I (*continued*)

Date (*UT*)	*MJD*	*Velocity km s*$^{-1}$	*Phase*	(*O*−*C*) *km s*$^{-1}$
1989 Mar. 27·17‡	47612·17	+2·4	1·365	−0·2
Apr. 30·11‡	646·11	+2·6	·369	0·0
May 27·04	673·04	+3·7	·372	+1·1
June 20·00	697·00	+2·3	·374	−0·2
July 11·96	718·96	+1·4	·377	−1·1
Oct. 17·76	816·76	+2·3	·388	−0·1
Nov. 1·75‡	831·75	+2·5	·390	+0·1
23·73	853·73	+2·7	·393	+0·3
1990 Jan. 31·25‡	47922·25	+2·7	1·401	+0·3
Mar. 13·51†	963·51	+1·6	·405	−0·7
May 27·06	48038·06	+2·9	·414	+0·6
July 5·97	077·97	+2·3	·419	+0·1
Oct. 6·85	170·85	+1·5	·429	−0·7
1991 Jan. 29·24‡	48285·24	+2·1	1·443	0·0
June 14·02	421·02	+1·9	·458	−0·1
July 28·90	465·90	+1·3	·464	−0·7
Oct. 29·75‡	558·75	+2·1	·474	+0·2
1992 Feb. 27·57†	48679·57	+1·5	1·488	−0·3
Apr. 25·12	737·12	+1·6	·495	−0·2
June 21·02	794·02	+2·0	·502	+0·3
Aug. 13·93	847·93	+1·4	·508	−0·3
Dec. 18·71	974·71	+1·6	·522	0·0
1993 Feb. 18·22	49036·22	+1·4	1·530	−0·2
Mar. 19·21	065·21	+1·8	·533	+0·2
July 7·04	175·04	+1·6	·546	+0·1
Sept. 13·81	243·81	+1·5	·554	+0·1
Nov. 5·01	296·01	+1·8	·560	+0·4
1994 May 3·09	49475·09	+1·2	1·580	−0·1
July 29·95	562·95	+0·8	·591	−0·4
Dec. 11·72	697·72	+0·8	·606	−0·3
1995 June 2·05	49870·05	+0·8	1·626	−0·2
1996 Mar. 30·18	50172·18	+0·8	1·661	0·0
Apr. 25·15	198·15	+0·7	·664	−0·1
Nov. 18·74¶	405·74	+0·7	·688	0·0
Dec. 15·71	432·71	+0·8	·691	+0·1
1997 Mar. 31·14¶	50538·14	0·0	1·704	−0·6
Apr. 16·15¶	554·15	+0·2	·705	−0·4
June 20·10¶	619·10	+0·7	·713	+0·2
July 19·98	648·98	+0·5	·716	0·0
Sept. 9·85	700·85	+0·1	·722	−0·4
Dec. 21·71	803·71	0·0	·734	−0·4
1998 Apr. 29·11	50932·11	+0·1	1·749	−0·2
May 4·11	937·11	+0·1	·750	−0·2
July 8·03	51002·03	0·0	·757	−0·2
1999 Apr. 2·49†	51270·49	+0·2	1·788	+0·2
July 9·36†	368·36	−0·2	·800	−0·2
Nov. 3·11†	485·11	+0·2	·813	+0·3

TABLE I (*continued*)

Date (*UT*)	*MJD*	*Velocity km s*$^{-1}$	*Phase*	(*O*−*C*) *km s*$^{-1}$
2000 Mar. 4·22	51607·22	−0·5	1·827	−0·2
Apr. 6·18	640·18	−0·5	·831	−0·2
May 14·10	678·10	−0·6	·836	−0·3
June 7·05	702·05	−0·4	·838	−0·1
July 18·03	743·03	−0·3	·843	+0·1
Aug. 14·03	770·03	−0·3	·846	+0·1
Sept. 20·85	807·85	−0·2	·851	+0·2
Oct. 13·79	830·79	−0·3	·853	+0·2
Nov. 1·81	849·81	−0·3	·856	+0·2
Dec. 3·70	881·70	−0·3	·859	+0·2
2001 Feb. 14·24	51954·24	−1·0	1·868	−0·4
Apr. 29·10	52028·10	−0·9	·876	−0·2
May 5·13	034·13	−0·8	·877	−0·1
June 8·07	068·07	−0·2	·881	+0·5
July 4·04	094·04	−0·1	·884	+0·6
Aug. 1·90	122·90	0·0	·887	+0·7
14·96	135·96	−0·5	·889	+0·3
Sept. 22·82	174·82	−0·8	·893	0·0
Oct. 18·78	200·78	−0·9	·896	−0·1
Nov. 22·71	235·71	−1·0	·900	−0·1
Dec. 7·70	250·70	−1·4	·902	−0·5
2002 Jan. 31·26	52305·26	−1·3	1·908	−0·4
Feb. 21·25	326·25	−1·1	·911	−0·1
Mar. 27·14	360·14	−1·1	·915	−0·1
Apr. 18·15	382·15	−0·9	·917	+0·1
May 16·07	410·07	−1·0	·920	0·0
June 1·06	426·06	−1·1	·922	0·0
July 4·00	459·00	−0·7	·926	+0·4
Aug. 6·97	492·97	−0·7	·930	+0·4
Sept. 1·87	518·87	−0·9	·933	+0·2
Oct. 3·80	550·80	−1·2	·937	0·0
Nov. 4·74	582·74	−0·8	·940	+0·4
Dec. 4·70	612·70	−1·3	·944	−0·1
2003 Feb. 15·24	52685·24	−1·5	1·952	−0·3
Mar. 15·22	713·22	−1·5	·956	−0·3
Apr. 7·17	736·17	−1·0	·958	+0·2
May 1·12	760·12	−0·9	·961	+0·3
June 11·08	801·08	−0·8	·966	+0·3
July 13·01	833·01	−0·8	·969	+0·2
Aug. 2·95	853·95	−0·4	·972	+0·4
Sept. 10·91	892·91	−0·4	·976	+0·1
Oct. 14·81	926·81	−0·3	·980	−0·2
Nov. 24·70	967·70	+0·5	·985	−0·3
Dec. 5·70	978·70	+1·0	·986	−0·2
2004 Feb. 9·24	53044·24	+5·0	1·994	−0·2
26·24	061·24	+7·0	·996	0·0
Mar. 2·24	066·24	+7·5	·996	0·0
17·18	081·18	+9·0	·998	−0·2
31·16	095·16	+10·7	2·000	0·0
Apr. 3·17	098·17	+11·0	·000	0·0
7·19	102·19	+11·9	·001	+0·5
15·16	110·16	+12·2	·002	+0·1
20·15	115·15	+12·6	·002	+0·1
May 6·10	131·10	+13·3	·004	0·0
17·09	142·09	+13·5	·005	−0·2

TABLE I (*concluded*)

Date (*UT*)	*MJD*	*Velocity* km s^{-1}	*Phase*	(*O*−*C*) km s^{-1}
2004 May 22·07	53147·07	+13·6	2·006	−0·1
31·06	156·06	+13·6	·007	−0·2
June 8·06	164·06	+13·9	·008	+0·1
15·10	171·10	+13·7	·009	−0·1
22·05	178·05	+13·7	·009	0·0
July 5·08	191·08	+13·4	·011	−0·1
Aug. 7·92	224·92	+12·8	·015	0·0
19·95	236·95	+12·5	·016	0·0
Sept. 3·93	251·93	+12·0	·018	−0·1
Oct. 5·83	283·83	+11·4	·022	−0·1
25·79	303·79	+10·9	·024	−0·2
Nov. 13·76	322·76	+10·7	·026	−0·1
Dec. 11·70	350·70	+9·7	·029	−0·6
2005 Mar. 12·23	53441·23	+9·5	2·040	+0·4
Apr. 19·17	479·17	+8·9	·044	+0·2
May 23·08	513·08	+8·7	·048	+0·3
June 14·03	535·03	+8·6	·051	+0·4
July 18·03	569·03	+8·1	·055	+0·1
Aug. 15·95	597·95	+7·9	·058	+0·1
Sept. 14·91	627·91	+7·7	·062	+0·1
Oct. 27·76	670·76	+7·4	·067	+0·1
Nov. 29·73	703·73	+7·3	·070	+0·2
2006 Mar. 23·19	53817·19	+6·5	2·083	−0·1
Apr. 26·14	851·14	+6·4	·087	0·0
May 30·07	885·07	+6·5	·091	+0·2
June 22·05	908·05	+6·5	·094	+0·3
July 18·02	934·02	+6·1	·097	0·0
Aug. 28·95	975·95	+5·9	·102	−0·1

*Observed with Palomar 200-inch telescope (weight 1/3).
†Observed with DAO 48-inch telescope (weight 1/3).
‡Observed with Haute-Provence *Coravel* (weight 1).
§Observed with ESO *Coravel* (weight 1/3).
¶Observed with Cambridge *Coravel* (weight 1).

is more likely to be a lower-main-sequence star of late-F, G, or early-K type. No evidence of it has been seen in radial-velocity traces, or reported by the authors who have taken spectra of HD 172401 for comparison with galaxies, although such spectra are probably not of the quality that could be obtained if the principal interest were in the star itself. If for the sake of illustration we take the mass of the secondary as being half that of the primary, the projected semi-major axis of the relative orbit is three times that of the orbit of the primary, or in round numbers 9 AU. Even at periastron, when the separation is reduced by a factor of $(1-e)$, it is still nearly $1\frac{1}{2}$ AU, so the system is very well detached. At the distance of about 230 pc implied by the parallax, the characteristic angular separation can be expected to be something like $9/(230 \sin i)$ seconds of arc, or about $0''\cdot04/\sin i$. The difficulty that it may present to optical interferometry therefore resides more in the Δm value, which is likely to be in the range 4–6 magnitudes (unless the companion is a white dwarf, in which case the disparity would be greater), than in the angular separation.

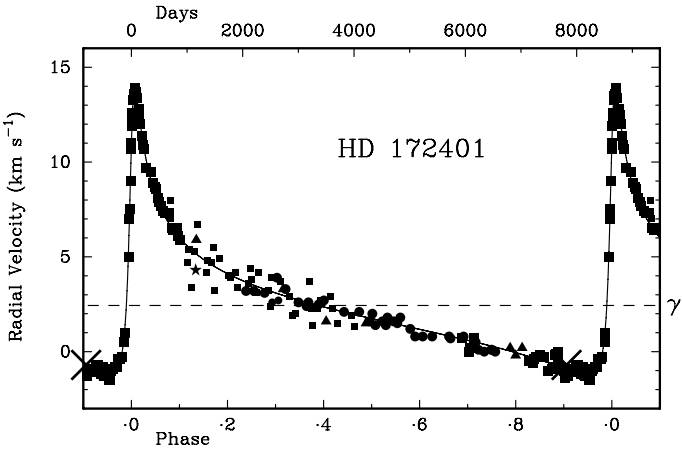

FIG. 1

The observed radial velocities of HD 172401 plotted as a function of phase, with the velocity curve corresponding to the adopted orbital elements drawn through them. The observations cover little more than one cycle, and although they are plotted in terms of phase they can also be viewed as plotted directly against time, the diagram running between calendar years 1978 at the left-hand end to 2006 at the right, although the earliest and latest observations reappear in the overlapping parts of the plot at the two ends. The initial Palomar observation (1978) is plotted at the extreme left as the large cross, which has deliberately been made conspicuous and allowed to project beyond the boundary of the figure. The next measurements were not until 1982, and were made with the original photoelectric spectrometer in Cambridge; they are plotted as small squares and have been weighted 0·15 in the solution of the orbit. The seven DAO velocities are shown as triangles, two ESO ones as small circles, and one further Palomar measure appears as a star symbol; they were all weighted $^1/_3$. Later observations were made successively with the *Coravel* spectrometers at Haute-Provence (circles, weight 1) and Cambridge (squares, weight 1). The seemingly unnecessary frequency of the measurements near the descending node around phase ·9 arose because when at last, after more than 20 years' observations, the velocity of the star approached the level that it had when it was first observed at Palomar, a rise of unknown and possibly extreme suddenness and amplitude was clearly imminent and was on no account to be missed. When it did occur, it was not covered observationally quite as well as might be wished, owing to its perverse timing at just the season when the star was scarcely accessible in the sky.

The two radial velocities published[2,3] for HD 172401 are clearly far outside the range of variation of the actual velocity. The paper[3] that gives the value $+23{\cdot}6$ km s^{-1} appears to have obtained it from its authors' own observation with a 'nebular spectrograph'. If that instrument could really give an error of $\sim$20 km s^{-1} on a bright star with a spectral type ideal for velocity measurement, its result hardly warrants quoting to 0·1 km s^{-1}. On the other hand, the other two 'template spectra' to which reference is made in the paper[3] are attributed velocities that are accurately those that were already to be found for them in the literature.

As a matter of curiosity, the writer took a look at the other radial-velocity standards in the paper[2] that lists a velocity of $-73{\cdot}0$ km s^{-1} for HD 172401. The authors of that paper say that their data were drawn from references, which they give, and none of which includes HD 172401, so the origin of the mistake remains obscure. They had 20 standards altogether, of which nine are to be recognized in the list (*not* one of the four that are referenced) that Heard[8] offered of 'faint standards', and the velocities that they are attributed[2] are indeed those published by Heard. All but one of the others have clearly been taken from Abt & Biggs' biblio-

graphical compilation[9], which is one of the four referenced listings. In most cases more than one value is given there for the star concerned, from different papers, and in every case the value selected by the authors of ref. 2 is that cited from Abt's catalogue[10] of Mount Wilson radial velocities that had not previously been published individually. It appears that those authors had not got a radial-velocity expert to advise them, for they must have made their selection on the basis that Abt's was the most recent publication (it appeared quite shortly before the bibliography[9] itself), notwithstanding that in many cases it presented the oldest and possibly least reliable velocities — they preferred Abt[10] even to Campbell & Moore[11]! Although the discrepancies between different papers as regards stellar velocities might be seen by galaxy experts as irrelevant niceties, one would hope that an error of more than 70 km s^{-1}, such as was made in the case of HD 172401, would have *some* significance even to *galactic* velocities!

References

(1) J. D. Fernie, *ApJ*, **130**, 611, 1959.
(2) K. R. Mueller *et al.*, *A&AS*, **140**, 327, 1999.
(3) I. Jørgensen *et al.*, *AJ*, **129**, 1249, 2005.
(4) R. F. Griffin & J. E. Gunn, *ApJ*, **191**, 545, 1974.
(5) R. F. Griffin, *The Observatory*, **126**, 338, 2006 (Paper 190).
(6) R. F. Griffin, *The Observatory*, **122**, 210, 2002; **124**, 210, 2004 (Papers 165 and 177).
(7) R. F. Griffin, *The Observatory*, **123**, 344, 2003 (Paper 173).
(8) J. F. Heard, *PDDO*, **3**, 11, 1972.
(9) H. A. Abt & E. S. Biggs, *Bibliography of Stellar Radial Velocities* (Kitt Peak Nat. Obs., Tucson), 1972.
(10) H. A. Abt, *ApJS*, **19**, 387, 1970.
(11) W. W. Campbell & J. H. Moore, *Publ. Lick Obs.*, **16**, 1928.

FIRST VISIBILITY OF THE LUNAR CRESCENT: BEYOND DANJON'S LIMIT

By A. H. Sultan
Physics Department, Sana'a University, Yemen

Many methods for predicting lunar first visibility have been proposed throughout history and new models are still being developed. All these models have to be compared with the published observations to test their validity.

In this paper, we use our photometric model to predict the naked-eye first visibility of the lunar crescent. We find that an elongation of about $7 \cdot 5°$ is the lowest naked-eye visibility limit. We also find that the lunar crescent may be seen — with a suitable telescopic magnification and ideal local conditions — when the Moon is about 5° from the Sun. Consequently, the thin lunar crescent may be seen in a telescope even at new moon when the Moon is at its greatest inclination.

Introduction

Methods for predicting first sighting of the new crescent moon have been around since the time of the Sumerians. Efforts for obtaining an astronomical criterion for predicting the time of first lunar visibility go back to the Babylonian era, with significant improvements and work done later by ancient Hebrew and Muslim scientists and others.

In the 20th Century, Fotheringham[1], Maunder[2], Danjon[3], Bruin[4], McNally[5], Schaefer[6], Ilyas[7], Yallop[8], Fatoohi[9], Caldwell[10], and recently Odeh[11] have developed empirical methods for predicting first sighting of the new crescent moon. Each of them made a collection of observations of first visibility of the crescent and used statistical analysis to find a minimum elongation for the Moon to be first seen: 12° for Fotheringham, 11° for Maunder, 10–10·5° for Yallop and Ilyas[9], 7·5° for Fatoohi, 7° for Danjon and Schaefer, 6·4 ° for Odeh, and 5° for McNally.

After testing all empirical models, Doggett & Schaefer[12] have claimed the model by Schaefer yielded a significantly better prediction than any other algorithm. Fatoohi and his colleagues at the University of Durham examined the Danjon limit by using 52 observations (with elongations $\leqslant 9{\cdot}4°$) extracted from 503 ancient and modern observations of first and last visibility of the lunar crescent. They deduced that Danjon's 7° limit should actually be revised to 7·5°.

In effect, within their empirical methods, Bruin, Schaefer, and Yallop have all tried to take into consideration some physical aspects concerning prediction of first lunar visibility. In this paper, we are following in their steps, benefitting from new technologies and recent researches, especially in eye perception[13–15].

Parameters to be considered

For evaluating a physical (photometric) method that predicts the first visibility of the lunar thin crescent, the factors to be considered are: (*i*) the geometry of the Sun, the Moon, and the horizon, (*ii*) the width and luminance of the crescent, (*iii*) the absorption of moonlight by the atmosphere, (*iv*) the scattering of light in the atmosphere, and (*v*) the psychophysiology of human vision. The first three factors can be calculated easily. Factor (*iv*) depends on the local conditions and we are obliged to make appropriate measurements[16]. Factor (*v*) has been discussed in one of our earlier works[17].

Discussion

As we have mentioned previously, prediction of the first sighting of the early crescent moon is a complex problem because it involves a number of highly non-linear variables simultaneously. It is very popular to use the age of the Moon (*i.e.*, the time of sighting since the instant of new moon) to predict if the young crescent will be visible. The naked-eye record (15·0 hours) set on 1990 February 25 by John Pierce[18] is still unbroken. However, sometimes even a 30-hour-old crescent can remain invisible if the Moon is low in the sky at sunset and well to the north or south of the sunset point. For this reason, we consider in our calculations the perfect geometrical situation when the difference in azimuth between the Sun and the Moon at the moment of observation equals zero.

By measuring the twilight-sky luminance and considering our site elevation, we fix the local atmospheric conditions. Moreover, we have calculated the optimum lunar altitude for first visibility[16], so the only variable still to be considered is the

lunar elongation. We know that the Moon can pass directly in front of the Sun at new moon (when a solar eclipse occurs) or can pass as far as five degrees away. That is, the Moon can start the (lunar) month with an elongation ranging from zero to about five degrees. To explore the idea that the Danjon limit might actually be smaller than 7° on the one hand, and to investigate the possibility of spotting the thin lunar crescent at new Moon when the Moon is at its greatest inclination on the other hand, we calculate the visibility criteria when the Moon is at the two extreme cases: near apogee and near perigee.

Naked-eye visibility limit calculations

We calculate the visibility criteria using our photometric-model equations[19], Blackwell's 1946 extensive data[20], our site elevation, and our local brightness of the background sky (see an illustrative example in reference 16). We perform these calculations starting with the phase angle of 175° (this angle corresponds to a topocentric elongation of 4°) and incrementing 0·5° in each step of calculations (possible error = ± 0·25°). The phase angle of 175° coincides with the instant of the new moon on 2002 March 14 when the Moon was near apogee (Table I). In the second case, when the Moon was near perigee, the Moon attained that angle 8 hours after the new moon of 2003 November 23; in this case the instant of the new moon occurred during a total solar eclipse (Table II).

We used data from MICA and IMCCE to calculate the visibility criteria ($C > C_{th}$) for the phase angles of between 175 and 171 degrees (Tables I and II). These angles correspond to the topocentric elongations between 4 and 8 degrees, respectively. The calculated visibility criteria are shown in the last columns of both tables.

From Tables I and II we find that an elongation of 7·5° (± 0·25°) is the lowest naked-eye-visibility limit. If the conjunction occurs when the Moon is near apogee, the Moon reaches this elongation 15 hours and 11 minutes after conjunction. If the conjunction occurs when the Moon is near perigee, the Moon — due to its high velocity — attains this elongation 14 hours after conjunction. Moreover, when the Moon is near perigee, at an elongation of 7·5°, the crescent has a width of 0·18′ and its luminance is $9 \cdot 5 \times 10^6$ nL. When the Moon is near apogee, it has a thinner width and more luminance for the same elongation. For this reason, we get the same visibility limit in both cases. After conjunction, the crescent width being thinner at the cusps, the Blackwell Contrast Threshold C_{th} is greater than C, so that cusp visibility becomes difficult, and the crescent seems shorter than 180 degrees[17].

Optically-aided visibility-limit calculations

If stars were perfect point sources, the issue of background light pollution or moonlight could be resolved by simply increasing magnification. The background becomes darker while the star keeps the same brightness. We can even observe the brighter stars in the daylight with suitably high magnification!

At night, as the skies get darker, we see more and more, fainter and fainter stars with the naked eye. With the telescope we see even more stars since the view is greatly magnified thus spreading out the background light but still gathering light from the star, which is a point source, into a relatively good point image. When looking at an extended object with a telescope, both the background and the object are spread out in a similar way so the actual contrast between them does not change, but the eye can discern contrast better if the objects viewed are larger.

TABLE I

Moon near apogee
(New moon: 2002 March 14 at 02:05 UT)

(67°S, 106°W), elevation: 2000m

Obs. time UT h	m	*Ph. angle* °	*R* ′	*Mag.*	*Elon.* °	% *ill.*	$L_\star$ (*nl*)	*L* (*nl*)	*W* ′	L_B (*nl*)	C_{th}	*C*	*Vis* $C > C_{th}$
2	5	175	14·68	−4·43	4	0·19	$4{\cdot}3\times10^{8}$	$2{\cdot}4\times10^{7}$	0·06	$1{\cdot}2\times10^{7}$	60	1	no
7	5	174·5	14·68	−4·48	4·5	0·23	$3{\cdot}7\times10^{8}$	$2{\cdot}1\times10^{7}$	0·07	$7{\cdot}5\times10^{6}$	43	2	no
9	20	174	14·68	−4·54	5	0·27	$3{\cdot}4\times10^{8}$	$1{\cdot}9\times10^{7}$	0·08	$4{\cdot}5\times10^{6}$	41	3	no
11	20	173·5	14·69	−4·6	5·5	0·32	$3{\cdot}0\times10^{8}$	$1{\cdot}7\times10^{7}$	0·1	$2{\cdot}6\times10^{6}$	38	6	no
12	50	173	14·69	−4·65	6	0·37	$2{\cdot}7\times10^{8}$	$1{\cdot}5\times10^{7}$	0·11	$1{\cdot}5\times10^{6}$	33	9	no
14	20	172·5	14·69	−4·7	6·5	0·42	$2{\cdot}5\times10^{8}$	$1{\cdot}4\times10^{7}$	0·12	$8{\cdot}5\times10^{5}$	31	15	no
15	50	172	14·69	−4·75	7	0·48	$2{\cdot}3\times10^{8}$	$1{\cdot}3\times10^{7}$	0·14	$4{\cdot}8\times10^{5}$	32	26	no
17	16	171·5	14·69	−4·81	7·5	0·55	$2{\cdot}1\times10^{8}$	$1{\cdot}2\times10^{7}$	0·16	$2{\cdot}7\times10^{5}$	37	43	yes
18	40	171	14·69	−4·86	8	0·62	$2{\cdot}0\times10^{8}$	$1{\cdot}1\times10^{7}$	0·18	$1{\cdot}5\times10^{5}$	39	72	yes

TABLE II

Moon near perigee
(New moon: 2003 November 23 at 23:00 UT, total solar eclipse)

Obs. time UT h	m	*Ph. angle* °	*R* ′	*Mag.*	*Elon.* °	% *ill.*	$L_\star$ (*nl*)	*L* (*nl*)	*W* ′	L_B (*nl*)	C_{th}	*C*	*Vis* $C > C_{th}$
7	0	175	16·73	−4·42	4	0·19	$3{\cdot}3\times10^{8}$	$1{\cdot}8\times10^{7}$	0·06	$1{\cdot}2\times10^{7}$	60	0·5	no
7	55	174·5	16·73	−4·48	4·5	0·23	$2{\cdot}7\times10^{8}$	$1{\cdot}5\times10^{7}$	0·08	$7{\cdot}5\times10^{6}$	37	1	no
8	45	174	16·73	−4·54	5	0·27	$2{\cdot}5\times10^{8}$	$1{\cdot}4\times10^{7}$	0·09	$4{\cdot}5\times10^{6}$	33	2	no
9	35	173·5	16·73	−4·59	5·5	0·32	$2{\cdot}3\times10^{8}$	$1{\cdot}3\times10^{7}$	0·11	$2{\cdot}6\times10^{6}$	35	4	no
10	25	173	16·73	−4·65	6	0·37	$2{\cdot}0\times10^{8}$	$1{\cdot}1\times10^{7}$	0·13	$1{\cdot}5\times10^{6}$	27	6	no
11	15	172·5	16·72	−4·7	6·5	0·43	$1{\cdot}9\times10^{8}$	$1{\cdot}1\times10^{7}$	0·14	$8{\cdot}5\times10^{5}$	26	12	no
12	5	172	16·72	−4·75	7	0·48	$1{\cdot}8\times10^{8}$	$1{\cdot}0\times10^{7}$	0·16	$4{\cdot}8\times10^{5}$	25	20	no
13	00	171·5	16·72	−4·81	7·5	0·55	$1{\cdot}7\times10^{8}$	$9{\cdot}5\times10^{6}$	0·18	$2{\cdot}7\times10^{5}$	28	34	yes
13	48	171	16·72	−4·86	8	0·62	$1{\cdot}5\times10^{8}$	$8{\cdot}3\times10^{6}$	0·21	$1{\cdot}5\times10^{5}$	32	54	yes

A faint extended object (*e.g.*, a thin lunar crescent, a galaxy, or nebula) should be viewed with enough magnification so that it appears several degrees across. A very thin crescent must be surrounded by a darker background if the eye is to detect the contrast; keep in mind that when we raise the magnification 10 times we decrease the surface brightness of both the crescent and background sky 100 times! Various magnifications should thus be tried to yield the best detection. At each magnification, considerable time should ideally be spent determining the quality of the detection. Unfortunately, this is not possible for detecting the very young crescent moon, as it appears only for a few minutes before disappearing in the haze of twilight. With such situations even experienced observers would be in trouble (see http://www.icoproject.org/icop/ram25.html).

Since magnifying the crescent enhances its visibility, one must consider optically-aided visibility criteria. In Table III, we recalculate the first row of Table I by assuming the following: dark-adapted eyes, normal acuity, properly aimed and focussed telescope, good optics, 200× magnification, high-elevation site, good transparency with minimum aerosols, and an experience observer!

TABLE III

Moon near apogee
(New moon: 2002 March 14 at 02:05 UT)

The lunar crescent could be seen when the Moon is at new moon

Obs. time UT *h*	*m*	*Ph.angle* °	*R* ′	*Mag.*	*Elon.* °	*% ill.*	$L_\star$ (*nl*)	*L* (*nl*)	*W* ′	L_B (*nl*)	C_{th}	*C*	*Vis* $C > C_{th}$
2	5	175	14·68	−4·43	4	0·19	$4{\cdot}3\times10^{8}$	$2{\cdot}4\times10^{7}$	0·06	$1{\cdot}2\times10^{7}$	60	1	no
	Magnification 200 ×							$0{\cdot}6\times10^{3}$	12	$0{\cdot}3\times10^{3}$	0·85	1	yes

Note (1): Abbreviations used in Tables I–III

Obs.time: Observation time in UT.
Ph.angle: phase angle in degrees.
R: Semi-diameter of the lunar disc.
Mag.: lunar magnitude.
Elon.: elongation in degrees (taking account of lunar parallax), DAZ = 0°, and site elevation = 2000 m.
%ill.: illuminated fraction of the lunar disc.
$L_\star$: actual (extra-atmospheric) luminance of the Moon.
L: The apparent (ground-observed) luminance of the Moon (nL).
W: Topocentric width of the illuminated lunar disc in minutes of arc.
L_B: Twilight-sky luminance (nL).
$C_{\rm th}$: Blackwell Contrast Threshold.
C: $(L–L_B)/L_B$.
Vis: Visibility (yes or no).

Note (2): Assumptions and applications adopted in Tables I–III

We consider the perfect geometrical situation with the difference in azimuth between the Sun and the Moon at the moment of observation being equal to zero (DAZ = 0°, see ref. 16).
We consider the Moon's altitude = 2° at the moment of observation.
We apply our site elevation (2000 m) to calculate *L*.
We use our measured L_B.

In Table III, using the 200 × magnification, we find that *L* drops from $2{\cdot}4\times10^{7}$ to 600 nL, and L_B drops from $1{\cdot}2\times10^{7}$ to 300 nL. So, *C* remains constant (= 1) while $C_{\rm th}$ drops from 60 to 0·85 (Fig. 1), which leads to the interesting result: the lunar crescent may be seen even when the Moon is precisely new!

Since we can spot the crescent at the moment of new moon (*e.g.*, 2002 March 14 at 0205 UT), we can also spot it one minute earlier at 0204 UT when it is an 'old moon' and one minute later at 0206 UT when it is a 'new moon', deducing that the Moon can pass from the 'old moon' phase to the 'new moon' phase without disappearing from sight. So, our calculations show that Danjon's limit is not only less than 7° but it vanishes completely. Moreover, by assuming the 200 × magnification and by using Fig. 1, we find that the dimensions[17] of the thin rectangle of light are about 233·2′ and 12′, concluding that the length of the arc of light of the lunar crescent at new moon, when the Moon is at its greatest inclination, is about 7·1° instead of 180°, *i.e.*, only 4% of the length of the normal few-days-old crescent moon.

Now, if it is possible to spot the thin lunar crescent at new moon when the Moon is at its greatest inclination, why has nobody claimed this observation before? The answer is because the coincidence of excellent conditions of observations and ideal parameters — discussed above — rarely happens. However, our model predicts

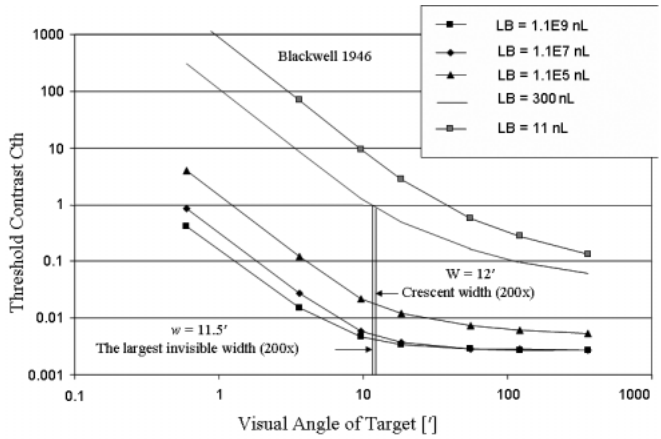

FIG. 1

This figure illustrates the possibility of spotting the thin lunar crescent at new moon when the Moon is at its greatest inclination, *e.g.*, on 2002 March 14 at 0205 UT. From Table III, a telescopic magnification (200×) makes L_B drop from $1{\cdot}2 \times 10^7$ to 300 nL. On the 300-nL Blackwell curve we find that the value of C_{th} corresponding to the magnified crescent width W (12′) is equal to 0·85. However, C does not change with magnification and keeps the same value, which is equal to 1; that value fits our visibility criterion ($C > C_{th}$), leading to the interesting result: the lunar crescent can be seen at new moon!

To calculate the visible crescent length, we use our relation deduced in a previous work[17]: $L = D - 2w\ (D + W)/2W$, where L represents the vertical component of the visible crescent length in arcminutes, D is the apparent diameter of the Moon in arcminutes, W is the width of the crescent in arcminutes, and w is the largest invisible width in arcminutes, *i.e.*, when $C_{th} = C$. From this figure we find that w is equal to $11{\cdot}5'$ (w corresponds to the point of intersection of the 300-nL curve and the line $C_{th} = 1$. This figure also gives a more accurate value for w than our previous approximate value[17]). The visible crescent length in degrees compared to the 180° normal crescent will be: $L/D \times 180°$.

that such an observation could be made in the future, and Stamm's observation of 2004 October 13 was only the first step in spite of the conservative comment made by *Sky & Telescope*'s editors[21].

New moon observations to be attempted in 2007

We urge the test of our model during the next months of this year. The following are the dates of the new moon when the lunar elongation will be around 5° at the instant of new moon: 2007 May 16 at 1929 UT, June 15 at 0314 UT, November 9 at 2304 UT, and December 9 at 1741 UT.

Conclusions

Our lunar-first-visibility model, based on Blackwell's 1946 data, employs more extensive data than those used by all other visibility models. Our calculation shows that 7·5° (± 0·25°) is the lowest naked-eye visibility limit. It also shows that — with suitable magnification — the lunar crescent may be seen even when the lunar crescent is at new moon provided that the Moon is at its greatest inclination.

The expected length of the lunar crescent is about 7·1° instead of 180°. Observing the lunar crescent at new moon is more favourable before sunrise than after sunset due to dark adaptation.

Stamm spotted the thin crescent when the apparent Moon's elongation was only 6·4°. With better equipment than that of Stamm and/or with better observing conditions than those of Mount Lemmon, Stamm's record would be broken again and again until arriving at our model prediction: the lunar crescent could be seen even when the lunar crescent is at new moon. In consequence, the Danjon limit is no longer valid!

We expect that our result will have considerable attraction for societies that use Danjon's limit as the basis for their religious calendars.

References

(1) J. K. Fotheringham, *MNRAS*, **70**, 527, 1910.
(2) E. W. Maunder, *JBAA*, **21**, 355, 1911.
(3) A. Danjon, *L'Astronomie*, **46**, 57, 1932.
(4) F. Bruin, *Vistas Astron.*, **21**, 331, 1977.
(5) D. McNally, *QJRAS*, **24**, 417, 1983.
(6) B. E. Schaefer, *QJRAS*, **29**, 511, 1988.
(7) M. Ilyas, *QJRAS*, **35**, 425, 1994.
(8) B. D. Yallop, *RGO NAO Tech. Note* **69**, 1997.
(9) L. J. Fatoohi *et al.*, *The Observatory*, **118**, 65, 1998.
(10) J. Caldwell & C. Laney, *African Skies*, **5**, 15, 2000.
(11) M. Odeh, *Experimental Astronomy*, **18**, 39, 2004.
(12) L. E. Doggett & B. E. Schaefer, *Icarus*, **107**, 402, 1994.
(13) S. H. DeVries and D. A. Baylor, *J. Neurophysiology*, **78**, 2048, 1997.
(14) X. Ying *et al.*, *J. Neurophysiology*, **93**, 2388, 2005.
(15) A. Vassilev *et al.*, *Journal of Vision*, **5**, 823, 2005.
(16) A. H. Sultan, *The Observatory*, **126**, 115, 2006.
(17) A. H. Sultan, *The Observatory*, **125**, 227, 2005.
(18) B. E. Schaefer, *QJRAS*, **37**, 759, 1996.
(19) A. H. Sultan, *The Observatory*, **124**, 390, 2004.
(20) H. R. Blackwell, *JOSA*, **36**, 624, 1946.
(21) A. M. MacRobert & R. W. Sinnott, *Sky & Telescope*, **109**, 75, 2005.

CORRESPONDENCE

To the Editors of 'The Observatory'

Spectroscopy of Edgeworth–Kuiper-Belt Objects

Recent discoveries of further objects in the Edgeworth–Kuiper Belt, especially those of comparatively large mass, have provoked much interest (particularly on the Internet), although astonishingly a number of authors in the USA appear to be quoting the temperatures of such objects in old-fashioned Fahrenheit.

Much useful information can be gained from wavelength-selective photometry of these objects, but for such difficult objects only colour indices using comparatively broad-band filters have generally proved practicable hitherto. Greater selectivity might be possible using multiplex spectrometry. The advantage of this

in signal-to-noise ratio goes as the square root of the resolving power, which can be only modest for such faint objects, but this nevertheless seems to present the best chance of securing actual infrared spectra. In case our colleagues in the USA, who have the best facilities, should have missed it, it seems worthwhile to record that an introduction to this technique is contained in *Notes and Records of the Royal Society*, **60**, 91–95, 2006 (see also *ApJ Lett.*, 2005 December 10).

Yours faithfully,
PETER FELLGETT

Little Brighter
St. Kew Highway
Bodmin
Cornwall, PL30 3DU

2006 August 8

The Living Orrery

In the August issue of this *Magazine*, the RAS meeting report for 2006 January 13 gave an account of Professor Mark Bailey's talk concerning the Human Orrery installed at Armagh Observatory[1,2]. What struck me after reading the discussion summary was the enduring historical presence of the orrery in both the public and scientific consciousness. Indeed, as long ago as 1713, Richard Steele[3] eulogized the orrery as "a Machine which illustrates, I may say demonstrates, a System of Astronomy … to the meanest Capacity". To which he added, "it is like receiving a new Sense, to admit into one's Imagination all that this Invention presents". This association of 'sense' and 'imagination' is seemingly intrinsic to the orrery, and was a topic developed by the Baptist minister, the Reverend John Collett Ryland (1723–1792), in his text book[4], *An Easy Introduction to Mechanics*, first published in 1768. Ryland's teaching method was to break down the topics that he intended to cover into 'study cards', and in his *Mechanics* he describes the "cards of astronomy, and living orrery, made with sixteen school-boys". He begins with the question, "Astronomy is a most sublime and delicious science.… but can any notion of this science be conveyed into the minds of school-boys?" His answer to this question is 'no' unless it is taught by 'play', by which he meant direct participation and physical involvement. The text for the 'living orrery' describes how to map out in the school ground, with a rope, the orbits for the planets as far out as the planet *Georgium Sidus* (Uranus). Lastly, Ryland explains that the circles indicating the limits for the Earth's Moon, as well as those for the larger moons of Jupiter and Saturn, should be added to the planetary 'paths'. And finally, Ryland commands, "Now begin your play, fix your boys in their circles, each with his card, in his hand, and then put the orrery in motion". The mind's-eye image of this scene is wonderful. Each participant moves around the Sun at the appropriate scaled rate, and in turn, each 'human' planet and moon reads aloud their card. Card 12 expounds, for example, "I represent stupendous Saturn. My diameter is 78,000 miles. I move around the Sun in $29\frac{1}{2}$ years at the distance of 907,000,000 miles, and at the rate of 22,000 miles an hour". It appears that Ryland placed greater pedagogical value on physical numbers, rather than description, there being no mention of Saturn's rings. "Half an hour spent in this play once a week," Ryland comments, "will in the compass of a year fix clear and sure ideas of the solar system, as they can never forget to the last hour of life".

It is interesting to note, as pointed out by Nicholas Roe[5], that John Ryland was the founder of Enfield Academy, to which the poet John Keats was sent in his adolescence (although after Ryland's death). The 'turning' of the living orrery was still being practised during Keats' tenure at the Academy, however, and this perhaps places new light on his lines within *On first looking into Chapman's Homer*: "Then felt I like some watcher of the skies when a new planet swims into his ken".

The cometarium[6], a specialized orrery to demonstrate the elliptical motion of a comet, was invented by John Theophilus Desaguliers (1683–1744) *circa* 1732, but to the author's knowledge no 'living cometarium' has ever been constructed for public use (until the Armagh example); that being said, Hughes[7] has described how one might be made to illustrate the full motion of Halley's famous comet with 76 year-posts. Perhaps the closest approximation to an historic 'living' cometarium is that described by Gilbert Vale[8] (1788–1866). The comet modelled in this case was Biela's comet of 1832, and the orbital track was "sixty feet" in length. The cometarium further incorporated an orrery showing the positions of the Earth, Moon, Venus, and Mercury. Exhibited at St. John's Hall in New York during the first half of 1832, this cometarium must have been an awe-inspiring installation.

In spite of John Herschel's 1833 dismissal[9] of orreries as "those very childish toys", the image of a mechanical (even peopled) model of the Solar System is still very much an engaging one. The wonderfully 'moody' painting[10] of an orrery, complete with surrounding observers, produced by Joseph Wright of Derby (1734–1797) in 1766, beautifully illustrates the depths to which the orrery can take the human imagination. That imagination and wonder is further encapsulated within the superbly crafted orrery recently completed for the Long Now Foundation[11]. And, finally, we can perhaps forgive Herschel his comments on the orrery, as noted above, since at that time he was deeply embroiled within the politics surrounding the construction of Babbage's difference engine (which is certainly not a toy[12]).

Yours faithfully,
MARTIN BEECH

Campion College,
The University of Regina,
Regina,
Saskatchewan,
Canada S4S 0A2

2006 September 3

References

(1) M. Bailey, *The Observatory,* **126**, 236, 2006.
(2) M. Bailey, D. Asher & A. Christou, *A&G*, **46**, 3·31, 2005; *S&T*, 2005 May, 107.
(3) R. Steele, *The Englishman*, no. 11 (27–29 October), 1713.
(4) J. C. Ryland, *An Easy Introduction to Mechanics. For the use of Schools, as well as Private Gentlemen* (Edward and Charles Dilly, London), 1768, pp. xix–xxi.
(5) N. Roe, *John Keats and the Culture of Dissent* (Clarendon Press, Oxford), 1997.
(6) M. Beech, *Bulletin Scientific Instrument Soc.*, **82**, 29, 2004.
(7) D.W. Hughes, *JBAA*, **95**, 162, 1985.
(8) G. Vale, *Cometarium, or the Astronomy of Comets* (Evans and Brooks, New York), 1832.
(9) J. A. Herschel, *Treatise on Astronomy* (Longman and Rees, London), 1833.
(10) http://www.geocities.com/jvertesi/wright/
(11) http://www.longnow.org/projects/clock/orrery/
(12) M. Beech, *JRAS Canada*, **100**, 118, 2006.

REVIEWS

The Last of the Great Observatories: Spitzer and the Era of Faster, Better, Cheaper at NASA, by G. H. Rieke (University of Arizona Press, Tucson), 2006. Pp. 228, 23·5 × 16 cm. Price $40 (about £22) (hardbound; ISBN 0 816 52522 6), $19·95 (about £11) (paperback; ISBN 0 816 52558 7).

An exciting title; "The Great" anything is almost certain to be exciting, and the last of these great things will be bathed in a sense of history and wisdom from the grand perspective of the last in the line. Alas none of that is true of this book. *The Last of the Great Observatories* is about the funding and management of a large space project in which all of the excitement of cutting-edge astrophysics and technology has been removed. My disappointment steadily increased as I ploughed on through page after page of descriptions of technical reviews and preparation for those reviews. So with very little astrophysics and even less technology, what do we discover about the last of the great observatories?

Rieke has been working on the *Spitzer* project (previously known as *SIRTF*) for 20 years, most of them before it became an approved mission with any real chance of flying. That alone would make you think of him as a forceful man of character — one who persists until he gets want he wants. In fact he and almost everybody else in the book come across as men with very little command of their own destiny, blown to and fro by the capricious forces of NASA funding, eccentric management, and faulty technology. The author's circumspect text none the less reveals his opinions of those capricious forces. For example, Ball Aerospace is good, Lockheed is bad, or more specifically Lockheed Sunnyvale is bad, Lockheed Denver is OK; JPL is good, Goddard is bad, and so on. His reasoning behind these opinions points to the different cultures at work, from the free-wheeling, highly communicative science types, generally based in universities, compared to the ploddingly dull and secretive workers in defence industries working under 'need to know' conditions.

The astronomy is dealt with in two sections: initially in a description of a colour book and crayons used to create a cartoon of how multi-spectra data could be used to enhance the astrophysics return from space; and in a final low-key section in which the *Spitzer* observatory achievements to date are outlined. The colour-book idea was used to sell the concept to NASA, and during this process the slogan "the Great Observatories" was born. Selling to NASA was not easy and the task of getting political support by door-stepping on Capitol Hill is described. Rieke acknowledges the astuteness of a master practitioner of this art, Francis Everett, in his long-term promotion of *Gravity Probe B*. The *SIRTF* astrophysics achievements are covered in a final short chapter of 11 pages — only three times the space he devotes to the experience of Charlie Pellerin's management course.

Anyone who has been involved in any scientific endeavour with a long-term struggle to get funding could appreciate the hoops through which the *SIRTF*/*Spitzer* team jumped in order to meet ever-changing cost targets. The noble concept of a space-research team being the scientific arm of the public's search into the unknown somehow gets lost in mundane cost-cutting that ultimately leads to the pragmatic view of "what is the credible minimum" we can do. The *SIRTF* team had their grand ideas tempered even beyond what is credible to come up with a cost 20% of their original estimate. Thus all ideas of fancy diagnostic capabilities and wide-ranging astrophysics were abandoned as they were forced to consider only key science programmes and avoid general capabilities.

In a short passage that comes as a relief from all the management, Rieke gives a realistic and insightful account of the process of building space instruments. He gives a nice simile in which the social structure of technical teams is compared to that of a medieval craft guild. Particular talented specialists use their skill and imaginations to hand-craft one-off examples of their work, which are combined again by specialist teams. Further, unintended, social observations emerge from the text: for example, the hierarchy that exists in the space world. Managers solve problems by long telephone conversations (in NASA speak this is called 'working' a problem), while the folk that cause all the technical difficulties are inevitably technicians and engineers. Scientists and managers are clearly an *élite*, who worry and discuss, and by this process make technical problems go away. Rieke illustrates the tricky business of making technical decisions under schedule and financial pressure — often with incomplete information — in relation to the degradation of a thin-film filter in the *SIRTF* cold flight dewar. As befits that *élite*, the decision, to do nothing, was made over a good dinner at a fancy Los Angeles restaurant.

The book's subtitle of *Spitzer and the Era of Faster, Better, Cheaper at NASA* refers to NASA administrator Dan Goldin's change in NASA's management culture in a praiseworthy attempt to get more science per dollar. As a great deal of the work for *Spitzer* was carried out under this faster, better, cheaper mantra, Rieke examines where it works and where it fails. He concludes that far from being a misguided concept dreamed up by fools, the 'faster, better, cheaper' theme actually captures many of the best aspects of the management of medium-scale, medium-complexity space missions. One of the aims was to delegate responsibility to the guy actually doing the job, and in the first few missions this worked fine. The well-publicized failures (think imperial to metric conversion) he believes were a consequence of pushing for higher performance with no matching cost increase and thus creating unrealistic goals. He also quotes some interesting statistics in the wider context of scientific satellites, looking at where failures actually occur. Surprisingly it is not the fancy new innovative technology that causes problems; rather it is poorly applied conventional technology that dominates the failure statistics. Equally, in spite of the perception of space agencies, science instruments hardly ever cause mission failure; launcher and spacecraft problems are the main culprits. It is a pity that these general lessons, and by far the most interesting section of the book, are relegated to a final short appendix.

In summary the book is probably a worthy historical account of some of the dullest aspects of building a science-led spacecraft. Written in a fairly flat style, it will not keep you awake and you will not refer to it for the technology or astrophysics of the *Spitzer* observatory (in fact the four-page index is bulked out with the names of various managers and space pundits). It is an honest attempt to document the management issues associated with building *Spitzer*; alas, honesty alone does not make interesting reading. — BARRY KENT.

Night Sky Tracker, by L. A. Horovitz (A. & C. Black, London), 2006. Pp. 224, 24 × 16·5 cm. Price £12·99 (hardbound; ISBN 0 713 67807 0).

Where to start? Perhaps with the cover, which glows in the dark, but for no obvious purpose. The book has a spiral binding, which means that the pages open flat, but the book is effectively 4-cm thick when opened. The last hundred or so pages are formatted as a logbook (a good idea in theory), two pages per night, it appears. At first I assumed the binding was to allow pages to be removed or added but this

is not so. Not that this matters much as even a non-astronomer would see that these pages are fairly useless. There are no drawing blanks and a strange allocation of space, *e.g.*, you have 6 cm to record the phase of the Moon but only 4·5 cm to record 'Visible Features'; variable stars don't get a mention although you do have space for two 'Notable Stars', each with 2 cm for 'Star Spotted', 1·5 cm for 'Apparent Magnitude', and another 2 cm for 'Notes'. The basic page colour for this section is dark blue so there is no chance to use the rest of the page. A 'Guide to Apparent Magnitude' box is provided with the familiar-sized printed circles to indicate magnitude! I have no idea what use this is meant to be as no charts appear in this section (charts that do appear elsewhere do not have a magnitude scale).

The first part of the book is in textbook style but I am not sure at whom it is aimed. Generally it seems to be for beginners but, if so, some sections, *e.g.*, that on black holes, seem a little advanced, while some basic information is missing. The book is not without merit: there are few typographic errors, it deals well with astrology, encourages binoculars and patience, and does not feature professional pictures that will never be matched at the eyepiece; but it certainly does present problems when you try to read it through. Some of these are minor ones of style (*e.g.*, commas are used to excess; and we have nebula/nebulae and aurora/auroras) but others are at best confused thinking, at worst wrong, misleading, or dangerous. For confused, try "Meteor showers are usually named after the constellation in which they are found...". Changing "they are" to "the radiant is" would be better. For wrong, try "These photons emit light ..."! For dangerous, "Welder's glass ... safe for solar viewing" — not true if it is less than grade 14. Perhaps my favourite could feature in *Here and There*: "Simply put, the ecliptic is the path that the Sun takes on its journey through the night sky".

It appears that information may have been obtained from various sources as the style does not seem consistent. This may be the cause of some contradictions, *e.g.*, in the section about Pluto (which is also where to find solar and lunar eclipses) p. 100 has "... the same as its lone moon Charon", whilst p. 101 has "... Pluto ... has three moons, ...".

I could go on but I'll resist. No doubt this book will sell; I expect mostly it will be bought by non-astronomers looking for a present for someone they believe to be interested in astronomy; but in my view although the cover may glow the contents most certainly do not. — RITA WHITING.

The Nature and Evolution of Disks Around Hot Stars (ASP Conference Series, Vol. 337), edited by R. Ignace & K. G. Gayley (Astronomical Society of the Pacific, San Francisco), 2005. Pp. 358, 23·5 × 15·5 cm. Price $77 (about £44) (hardbound; ISBN 1 583 81203 2).

More often than not, workshop meetings, such as that recorded here, are scarcely distinguishable from any other conferences. The effort that evidently went into making this three-day gathering, held in Tennessee in mid-2004, a *real* 'workshop' is therefore noteworthy. Each day, three fairly lengthy reviews were presented in the morning, followed after lunch by an extended discussion session, wrapping up with semi-tutorial focus sessions. The resulting book is far more useful than the typical conference proceedings, both because there's space for material to be developed in significantly greater depth than is usual, and because of the effective didactic functionality of the focus-session write-ups. This volume is thus an unusual blend of reports of active research and the sort of advanced background material one might expect of a summer school.

This all works well not only because of the foresight of the organizers and the authority of the contributors, but also because of the subject matter, dominated by Be-star discs but with substantial nods towards Herbig Ae/Be stars and related topics. There's lots of well-developed astrophysics that's evidently pertinent (magnetic fields, radiation hydrodynamics), but no-one's sure *exactly* how — leaving plenty of room for theoretical speculation, and plenty of room for observations to provide guiding insight. That's reflected in the hundred or so pages of reports of poster presentations (each allowed a reasonably generous five pages) which, alongside a lot of theory and modelling, include summaries of work involving optical interferometry, spectroastrometry, circular spectropolarimetry, linear photopolarimetry, and X-ray spectroscopy; one can hardly complain about a lack of observational effort!

Most conference proceedings become obsolete rather too quickly, but I expect this one to stay within easy reach as long as I remain interested in the topic. Well worth a look by anyone working on Be and related stars. — IAN D. HOWARTH.

Astrophysics of Variable Stars (ASP Conference Series, Vol. 349), edited by C. Sterken & C. Aerts (Astronomical Society of the Pacific, San Francisco), 2006. Pp. 480, $23 \cdot 5 \times 15 \cdot 5$ cm. Price $77 (about £44) (hardbound; ISBN 1 583 81217 2).

Nearly a century ago (1908) Henrietta S. Leavitt published her catalogue of Cepheids in the Magellanic Clouds and her observation of the period–luminosity relation. Stellar oscillations have ever since been a main tool for measuring distances and, more recently, for studying stellar properties by means of seismology techniques such as demonstrated for the Sun, white dwarfs, and β Cephei stars. Another major tool in stellar astrophysics goes even further back in time. It is the study of binary or multiple stellar systems, which remains the best source for determination of stellar masses and radii. The variable-star astronomers of today and the future face vast amounts of observational data from ground-based surveys and from space (*e.g.*, *OGLE*, *MACHO*, and the *Gaia*, *BRITE-Constellation*, and *COROT* missions). In addition, the tools for visualizing, modelling, and analysing the observations have developed rapidly in complexity and number over the past decade. Thus for PhD students in this research field there is a lot to acquaint themselves with before choosing the topic of their research and how to do it.

In 2005 September, a highly successful PhD conference on 'Astrophysics of Variable Stars' was held in Pécs, Portugal, with the main purpose of offering the students a course in the field of variable-star research and improving their skills in scientific communication. There were about 70 international participants, including nine senior scientists who are among the world's leading experts in the fields of variable B stars, roAp stars, binary-star modelling, databases of variable stars, and pulsation theory. These proceedings are therefore valuable as a broad introduction and brief update on the current open questions, tools, and facilities in this research field. Not unexpected of the proceedings of a meeting of this format, the book is not totally devoid of typographical errors. That this is also the case for the chief editor's long but insightful article on writing scientific papers (Sterken has considerable experience as author and editor), is undoubtedly the result of also dealing with the over-100 papers, of which most were student papers submitted twice for training purposes. This has, however, greatly improved the readability of the PhD texts.

The book's four parts start with a broad introduction to databases, and to binaries and pulsating variables. I enjoyed reading Terrell's article on 'Eclipsing Binaries: Future Work' which, *e.g.*, discusses the possible existence of planets in binaries. An 'eye-opener' for me was the article by Henden on the potential of professional–amateur collaboration in organizations like the very productive AAVSO. He gives practical advice on how to maintain such collaborations and demonstrates the value of visual data. A well-written, concise overview of stellar pulsation is given by Kurtz, who also gives examples of the most promising results from asteroseismology. Then follow two parts with PhD contributions (half of the book) from student talks and poster presentations. All articles appear alphabetically after author, but I would have preferred a topic-based division. Several of the PhD projects are comprehensive studies, and some include very useful comparisons of commonly used photometry software and photometric calibrations. Noteworthy also are some very relevant theoretical considerations of stellar pulsations in δ Scuti and β Cephei stars. The book's final part is about communication of scientific results and the diverse aspects of a scientist's activities. These articles make pleasant, often amusing, reading, full of practical advice for the young scientist (and some senior ones as well). The book may serve both as a handbook on the subject of variable stars, with snapshots of contemporary research projects, and a mini-guide for the young scientist on his/her way up the career ladder. — LARS FREYHAMMER.

Astrophysics in the Far Ultraviolet: Five Years of Discovery with FUSE (ASP Conference Series, Vol. 348), edited by G. Sonneborn, H. W. Moos & G.-G. Andersson (Astronomical Society of the Pacific, San Francisco), 2006. Pp. 591, 23·5 × 15·5 cm. Price $77 (about £44) (hardbound; ISBN 1 583 81216 8).

In the early 1980s, only a few years after the launch of the *IUE* satellite, a successor spectroscopic UV mission was already being actively discussed. At the time, few would have foreseen that *IUE* operations would continue until late 1996, but the 'imminent' launch of the *Space Telescope* was widely recognized as an important constraint; anything that duplicated (or even worse, exceeded) the functionality of *HST* was a non-starter. This dictated wavelength coverage shortwards of ∼ 120 nm for UV spectroscopy, but the resulting narrow spectral window down to the Lyman limit (91·2 nm) holds sufficient riches amply to justify a dedicated mission, manifested (after many trials and tribulations) in *FUSE*, the *Far Ultraviolet Spectroscopic Explorer*. *FUSE* was finally launched in 1999 June; five years into the mission, in 2004 August, a conference was held in Victoria, BC, to review scientific results to date, and the proceedings are recorded in this volume.

The attraction of mission-based conferences of this nature is the diversity of topics covered — ranging, in this case, from the Martian atmosphere to active galactic nuclei. In this sense *FUSE* is indeed a successor to *IUE*, but, through its strength in conducting absorption-line studies of the gas phase of the diffuse interstellar medium, its antecedents are easily traced back still further, to the *Copernicus* satellite. For example, the original top-level driver for the mission was investigation of the deuterium:hydrogen ratio (at the time, a critical diagnostic of Ω_B), and *FUSE* data have indeed brought about important advances both in the measurement of the 'cosmic' D/H ratio and in the study of the astration processes that modify that ratio. At the other end of the temperature scale, the O VI resonance lines, accessible with good sensitivity with *FUSE*, probe the hot gas, and its interface with cooler phases of the ISM.

Stellar astrophysics has also benefitted considerably from *FUSE* — perhaps more so than suggested by the conference summarizer's rather laconic remark that, where cool stars are concerned, "FUSE has shown that the main sequence can be quite interesting". In particular, surveys of the P V resonance doublet in stellar winds, superficially a somewhat arcane pursuit, have shaken the 'well established' foundations of our understanding of mass loss, demanding downward revisions of mass-loss rates by an order of magnitude.

One could easily pick out many more examples of interesting science from this wide-ranging and versatile mission. The 120+ papers published here make for a nice *smorgasbord* at which one can nibble, and they convincingly demonstrate the strengths of UV spectroscopy for quantitative astrophysics; the diversity of topics gives a proceedings volume that, for a change, makes a virtue of numerous short reports of work that in many cases has been published in full in the refereed literature. The introductory potted history of the mission, recounting the lurches from financial crisis to crisis pre-launch and the successive hardware problems post-launch, also makes entertaining reading — given the luxury of hindsight and a now mature, successful spacecraft. — IAN D. HOWARTH.

Large-Scale Structures and their Role in Solar Activity (ASP Conference Series, Vol. 346), edited by K. Sankarasubramanian, M. Penn & A. Pevtsov (Astronomical Society of the Pacific, San Francisco), 2005. Pp. 432, 23·5 × 15·5 cm. Price $77 (about £44) (hardbound; ISBN 1 583 81214 8).

These proceedings contain the presentations given at the 22nd NSO Sacramento Peak workshop held in 2004 October at Sunspot, New Mexico. There is a healthy mix of long (invited reviews) and short papers. At the conference itself the invited reviews were unusually long, lasting a whole hour. At 12 000 ft this meant that all sea-level speakers required significant stamina to keep going for the duration. Thankfully most of the articles do not make the reader suffer similarly!

The conference was attended by a significant number of the key people in this particular field on both the observational and theoretical sides and these proceedings provide a nice review of each researcher's current interests. Overall, the collection of articles provides a coherent overview, from the solar interior to the solar surface and up into the atmosphere, of the large-scale activity on the Sun. In particular, the articles discuss large-scale flows in the interior such as the possibility of giant convection cells. Photospheric signatures of magnetoconvection lead on to articles looking at the long-term, large-scale dynamics of surface magnetic fields. The major questions considered in the solar atmosphere involve the formation of phenomena such as prominences, open magnetic-flux regions, and the large-scale build-up of energy leading to eruptions. Although the main focus of the conference was on large-scale phenomena, connections are made to small-scale phenomena. Also the magnetic activity on Sun-like stars is compared to that on the Sun.

There are a number of articles I found particularly interesting or timely. These involved predicting the sunspot number of the new solar cycle — predictions that can soon be tested — and an overview of filament observations with a discussion indicating which is the most likely theoretical model to explain each particular type of filament. Other interesting articles reviewed the solar dynamo and considered its photospheric signatures on the entire range of scales from small network fragments with fields of just tens of Gauss up to sunspots that have fields of a few thousand Gauss.

The range of articles is clearly of interest to those working on large-scale solar activity, but this book may also be of interest to new students entering the field or researchers on stellar magnetic activity who would like an overview of solar research in this area. Indeed, it also serves as a useful update to the field for solar physicists like me, who focus on different aspects of the Sun. — CLARE PARNELL.

Direct Imaging of Exoplanets: Science and Techniques (IAU Colloquium No. 200), edited by C. Aime & F. Vakili (Cambridge University Press), 2006. Pp. 638, 23·5 × 15·5 cm. Price £60/$95 (hardbound; ISBN 0 521 85607 8).

The study of exoplanets is, without doubt, one of the hottest topics in modern-day astronomy. In such a rapidly moving field, it is essential that conference proceedings are published as quickly as possible to prevent them becoming outdated. The editors of these proceedings, the 200th IAU Colloquium (held during 2005 October 3–7), have delivered their volume, in conjunction with the Cambridge University Press, only nine months after the conference. This is certainly an impressive effort and gives the contents of the book an immediacy often lacking in many similar volumes.

Most of what we know about extra-solar planets has been obtained through indirect means, by the use of radial-velocity or occultation techniques. There has been a direct detection of the extended atmosphere of one object, through absorption against the spectrum of the host star, but otherwise information on the planets, such as their composition, is virtually non-existent. Therefore the direct imaging of extra-solar planets and, ultimately, their spectroscopic study is the Holy Grail of planetary exploration outside the Solar System. As indicated in the title, this book delivers a timely summary of the state of the art in both the science to be gained from exoplanet imaging and the variety of techniques being developed to achieve this ultimate goal. The proceedings are split into two sections covering both areas, with the majority (about 2/3) of the volume devoted to 'Instrumentations and techniques'. Almost 80 papers cover a large variety of different existing and proposed instruments, including interferometers, coronagraphs, and adaptive optics. Unfortunately, there is quite a lot of duplication of technical information across these, and inclusion of a general review among the invited papers, drawing all the basic information together, would have been helpful. Another limitation is that most of the contributions concentrate on ground-based techniques, with only a few papers devoted to space-based instrumentation. However, this might be a reflection of greater maturity of the former.

Although the initial science section of the book is the shorter, it contains some of the most fascinating papers in the proceedings. As yet there are no real results to present, but there are a few key invited reviews which are rather thought-provoking in their examination of how the data ultimately obtained might be interpreted. Of course, one of the key questions is whether or not we will be able to find planets like our own and the chances of being able remotely to detect evidence of life. Two excellent reviews, by Meadows and Woolf, on these respective topics are the highlights of the book for me. Their topicality will probably outlast most of the other papers. In general, the book is well produced, with a nice uniformity of style and clear figures, avoiding the all-too-common pitfalls of many conference proceedings. It may well be superseded in a fairly short time, given the intense activity in the field, but I would definitely recommend that anyone who wants a thorough update on extra-solar planetary imaging obtain a copy. — MARTIN BARSTOW.

Einstein's Jury: The Race to Test Relativity, by J. Crelinsten (Princeton University Press, Woodstock), 2006. Pp. 428, 24 × 16 cm. Price £22·95/$35 (hardbound; ISBN 0 691 12310 1).

I still recall the haunting theme, taken from Stravinsky's *The Rite of Spring*; it heralded each programme of Sir Herman Bondi's TV series $E = mc^2$, an introduction to relativity that held me spell-bound during my last years at secondary school in the early 1960s. Each step of the way seemed so logical (true also of the booklet that accompanied the series) and yet, after a while, I found myself in a fantastic and unreal — or at least unworldly — relativistic wonderland. I imagine many had similar feelings when Einstein brought forth his Special and (more particularly) General Theories of Relativity in the early years of the 20th Century, so it was with great interest that I began to read *Einstein's Jury*.

It seems I was right: at the outset many famous names in astronomy were clearly struggling with the new concepts. Crelinsten has gathered in a harvest of detailed material from correspondence, public talks, the press, the scientific media (including more than a few items from the pages of this *Magazine*), and elsewhere to demonstrate that really rather few astronomers had a firm grip on the matter. His thesis is actually quite interesting: it seems that in Europe, and especially in Britain, relativity took root fairly quickly, thanks especially to the prestige of Sir Arthur Eddington, whose results from the 1919 eclipse and whose clear understanding and consequent championing of relativity was a dominant force.

On the other hand, the situation in America was very different: the East Coast was home to a considerable force of 'traditional' (almost, one might say, 'Newtonian') astronomers, whose bread and butter was classical and dynamical astronomy, while the West Coast harboured the great observational battalions who wanted experimental proof before taking the new ideas on board; even the top US astrophysicist of the day, Henry Norris Russell, seemed unsure about relativity!

The 'Jury' of this book, then, is primarily the American astronomical community, and the 'trial' is based around the three principal tests of relativity: Mercury's anomalous perihelion motion, the deflection of light as it passed by the Sun, and the redshift of light escaping from the surface of a massive body — initially the Sun and latterly the white dwarf Sirius B. The witnesses for the prosecution (anti-relativity) were many to begin with, prime amongst them being a professor at Columbia University, Charles Lane Poor, and Heber D. Curtis, both of whom fought a long and often vitriolic campaign to demonstrate that their observational results (and those of others) disproved relativity. To begin with, there were few witnesses for the defence of Einstein's ideas, but as further eclipse results came in during the mid-1920s, especially from Lick observers (W. W. Campbell *et al.*, but particularly R. Trumpler, a Swiss astronomer who actually understood relativity and who was also clearly a first-rate observer), and increasingly accurate spectroscopic measurements were made, primarily by astronomers from Mount Wilson (W. S. Adams and his colleagues), the tide turned and Einstein was acquitted *cum laude*.

Along the way we get a useful synopsis of the 'birth' of relativity in Europe (and its passionate defence by Erwin Finlay-Freundlich, later Napier Professor of Astronomy at St. Andrews), discuss some of the finer points of the measurements and theories (such as the various factors that influence the radial velocities of spectrum lines across the disc of the Sun, and whether light might be refracted near the solar surface), encounter some strange characters, like T. J. J. See — an astro-

nomical 'loose cannon' if ever there was one — and examine related work such as the search for the ether and Michelson's experiments.

This will be a valuable book for historians, with useful annotation, extensive bibliography, and comprehensive indices. A number of historically significant monochrome pictures add flavour to a work from which a small number of proof-reading errors (including several times a reference to "the Lick" where presumably "the Lick astronomer(s)" is meant) hardly detract. — DAVID STICKLAND.

Fundamentals of Plasma Physics, by P. M. Bellan (Cambridge University Press), 2006. Pp. 609, 25·5 × 18 cm. Price £45/$75 (hardbound; ISBN 0 521 82116 9).

I am a mathematician by training and have never actually taken a course in plasma physics. However, since I work mostly on theoretical solar physics I do know some plasma physics. Therefore it was with some trepidation that I picked up the book by Paul Bellan and started to read. The preface was reassuring: "The prerequisites for this text are a reasonable familiarity with Maxwell's equations, classical mechanics, vector algebra, vector calculus, differential equations, and complex variables". Phew! I should be okay then. Indeed, I was pleasantly surprised as to at how low a level the book starts. In many places there is not only the mathematical working, but also a written description of the steps taken, although I felt in places that this was a bit over-done and distracted from the real problem; but for a physics or engineering undergraduate student it may be helpful. Furthermore, there are several assignments at the end of each chapter, which again will appeal to students. However, I think what would have been even more appealing is an appendix with the answers to these assignments!

The book considers all three approaches to plasma physics, namely, the Vlasov, two-fluid, and MHD models. Throughout the book these approaches are all used to tackle the same or different problems, illustrating their strengths and weaknesses in various situations. After the introductory chapters the topics covered are single-particle motion, waves in different types of plasma, MHD equilibria, magnetic helicity, and magnetic reconnection. The latter chapters discuss the Fokker–Planck theory of collisions, non-neutral plasmas and dusty plasmas, and more waves. There is considerable discussion about each problem in order to give as full an explanation as possible. This does mean that in some chapters only the very basics are covered. I was a little surprised and disappointed to find that work by key authors in certain areas was not discussed at all.

In many ways, therefore, I would see this as being an ideal book for undergraduate students if it were not for the numerous minor mistakes or inconsistencies that occurred far too frequently for my liking. Clearly, during the writing of the book the notation has changed, but often not consistently. Furthermore, I found that the same Greek letter was used to mean two different things within the same chapter or even on the same page. This can be quite confusing even if one is a subscript and the other not. This, I think, would be very off-putting for students who expect lecturers to produce perfect notes for every university course. To discover that a text book has a number of mistakes or a notation that occasionally switches is going to cause them no end of trouble.

Overall I liked the book and found it one of the easiest plasma-physics books I have read. I would recommend it to a PhD student for directed reading, with the warning that there are mistakes. As I have already said, it would make a good undergraduate student text book if it were not for those mistakes. In a large class,

though, it is just not possible to explain why subscripts magically change from one equation to the next for no reason! Hopefully, many of these problems can be ironed out if it is ever reprinted. — CLARE PARNELL.

THESIS ABSTRACTS

LUCKY IMAGING: DIFFRACTION-LIMITED ASTRONOMY FROM THE GROUND IN THE VISIBLE

By Nicholas M. Law

This thesis describes the development and use for science of the Cambridge 'Lucky Imaging' system, *LuckyCam*, designed for astronomical imaging through Earth's turbulent atmosphere. I demonstrate that in good conditions *LuckyCam* gives diffraction-limited images in the *I* band, matching from the ground the resolution of the *Hubble Space Telescope*. In poorer conditions, the system improves the imaging resolution by factors of 3–4. The system is shown to achieve reliably very-high-resolution output images that are useful for a wide variety of astronomical programmes. The L3CCD (EMCCD) detector allows noise-free photon counting at CCD quantum efficiencies; calibration methods developed for astronomy with this detector are presented. My design and implementation of both fast *LuckyCam* data-acquisition software and an automated Lucky Imaging pipeline are discussed in detail. I also present several methods for the measurement of the parameters of close-binary systems using *LuckyCam* data, as well as calibration methods for speckle imaging using L3CCD detectors.

In the second part of this thesis, I detail the *LuckyCam* very-low-mass (VLM) binary survey, a search for close companions to nearby late-M-dwarf stars. One hundred and ten targets were imaged at 0·1-arcsec resolution in only 16 hours on-sky, a very fast rate compared to other high-resolution imaging systems. Twenty-one new VLM binaries were found, a ∼25% increase in the known number. Several more-exotic systems were discovered during the surveys, such as a possible substellar companion, and a wide triple system. The orbital-radius distribution of the binaries is found to have an apparently sharp change at around the M5·0–5·5 spectral type, with the earlier-type stars having a large population of binaries wider than 10 AU. — *University of Cambridge; accepted 2006 July.*

The full thesis is available electronically at:
http://www.ast.cam.ac.uk/~optics/Lucky_Web_Site/

SOLAR-WIND–MAGNETOSPHERE COUPLING AT SATURN

By Caitríona M. Jackman

The studies contained within my thesis concern the interaction of the solar wind (the stream of charged particles from the Sun), with the magnetosphere of the gas-giant planet, Saturn. Saturn's magnetosphere is the enormous cavity that surrounds that planet and contains the planet's magnetic field.

The first study used data obtained by the *Cassini–Huygens* spacecraft while it was cruising toward Saturn, to investigate the large-scale structure of the heliosphere and the interplanetary magnetic field (the field contained within the solar wind). The medium was found to be consistent with that expected during the declining phase of the solar cycle, structured by co-rotating-interaction-region (CIR) compressions and rarefactions. An empirical formula for open-flux production at Saturn's magnetopause was presented. Use of this formula enabled investigation of the effect of solar-wind-driven reconnection on large-scale magnetospheric dynamics.

The second study again used data from *Cassini*'s magnetometer, but this time combined with information on Saturn's kilometric radiation (SKR) emissions, and images of Saturn's UV aurora taken by the *Hubble Space Telescope* in 2004 January. This combination of data sets enabled me to study in detail the effects of a compression (high field) region hitting the planet. I then went on to infer conditions inside the magnetosphere during the Saturn orbit-insertion fly-through in 2004 July, when *Cassini* had its closest approach to the planet of 1·33 Saturn radii. This work provided evidence for the first specific link between SKR emission features and *in-situ* dynamics inside Saturn's magnetosphere.

The third study developed a theoretical model of the flows and currents in Saturn's polar ionosphere which cause the dynamic aurora as observed with the *Hubble Space Telescope*. The model described a number of processes (sub-co-rotation, convection, *etc.*) which combine to produce the observed aurorae, which commonly display a dawn–dusk asymmetry in brightness. This was the first fully quantitative model of its kind, and has sparked many ideas for future work. — *University of Leicester; accepted 2006 June.*

Here and There

THE ATTRACTION OF ACADEME

An Apparent University Magnetic Constant for Cool Stars. — *PASP*, **97**, Contents page.

LIKE FATHER, LIKE SON?

… the techniques [in galaxy dynamics] first introduced by Karl Schwarzschild in the late 1970s … — *Gemini Focus*, 2005 December, p. 25.

GRAMMATIC ABERRATION

Alfred Jensch, head designer in the astrology department at Carl Zeiss … — *Innovation 16* (Carl Zeiss AG), 2005, p. 25.

HARD GOING FOR *GAIA*

Distance to the center of the galaxy: approx 210,000,000 light years. — *Innovation 16* (Carl Zeiss AG), 2005, p. 24.

A SERIOUS PERTURBATION

… Uranus's largest moon, Triton, … — *A & G*, **47**, 2·42 (2006 April).

PLATE 1. The waning gibbous Moon. Taken by Robert Gendler in 2003 December from Connecticut, this image is a mosaic of six individual exposures, made with a 12.5-inch *f*/6 Ritchey-Chrétien telescope and an ST10XME CCD camera ($2184 \times 1472 \times 6.8$-micron pixels). Copyright R. Gendler 2006. (For many more superb images, go to http://www.robgendlerastrotopics.com.)

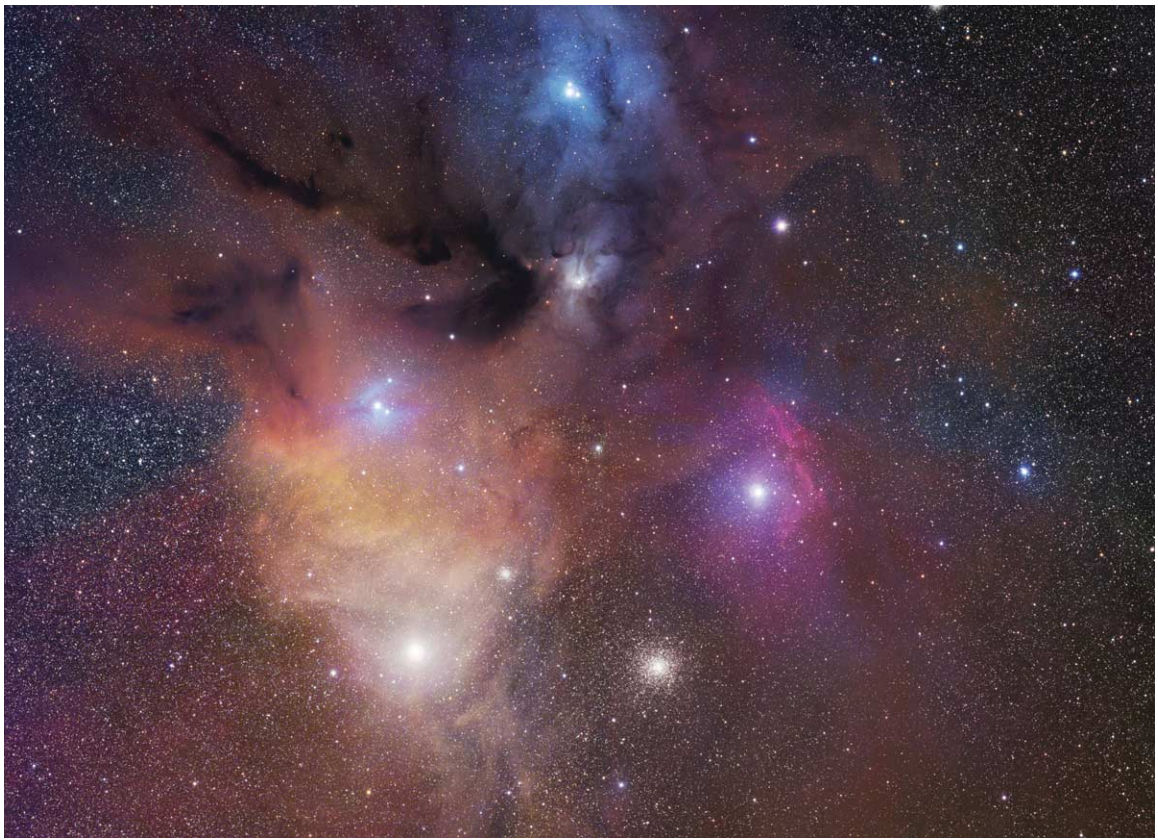

PLATE 2. Rho Ophiuchi nebula. A four-frame mosaic image taken with an FSQ 106 (4.2-inch *f*/5.5) Takahashi refractor and an STL11000 CCD camera (4008 × 2672 × 9-micron pixels) from Arizona in 2006 July. Copyright R. Gendler, J. Misti and S. Mazlin 2006.

PLATE 3. Double cluster in Perseus (h and χ Persei). This image is a mosaic of two frames with a total exposure time of 14 hours taken with a 12.5-inch Ritchey-Chrétien telescope and STL11000 camera in 2006 November at the Nighthawk Observatory in the Sacramento Mountains of New Mexico. Dr. Gendler has been carrying out CCD imaging since 1996 and one of his early influences was the work of David Malin at the AAO (see Plate 4 for an example). Copyright R. Gendler 2006.

PLATE 4. M43. The circular nebula at the top of this image, M43, is a part of the Orion nebula, but separated from it by a dark lane, so that M43 and M42 (below) appear as separate objects to the eye. It is clearly centred on a bright star, NU Orionis, whose light is scattered, absorbed, reflected, and re-emitted to produce the range of colours and textures seen here. Anglo-Australian Observatory/David Malin Images.

Advice to Contributors

The Observatory magazine is an independent journal, owned and managed by its Editors (although the views expressed in published contributions are not necessarily shared by them). The Editors are therefore free to accept, at their discretion, original material of general interest to astronomers which might be difficult to accommodate within the more restricted remit of most other journals. Published contributions usually take one of the following forms: summaries of meetings; papers and short contributions (often printed as *Notes from Observatories*); correspondence; reviews; or thesis abstracts.

All papers and *Notes* are subject to peer review by the normal refereeing process. Other material may be reviewed solely by the Editors, in order to expedite processing. The nominal publication date is the first day of the month shown on the cover of a given issue, which will normally contain material accepted no later than four months before that date. There are no page charges. Authors of papers, *Notes*, correspondence, and meeting summaries are provided with 25 free reprints if required; additional reprints may be purchased.

LAYOUT: The general format evident in this issue should be followed. ALL MATERIAL MUST BE DOUBLE SPACED. Unnecessary vertical spreading of mathematical material should be avoided (*e.g.*, by use of the solidus or negative exponents). Tables should be numbered with roman numerals, and be provided with a brief title. Diagrams should be numbered with arabic numerals, and have a caption which should, if possible, be intelligible without reference to the main body of the text. Lettering should be large enough to remain clear after reduction to the page width of the *Magazine*; figures in 'landscape' format are preferable to 'portrait' where possible.

REFERENCES: Authors are requested to pay particular attention to the reference style of the *Magazine*. References are quoted in the text by superscript numbers, starting at 1 and running sequentially in order of first appearance; at the end of the text, those references are identified by the number, in parentheses. The format for journals is:

(No.) Authors, journal, volume, page, year.

and for books:

(No.) Authors, [in Editors (eds.),] Title (Publisher, Place), year[, page].

where the bracketed items are required only when citing an article in a book. Authors are listed with initials followed by surname; where there are four or more authors only the first author '*et al.*' is listed. For example:

(1) G. H. Darwin, *The Observatory*, **1**, 13, 1877.
(2) D. Mihalas, *Stellar Atmospheres (2nd Edn.)* (Freeman, San Francisco), 1978.
(3) R. Kudritzki *et al.*, in C. Leitherer *et al.* (eds.), *Massive Stars in Starbursts* (Cambridge University Press), 1991, p. 59.

Journals are identified with the system of terse abbreviations used (with minor modifications) in this *Magazine* for many years, and adopted in the other major journals by 1993 (see recent issues or, *e.g.*, *MNRAS*, **206**, 1, 1993; *ApJ*, **402**, i, 1993; *A&A*, **267**, A5, 1993; *A&A Abstracts*, §**001**).

UNITS & NOMENCLATURE: Authors may use whichever units they wish, within reason, but the Editors encourage the use of SI where appropriate. They also endorse IAU recommendations in respect of nomenclature of astronomical objects (see *A&AS*, **52**, no. 4, 1983; **64**, 329, 1986; and **68**, 75, 1987).

SUBMISSION: Material may be submitted as 'hard copy', or (preferably) by electronic mail to the address on the back cover.

Hard copy: *Three* copies should be submitted. Photocopies are acceptable only if they are of high quality.

Email: contributions may be submitted by email, preferably as standard (LA)TEX files. REFERENCE TO PERSONAL MACROS MUST BE AVOIDED. Those submitting letters, book reviews, or thesis abstracts are encouraged to use the *Magazine*'s LATEX templates, which are available on request. Word files are also welcome provided they conform to the *Magazine*'s style.

Figures may be submitted, separately, as standard Adobe PostScript files, but authors must ensure that they fit properly onto A4 paper.

The Editors welcome contributions to the *Here and There* column. Only published material is considered, and should normally be submitted in the form of a single legible photocopy of the original and a full reference to the publication, to facilitate verification and citation.

CHECKLIST: Double-spaced? Reference style? Three copies?

CONTENTS

NOTES TO CONTRIBUTORS

'THE OBSERVATORY' is an independent magazine, owned and managed by its Editors, although the views expressed in submitted contributions are not necessarily shared by the Editors. All communications should be addressed to

The Managing Editor of 'THE OBSERVATORY'

16 Swan Close, Grove

Wantage, Oxon., OX12 0QE

Telephone Abingdon (01235) 767509

Email: manager@obsmag.org

URL: www.obsmag.org

Publication date is nominally the first day of the month and the issue will normally include contributions accepted four months before that date.

Publishers: The Editors of 'THE OBSERVATORY'

Subscriptions for 2007 (six numbers, post free): £58 or U.S. $110

A lower subscription rate is available, on application to the Editors, to personal subscribers who undertake not to re-sell or donate the magazine to libraries.

Printed in 9/10 Plantin by
Cambridge University Press.

For advertising contact the Editors

ISSN 0029-7704